ORNL/TM-9561

ornl

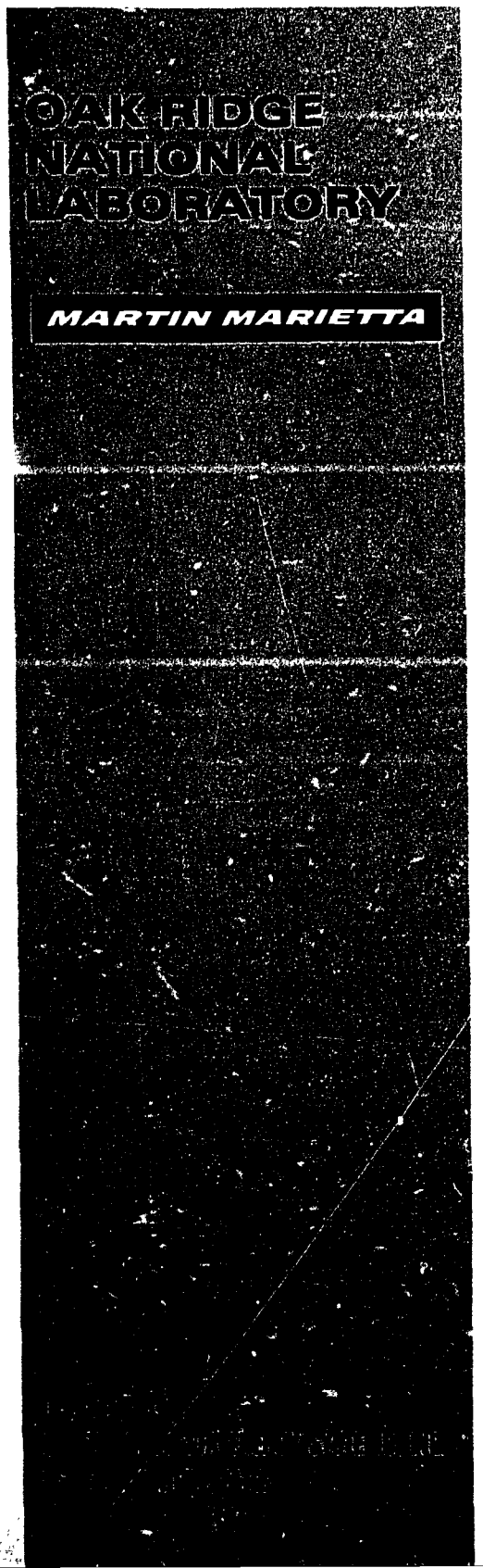

An NE-213-Scintillator-Based Neutron Detection System for Diagnostic Measurements of Energy Spectra for Neutrons Having Energies ≥ 0.8 MeV Created During Plasma Operations at the Princeton Tokamak Fusion Test Reactor

J. K. Dickens
N. W. Hill
F. S. Hou
J. W. McConnell
R. R. Spencer
F. Y. Tsang

ORNL/TM--9561

DE85 018079

ORNL/TM-9561
Dist. Category UC-20d

Engineering Physics and Mathematics Division

AN NE-213-SCINTILLATOR-BASED NEUTRON DETECTION SYSTEM FOR DIAGNOSTIC MEASUREMENTS OF ENERGY SPECTRA FOR NEUTRONS HAVING ENERGIES ≥ 0.8 MeV CREATED DURING PLASMA OPERATIONS AT THE PRINCETON TOKAMAK FUSION TEST REACTOR

J. K. Dickens, N. W. Hill, F. S. Hou,* J. W. McConnell,
R. R. Spencer, and F. Y. Tsang**

Manuscript completed: June 15, 1985

Date published: August 1985

Research supported by
U. S. Department of Energy
Office of Basic Energy Sciences
and
Work partially performed by
Princeton Plasma Physics Laboratory
Princeton, NJ
under
Subcontract No. S-02576-G

*Princeton Plasma Physics Laboratory, Princeton, NJ, operated by Princeton University under contract DE-AC02-76CH03073 with the U.S. Department of Energy.
**Idaho National Engineering Laboratory, Idaho Falls, Idaho.

Prepared by the
OAK RIDGE NATIONAL LABORATORY
Oak Ridge, Tennessee 37831
operated by
Martin Marietta Energy Systems, Inc.
Under Contract No. DE-AC05-840R21400
for the
U.S. DEPARTMENT OF ENERGY

CONTENTS

AN NE-213-SCINTILLATOR-BASED NEUTRON DETECTION SYSTEM FOR DIAGNOSTIC MEASUREMENTS OF ENERGY SPECTRA FOR NEUTRONS HAVING ENERGIES ≥ 0.8 MeV CREATED DURING PLASMA OPERATIONS AT THE PRINCETON TOKAMAK FUSION TEST REACTOR

J. K. Dickens, N. W. Hill, F. S. Hou, J. W. McConnell,
R. R. Spencer, and F. Y. Tsang

ABSTRACT

A system for making diagnostic measurements of the energy spectra of ≥0.8-MeV neutrons produced during plasma operations of the Princeton Tokamak Fusion Test Reactor (TFTR) has been fabricated and tested and is presently in operation in the TFTR Test Cell Basement. The system consists of two separate detectors, each made up of cells containing liquid NE-213 scintillator attached permanently to RCA-8850 photomultiplier tubes. Pulses obtained from each photomultiplier system are amplified and electronically analyzed to identify and separate those pulses due to neutron-induced events in the detector from those due to photon-induced events in the detector. Signals from each detector are routed to two separate Analog-to-Digital Converters, and the resulting digitized information, representing (1) the raw neutron-spectrum data and (2) the raw photon-spectrum data, are transmitted to the CICADA data-acquisition computer system of the TFTR. Software programs have been installed on the CICADA system to analyze the raw data to provide moderate-resolution re-creations of the energy spectrum of the neutron and photon fluences incident on the detector during the operation of the TFTR. A complete description of, as well as the operation of, the hardware and software is given in this report.

1. INTRODUCTION

The presently-described program was initiated in April 1984 as a joint venture between our group at the Oak Ridge National Laboratory (ORNL) and the Radiation Shielding Section of the Tokamak Fusion Test Reactor (TFTR) at the Princeton Plasma Physics Laboratory (PPPL). The goal of this program is to experimentally deduce the transport of neutron and photon radiation (created during TFTR operation) from the sources of the radiation to designated critical areas of the Test Cell Basement (TCB) of the TFTR. Responsibilities were divided broadly into two areas: (1) ORNL personnel were responsible for the design, fabrication, and testing of the detector hardware and for the software package necessary to analyze the raw spectral data; (b) PPPL personnel were responsible for on-site installation (including choice of locations for measurements) and for the software programs necessary for data acquisition and display utilizing the TFTR computer system CICADA. The resulting system has been in operation as of this writing (March 1985) for several months. The purpose of this report is twofold: (1) to document the hardware and software that have been developed for this task; and (2) to provide a "users' manual" for subsequent users of this equipment at PPPL, since it is planned to leave the equipment at the TFTR when the present experimental needs are fulfilled.

2. DETECTION SYSTEM

2.1 DETECTORS

Three different-sized right circular cylinder detectors were fabricated, the sizes chosen to span the estimated neutron and photon fluences expected to be encountered in the TCB. The chosen sizes are given in Table 1. After initial scoping studies to obtain a better estimate of these fluences, the two larger detectors were chosen for the first series of final measurements in the TCB.

Table 1. NE-213 detector sizes

No.	Diameter (cm)	Height (cm)	Designation
1	4.6	4.6	"Large"
2	4.6	2.2	"Medium"
3	2.1	2.2	"Small"

The detector configuration for the largest detector is shown schematically in Fig. 1. The cell is an aluminum turning, painted white on the inside with an insoluble epoxy (Varian Torr Seal Vacuum Epoxy) and glued (National Diagnostics ND-707) onto the photocathode of the photomultiplier tube (an RCA-8850). The liquid NE-213 scintillator was put into the cell via the filling hole (a threaded hole), was "bubbled" to allow removal of trapped gases, and was then sealed in. The cell assembly is wrapped in black teflon tape. As shown in Fig. 1, the detector system is enclosed in (a) a standard μ-metal shield and (b) a 1-cm-thick soft-iron shield which is designed to protect the photomultiplier tube in magnetic fields up to 0.8 Tesla (8K Gauss).

An RCA-recommended, high-gain, high-current resistive chain was adopted to control the voltage among the dynodes between the photocathode and the anode. These electronics are housed in the item labelled "Tube Base" in Fig. 1.

2.2. ELECTRONICS

The technique adopted to differentiate events due to neutron detection from those due to photon detection depends on pulse-shape analysis, and is known as Pulse-Shape Discrimination (PSD). It is a measurement of time which is then converted to pulse height. The resulting pulse-height spectrum exhibits two distinct peaks, one corresponding to neutron events and the other corresponding to photon events.

The electronics connected to a detector in the experimental measurement area is exhibited in Fig. 2. It consists of the aforementioned tube base, a PreAmplifier (PA), a constant-fraction discriminator (CFD) (ORTEC Model No. 473A or Model No. 934), a NIM Bin to provide power for the PA and the CFD, and a high-voltage (HV) supply to supply the high voltage (bias) to the photomultiplier tube. All of these items are housed in a relatively thin-walled steel box designed as a Faraday shield against possible substantial electric field transients while also allowing heat dissipation. This steel box is electrically insulated from its environment. The box may also be insulated from the soft-iron magnetic shield surrounding the detector.

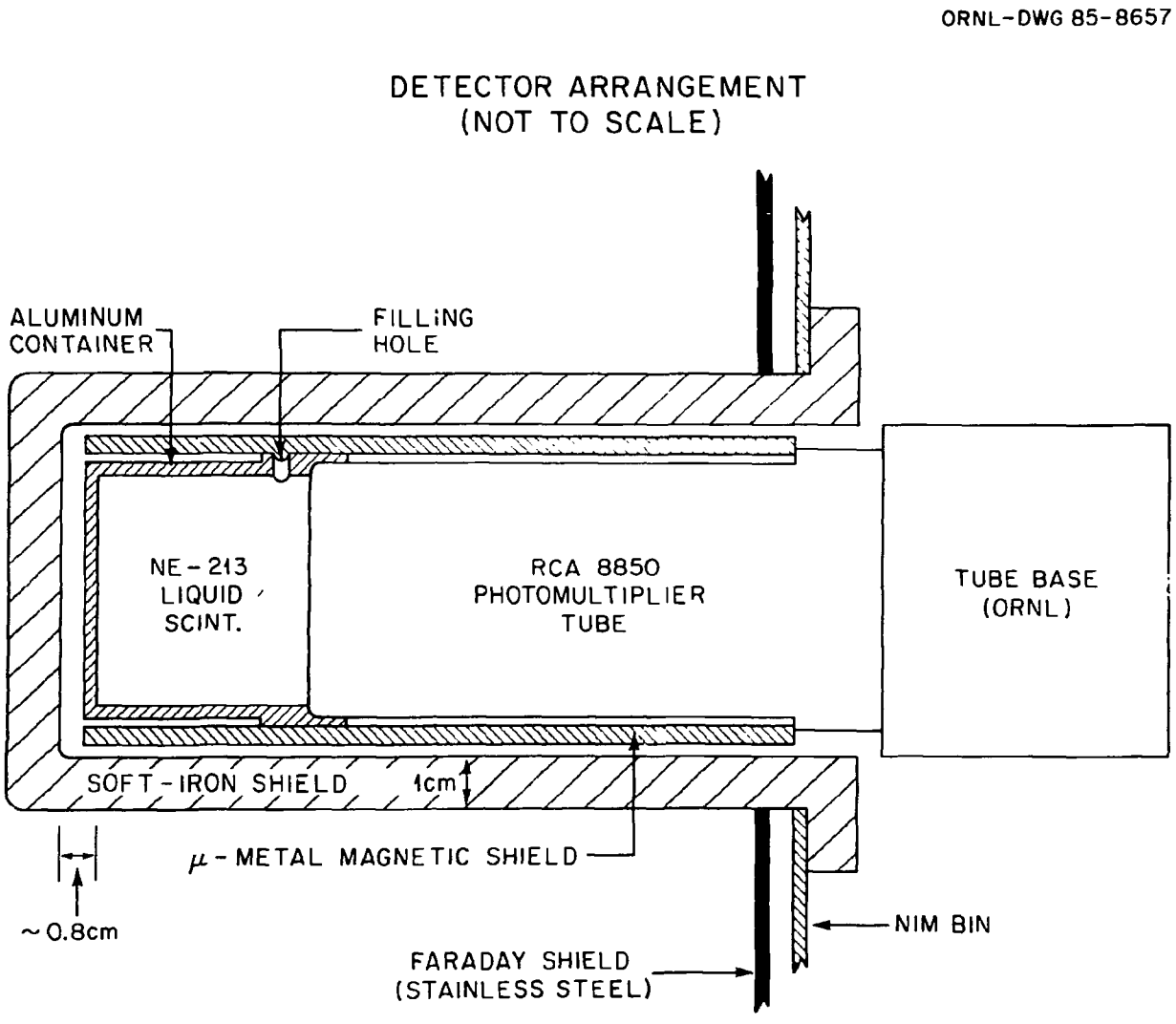

Fig. 1. Detector arrangement showing details of the scintillator inside the soft-iron shield for the largest detector. For the two thinner detectors, the photomultiplier tube occupies the same position as shown, so the front face of the detector is ~3.0 cm behind the inside of the front of the iron shield. The aluminum container is machined to yield an accurately known inside dimension; its walls are <1 mm thick except at the base where it is glued to the photomultiplier tube.

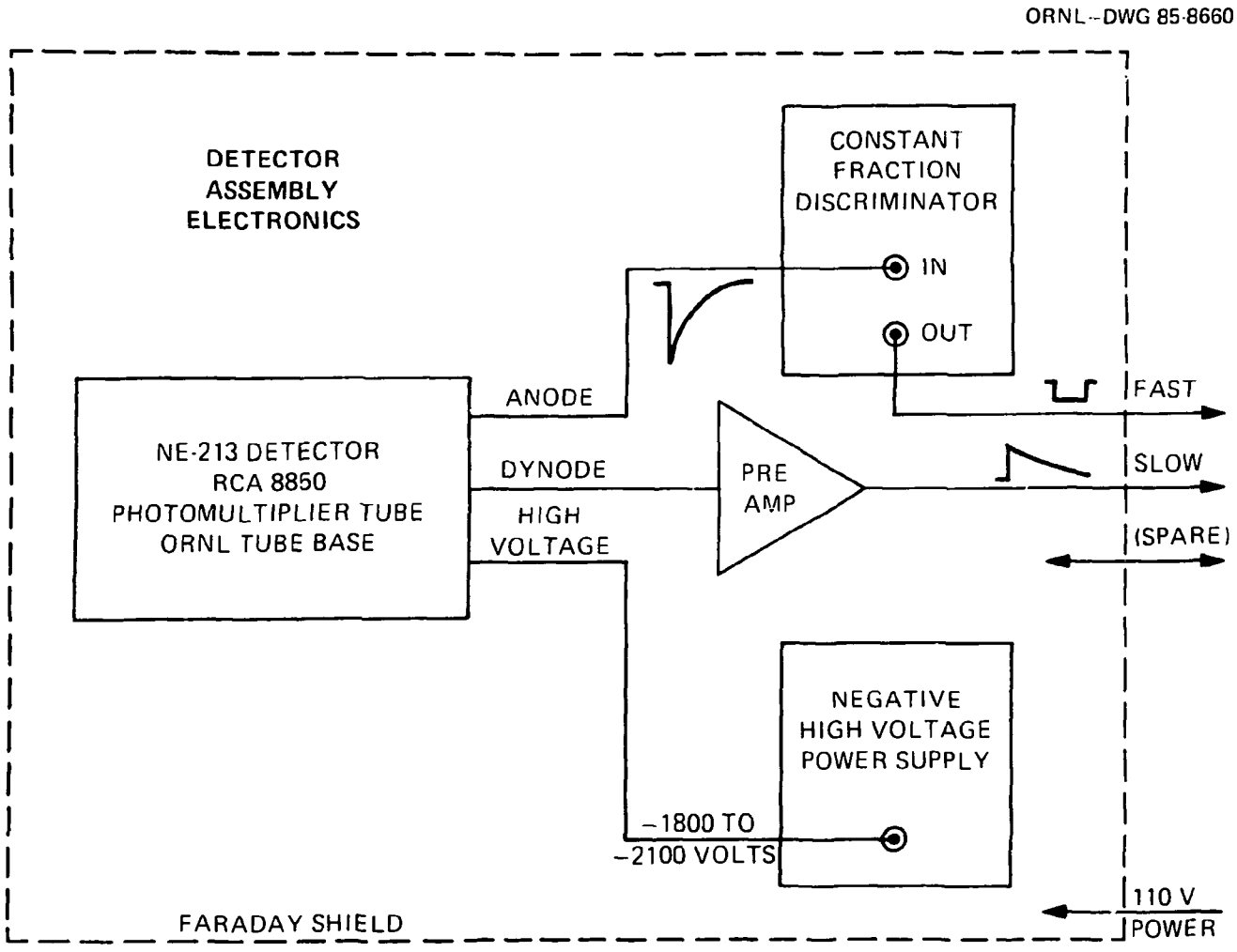

Fig. 2. Electronics for the detector assembly. The Faraday shield consists of a box made of stainless steel. It houses a standard NIM bin, which unit provides power for the Preamplifier and the Constant Fraction Discriminator units.

The output of the anode (of the photomultiplier tube) is connected to the input of the CFD using a short piece of 50-Ω cable. The PA is connected (on the tube base) to the dynode output; the PA power is obtained directly from one of the NIM bin slots. The HV supply is set to negative (switch on the back) before connecting it to the appropriate connector on the tube base. The bias used for these detectors ranges between −1800 and −2100 volts. The outputs of the PA and the CFD are connected to BNC-type connectors fixed on, and insulated from, the steel box. Approximate pulse shapes at these points are indicated in Fig. 2.

In the present arrangement, the detectors are connected to the rest of the electronics via RG-59/U cable, a 75-Ω cable, and these cables are of different lengths depending on the location of the detector. IT IS IMPORTANT TO NOTE THAT THE PSD ELECTRONIC TIMING MUST BE REDONE WHEN THESE CABLES ARE CHANGED.

The PSD electronics are housed in the Safety Check Area of the TCB. A schematic of these electronics is given in Fig. 3. The "Fast" pulse from the CFD of Fig. 1 is connected through a 25-Ω resistor to a second discriminator. The resistor is needed because the long cables are 75-Ω cables, whereas the fast electronics equipment has 50-Ω inputs; a second discriminator is used to compensate for substantial degradation of the fast logic signal after it has traversed ~135 ft of RG-59/U cable. The subsequent logic pulse is delayed and provides the "Stop" pulse to the Time-to-Amplitude Converter (TAC). The "Slow" pulse, from the PA of Fig. 1, is split and fed into two amplifiers. The ORNL Q-5695 Timing-filter amplifier is especially designed to provide a pulse of ~0.6 μsec total duration with an exceptionally fast crossover; this crossover is sensed by the ORNL Q-5686 Fast Zero-crossing discriminator, and the output logic pulse provides the "Start" pulse to the TAC. The LENGTHS of the two cables connected to the Start and Stop connectors of the TAC are very critical and provide the fine tuning needed for optimal operation of the PSD logic (see Sect. 4). When properly set up, the PHA output of the TAC should exhibit pulses similar to that schematically shown near point H of Fig. 3. If this signal is analyzed using a pulse-height analyzer (PHA), the spectrum should closely resemble that shown in Fig. 4. Once this spectrum has been obtained, the lower-level discriminator (LLD) and the upper-level discriminator (ULD) of the TAC-and-SCA (Single-Channel Analyzer) unit are set to bracket the "peak" corresponding to neutron detection. The SCA output will provide a positive gating pulse for a TAC-identified neutron pulse; this gate pulse is connected to the coincidence input pulse of a LeCroy Model No. 3512 Analog-to-Digital Converter (ADC). For gamma-ray identification, the commercially obtained TAC-and-SCA unit has been modified by adding an output connector to the rear panel of this unit; a positive gate pulse appears at this connector when the TAC output is larger than the ULD setting but smaller than the range setting. Hence, this gate pulse corresponds to detection of a gamma ray in the detector and is used at the coincidence input of a second LeCroy 3512 ADC. The signal inputs of these ADC units are connected to an amplified, doubly-differentiated, and delayed pulse. These ADC units require pulses having time constants of 1 μsec or longer and will not work on the ORNL Q-5695 amplifier output pulses. Therefore a "standard" linear amplifier connected in parallel with the ORNL Q-5695 amplifier is used to provide pulses to be input into the LeCroy 3512 ADC units.

The relative times-of-arrival of the various signals must be set for operation of the PSD electronics. Shown in Fig. 5 are signals obtained at designated locations in the set up diagramed in Fig. 3. The setup procedure will be discussed in more detail in Sect. 4.

There are two complete detector configurations in the present experiment, each with the set of electronics shown in Figs. 2 and 3. Thus, in a "permanent" location in the Safety Check Area of the TFTR TCB there is a CAMAC crate containing electronics including four LeCroy Model No. 3512 ADC units. These four units are daisy-chain connected to a LeCroy Model No. 3588 Histogram Unit, which, in turn, is connected to the CICADA data-acquisition computer system via an optic-fiber link.

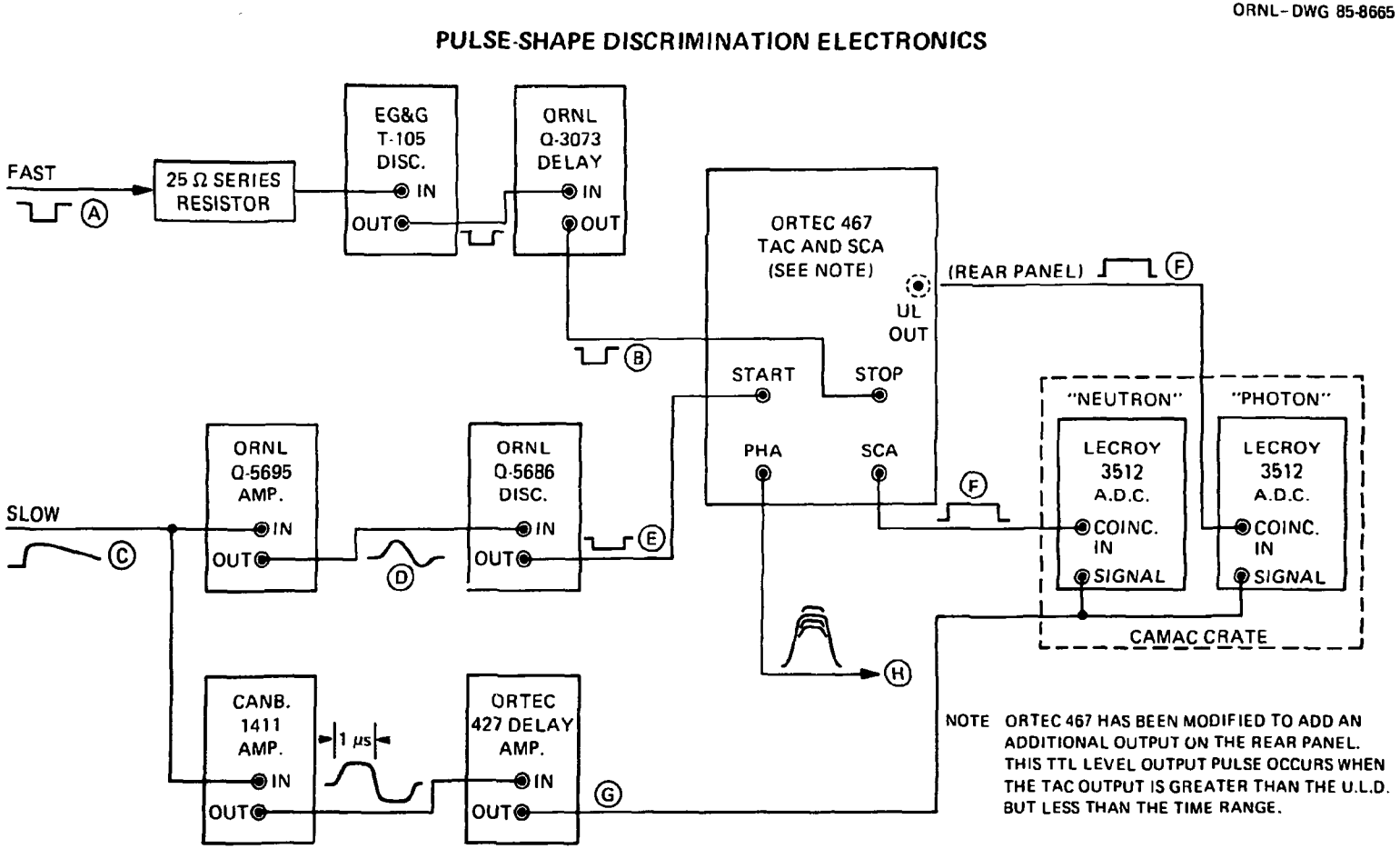

Fig. 3. Pulse-shape discrimination electronics for one detector. There are two complete sets of these electronics. Not shown is a LeCroy Model No. 3588 Histogram Unit which is connected to the (four) ADC units and serves as a pulse-height memory for the data acquired using the ADC units.

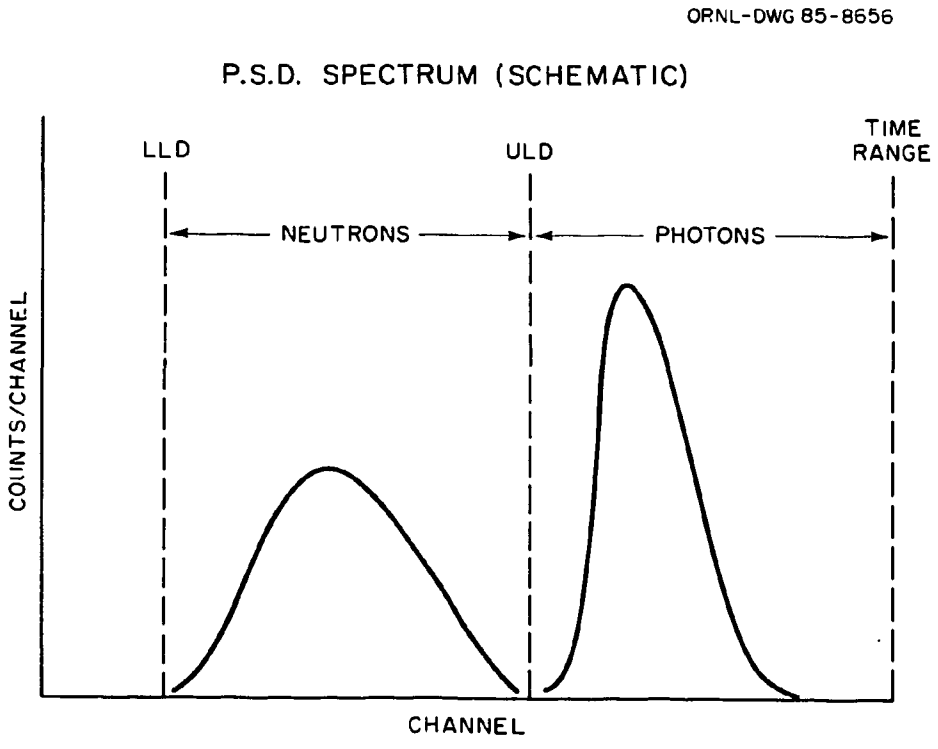

Fig. 4. Schematic pulse-shape discrimination spectrum. The dashed lines indicate probable discriminator settings on the TAC-and-SCA unit of Fig. 3.

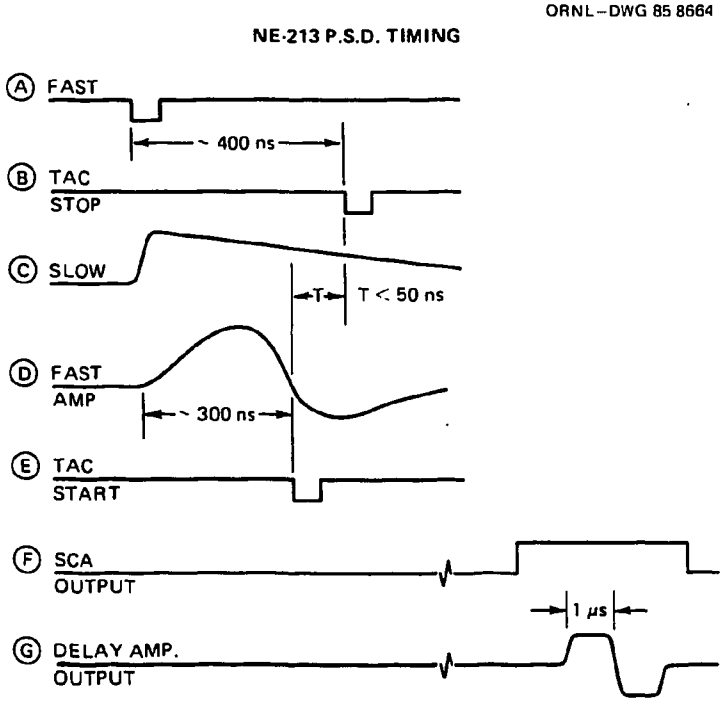

Fig. 5. Pulse-shape discrimination time and pulse shapes. The timing scale for the pulses labelled C, F, and G is much more compact than for the pulses labelled A, B, D, and E.

These ADC units are preset for 250 channels total, and each ULD is set at maximum, corresponding to about a 7.7-volt pulse, which (pulse) must be at least 1 μsec wide. The LLDs on these units are set to cut off the spectrum at about channel no. 4, i.e., corresponding to about a 0.13-volt pulse. There is a switch on the front of each ADC unit that is set to designate that the unit is to be operated in the mode requiring (time) coincidence of the amplified (and delayed) pulse with its associated coincidence pulse from the PSD electronics. One may note, in passing, that the hardware of the LeCroy units does set priorities for the transfer of data from the ADC units to the Histogram unit.

2.3. COUNTING-RATE CAPABILITIES OF A COMPLETE SYSTEM

The LeCroy Model No. 3512 ADC units require 5 μsec (minimum) to properly process a pulse for transmission to the Model No. 3588 storage unit. This 5-μsec processing time would imply a maximum upper-limit counting rate of 200,000/sec, but for practical purposes, one should strive for no more than ~25% of this maximum, or 50,000/sec. The PSD decision-making process is designed to be accomplished in 0.6 μsec; tests with units similar to those in the present systems verify accurate PSD for count rates in excess of 500,000/sec, indeed with very little distortion for count rates approaching 10^6/sec. The Canberra Model No. 1411 amplifier is set to 1-μsec time constants and should recover within 5 μsec to properly amplify the next pulse; i.e., its counting-rate limitations are comparable to those of the LeCroy ADC units.

Overload pulses in the Canberra Model No. 1411 amplifier, however, will result in a much longer recovery period, of ~10 μsec or longer. Overload pulses in the ORNL Q-5695 timing-filter amplifier are rejected by an ULD in the Q-5686 unit, and as a result neither unit is "disabled" by an extended recovery nor is there an output pulse from the Q-5685 unit to start the PSD action.

3. SOFTWARE PROGRAMMING

At present all software is resident in the CICADA system's PDP-11/23 microcomputer. Data are stored on the PDP-11/23 microprocessor's hard disk (10Mb Winchester drive) and transferred via floppy disks to another PDP-11/23 computer for further analysis, i.e., unfolding. This transfer is a "manual" operation, and it can be done at any time. They are not (yet) accessible by any other diagnostic system, nor are results of other diagnostic programs accessible to the present program. In addition, only limited input and output (I/O) capabilities exist for the present program.

3.1 DATA-ACQUISITION PROGRAM

This program is resident in core and operates automatically (i.e., without operator commands). About 1 sec prior to a plasma "shot" in the TFTR the program transmits a signal to enable the CAMAC equipment, and data taking commences. Six seconds later a second signal is transmitted to the CAMAC equipment to (a) disable data taking, (b) transmit the contents of the LeCroy Model No. 3588 histogram unit to CICADA storage, and (c) reset the histogram unit memory to zero. Details of this program are given in Appendix D.

There is a second version of this program which may be used when the TFTR is not being operated. This second version requires operator action. It is called into operation by the command RUN NETST and allows the operator to accumulate data for any desired period of time up to 500 sec, a value for which is input following a prompt to do so. This version is used during equipment setup and to obtain energy-vs-pulse-height energy calibrations.

One limitation to these codes should be noted: the data are transferred and stored as single-precision (signed) integers, and so there is an effective upper limit to $2^{15}-1$ (or 32768) counts/channel that may be transmitted.

3.2 DATA-REDUCTION PROGRAMS

Data acquired with the present system are difficult to interpret without subsequent analysis. The required primary data analysis is designated as "unfolding" and comes about because of the nonspecific response of the NE-213-based detection system to the radiation, neutrons and/or photons, being detected. The response of this type of detector to (both) neutrons and photons of a specific energy is a distribution that has the general characteristic shown in this small figure:

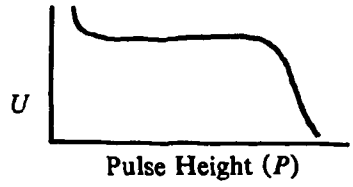

If we designate the plotted analog function by $U = U(E, P)$, where E is the energy of the incident radiation (assumed monoenergetic) and P is the pulse-height value, then what we measure when we measure a detector response are yields/channel, which, for a specific channel C_j of the analysis equipment is given by

$$R_j(E) \equiv R(C_j,E) = \int_{P_j-\Delta P/2}^{P_j+\Delta P/2} U(E,P)dP \quad , \tag{1}$$

where P_j corresponds to the centroid pulse-height of the channel C_j, and ΔP corresponds to the equivalent pulse-height spread (or bin) associated with the channel C_j. Here we must be careful in the understanding of the several variables. The pulse height, P, has real units of voltage. The LeCroy Model 3512 ADC will process pulses of height, P, up to ~7.8 volts. The channel, C_j, is a designation for a particular digitized output of the ADC. For the present experiment, the ADC has been set to output $p = 240$ channels, and so the channel designations are C_1, ..., C_j, ..., C_p, where now $C_p = 240$ corresponds to $P_{max} \sim 7.8$ volts, $C_1 = 1$ corresponds to $P_{min} \sim (7.8/240)$ volts, and C_j $(1 < j < p)$ corresponds to a value of P between P_{min} and P_{max}. The functional dependence of C_j on P is nearly but (usually) not exactly linear, and may be determined using a variable electronic pulse generator.

In our experiment, the pulse height, P, is the maximum voltage value of the pulse generated by the electronics; as such P is a function of the amount of energy deposited in and recorded by a detector. Therefore, we set our electronic equipment so that *for events of interest* the maximum energy deposited in the detector will result in a pulse height $P < P_{max}$. Evidently, one needs to determine the functional relationship between P and the energy deposited, i.e., an energy-to-pulse-height calibration. This calibration task would be straightforward if the detector response were a delta function for incident monoenergetic radiation. However, the real response is not a delta function but a distribution exhibited in the small figure above, and so some interpretation is required.

The calibration procedure used is based upon the response, $U_0(E,P)$, that might be expected for the case where the incident monoenergetic radiation interacts only once (i.e., no multiple scattering) in an ideal detector. In this case, $U_0(E,P) = 1$ (in relative units) for $0 \leq P \leq P_{edge}$, and $U_0(E,P) = 0$ for $P > P_{edge}$. Now, P_{edge} is a function of E. For gamma rays, P_{edge} is a function of the maximum Compton-electron energy, and for neutrons, P_{edge} is a function of the recoil-proton energy.

The real response approximates U_0 for the larger P with the modification that for $P \sim P_{edge}$,U_0 is "smeared" by an approximate Gaussian distribution of some finite width. The calibration technique, then, involves analyzing the obtained calibration spectrum to deduce a value of P which would approximate the P_{edge} of the U_0 response. What is done is to determine the value of U for the measured response for the "flat" region, and then determine the position, P_h, where the value of U is one-half of that for the "flat" region, as generally indicated in the next small figure:

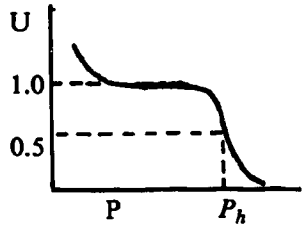

Standard practice is to set $P_h = P_{edge}$, since P_{edge} can be computed exactly, so that the P-axis can be labelled with an "equivalent" particle energy. Some care in interpretation is required, however, for there are real data having $P > P_h$. Clearly, there can be no data resulting in P larger than the size of a pulse corresponding to the energy of the detected neutron or photon. The use of the "equivalent" particle energy is very convenient but will lead to the above contradiction if taken as the actual particle energy.

As mentioned above, the pulse-height, P, has real units of voltage. However, voltage is an inconvenient unit since it depends upon electronic settings and is, therefore, different for every experimental setup. So, an intermediate unit was developed as a pulse-height unit, and this unit goes by the designation of a "light" unit. This unit is a linear function of voltage, or nearly so. However, while neither neutron energy nor photon energy is a linear function of "light" units, the functional dependence of each (with respect to "light" units) is single-valued and monotonically increasing, and each functional dependence has been experimentally deduced. The calibration procedure, then, is to deduce the "light"-unit curve as a function of the experimental pulse-height setting, and to use "light" units as pulse-height units for subsequent data analysis.

The actual data that we obtain are due to neutrons and photons having a spectrum of energies. We may define, say, the neutron fluence, as being composed of m discrete energy groups (m may be a very large value, but we assume it is finite). Let us designate separately each energy by E_k (where $1 \leq k \leq m$) and measure the detector response to some incident neutron fluence made up of $n(E_k)$, where n is the number of neutrons having energy E_k. In this case, the yield, Y_j, in the j^{th} channel is given by the "folding" process,

$$Y_j = \sum_{k=1}^{m} R_j(E_k)n(E_k) \quad . \tag{2}$$

In our real measurements, however, it is the spectrum $n(E_k)$ that is unknown. One first measures a spectrum of Y_j. The data reduction then consists of applying the $R_j(E_k)$ and the Y_j properly to deduce the spectrum corresponding to the $n(E_k)$. It is the inverse nature of the mathematical process that has led to the term "unfolding."

As might be expected, the simple description given by Eq. (2) becomes substantially more complicated when uncertainties are included in the unfolding process. We use an application[1] of Bayes theorem as the mathematical basis for the unfolding software. Responses of each detector to approximately monoenergetic neutrons having energies >0.8 MeV were determined experimentally using neutrons generated by the Oak Ridge Electron Linear Accelerator (ORELA). Examples are shown in Figs. 6, 7, and 8, which exhibit, in particular, that the detector responses are not simple multiples of a very similar relative response. Absolute normalization was deduced using the Monte Carlo computer program[2] O5S. Responses for each detector to gamma rays were determined experimentally using well-calibrated gamma-ray sources for photon energies ≤2.6 MeV. Interpolation was used to deduce $R_j(E_l)$ values for $(E_\gamma)_l < 2.6$ MeV; for larger-energy gamma rays assumptions were made about the relative shape of the response vs pulse height, and these were normalized to the total interaction probability deduced from known attenuation coefficients.

All of these responses were determined for radiation impinging on the front face of the detector. Experience has shown that detector response is essentially insensitive to the angle of entry,[3] and so that assumption is made for these detectors also. It should be noted that no corrections have been made for attenuation by the 1-cm iron magnetic shielding. Such corrections will depend on detector orientation with respect to the incident flux and will need to be computed as part of a radiation transport calculation. An estimate of the magnitudes of the effects of this iron shield on neutron spectra was obtained from an ANISN[4] calculation done for us by J. M. Barnes and R. T. Santoro for an isotropic source incident on the iron shield. Their results confirm our original estimates of neutron attenuation in the iron, and, in addition, indicate the amount of the moderate shift in overall response toward smaller response energies. More detail on this calculation is given in Appendix B.

In order to relate the measured responses to the *in situ* plasma-produced neutron and gamma-ray fluences, a decision on pulse-height binning was needed. It was evident that a very fine binning (i.e., pulse-height bin width << average pulse-height bin magnitude) would result in data arrays much too large to be handled by the available CICADA computer, and, indeed, would result in detail that present-day radiation-transport calculations cannot hope to reproduce, again because of the overwhelming magnitude of the calculation. We have chosen a somewhat coarse grouping which spans the neutron energy region between 0.75 and 15 MeV and yet provides some detail of the 1- to 3-MeV neutron energy region so that some inferences can be made about scattering of D+D neutrons. Primarily for simplicity in the programming and calculations, the same pulse-height binning was adopted for the gamma-ray responses, even though the resulting gamma-ray energies at the bin limits may not be ideal. The final pulse-height binning is given in Table 2. The units for pulse height are the "light" units[5] presented above and discussed in more detail in Sect. 4. Again more for ease of programming, responses were computed for radiation (i.e., neutron or gamma ray) energy groups identical to those of the pulse-height binning; that is, the response arrays are "square." Actually, the response arrays contain one additional bin corresponding to $E_n > 15.2$ MeV. Clearly, we do not expect to observe *any* neutrons corresponding to $E_n > 15$ MeV (except possibly during a plasma disruption); this added pulse-height bin allows a full description, including detector resolution effects, for a detector response to 14-MeV neutrons.

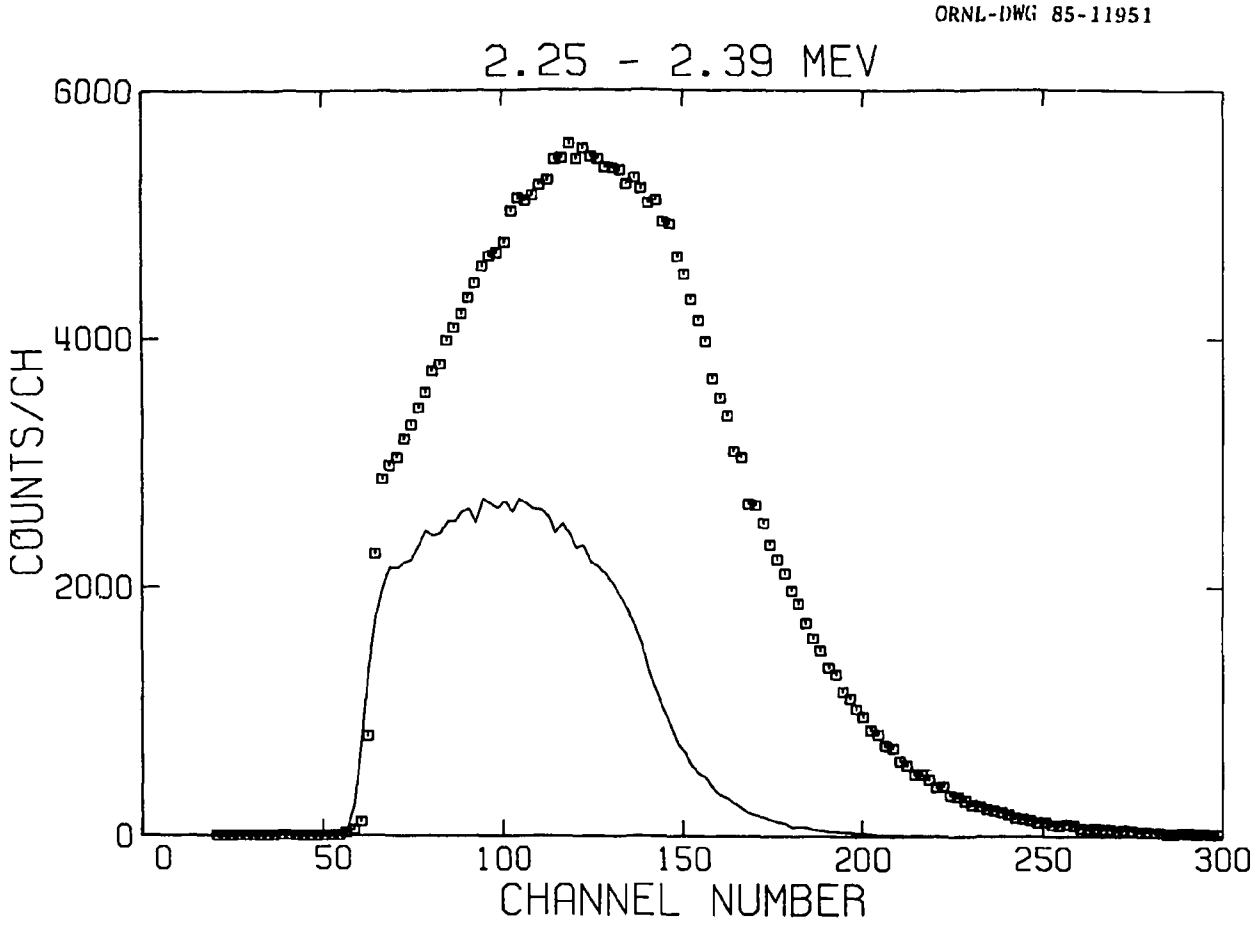

Fig. 6. Measured responses for E_n = 2.25 to 2.39 MeV. The squares exhibit the raw data obtained for the Large detector and the line indicates data for the Medium detector. The data were obtained on Flight Path 8 at the 20-m station of the ORELA. The incident neutron energy was determined by time-of-flight techniques. These data are not normalized; the figure is to illustrate relative yields $R(C_j,E)$ of Eq. (1).

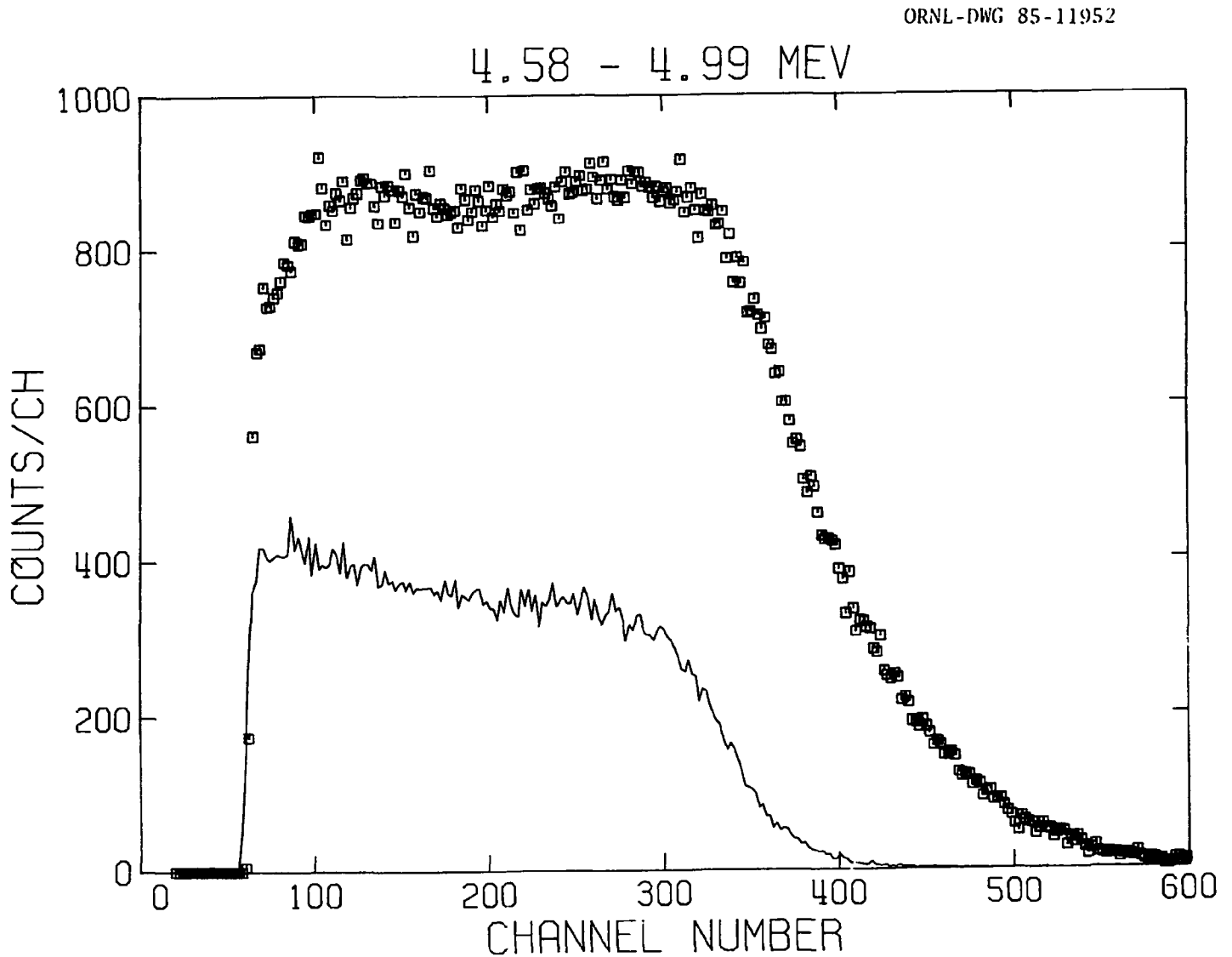

Fig. 7. Measured responses for E_n = 4.58 to 4.99 MeV, similar to data exhibited in Fig. 6.

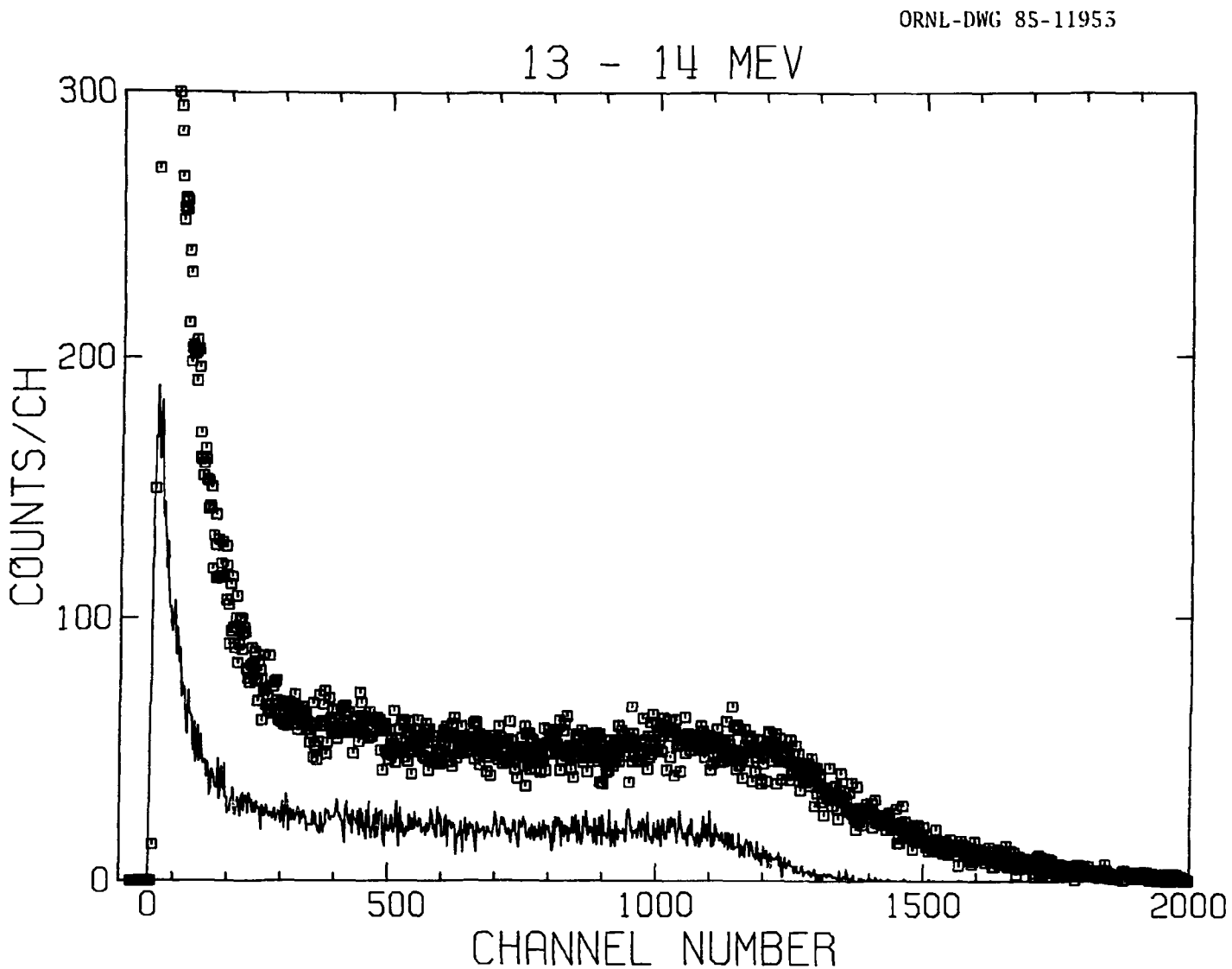

Fig. 8. Measured responses from E_n = 13 to 14 MeV, similar to data exhibited in Fig. 6.

Table 2. Adopted pulse-height bins and associated neutron and gamma-ray energies

Bin no.	Pulse height (light units)	Neutron energy (MeV)	Gamma-ray energy (MeV)
1	0.097 - 0.132	0.75 - 0.90	0.24 - 0.29
2	0.132 - 0.164	0.90 - 1.03	0.29 - 0.34
3	0.164 - 0.215	1.03 - 1.22	0.34 - 0.41
4	0.215 - 0.272	1.22 - 1.41	0.41 - 0.49
5	0.272 - 0.333	1.41 - 1.60	0.49 - 0.57
6	0.333 - 0.400	1.60 - 1.80	0.57 - 0.66
7	0.400 - 0.4725	1.80 - 2.00	0.66 - 0.75
8	0.4725 - 0.565	2.00 - 2.25	0.75 - 0.87
9	0.565 - 0.645	2.25 - 2.45	0.87 - 0.97
10	0.645 - 0.742	2.45 - 2.70	0.97 - 1.09
11	0.742 - 0.911	2.70 - 3.10	1.09 - 1.30
12	0.911 - 1.424	3.10 - 4.20	1.30 - 1.92
13	1.424 - 2.05	4.20 - 5.48	1.92 - 2.67
14	2.05 - 3.06	5.48 - 7.40	2.67 - 3.88
15	3.06 - 4.15	7.40 - 9.32	3.88 - 5.17
16	4.15 - 5.8	9.32 - 12.09	5.17 - 7.14
17	5.8 - 6.5	12.09 - 13.23	7.14 - 7.97
18	6.5 - 7.7	13.23 - 15.20	7.97 - 9.40
19	7.7 - 8.5	15.20 - 16.48	9.40 - 10.35

There are four responses built into the unfolding program installed on the CICADA at PPPL. These are one each for neutrons and for gamma rays for each of the Large and Medium systems given in Table 1. These responses, and those for the Small detector, are tabulated in Appendix A. Should any measurements be made using the Small detector, it is a simple matter to enter the last two responses into the present code.

Gamma-ray responses were tested by unfolding photon source spectra. An example is given in Fig. 9 for ^{54}Mn. If the unfolding were "perfect", the bin corresponding to $E_\gamma \sim 0.83$ would contain the total yield and the rest of the bins would contain zeroes. Obviously, the ideal has not been (quite) obtained. There are two caveats for this particular source measurement: one, there were background radiation taken at the same time; and, two, in most cases, the unfolding process simply will generally not reproduce ideally the overall resolution because of small differences between the actual test data and the effectively smoothed response. For this case, the only datum that may be cause for concern is that at $E_\gamma \sim 0.375$ MeV, which suggests the possibility of small errors in the lowest-energy pulse-height bins for one or more responses for $0.4 \leqslant E_\gamma \leqslant 0.9$ MeV. The maximum possible incorrect determination is, however, $\leqslant$7% (after estimated background and resolution effects are considered) of the total yield, and will be of essentially no consequence for spectra obtained at the TFTR. One might be more concerned about unfolded gamma-ray spectra for $E_\gamma > 2.6$ MeV since the deduced $R_j(E_i)$ are extrapolated from experimental measurements and not based directly on measurements. Again, however, we expect rather fewer high-energy than low-energy gamma rays, at least during normal (i.e., nondisrupted) plasma shots, and so any errors in $R_j(E_i)$ due to incorrect extrapolation should not impact substantially conclusions regarding unfolded spectra.

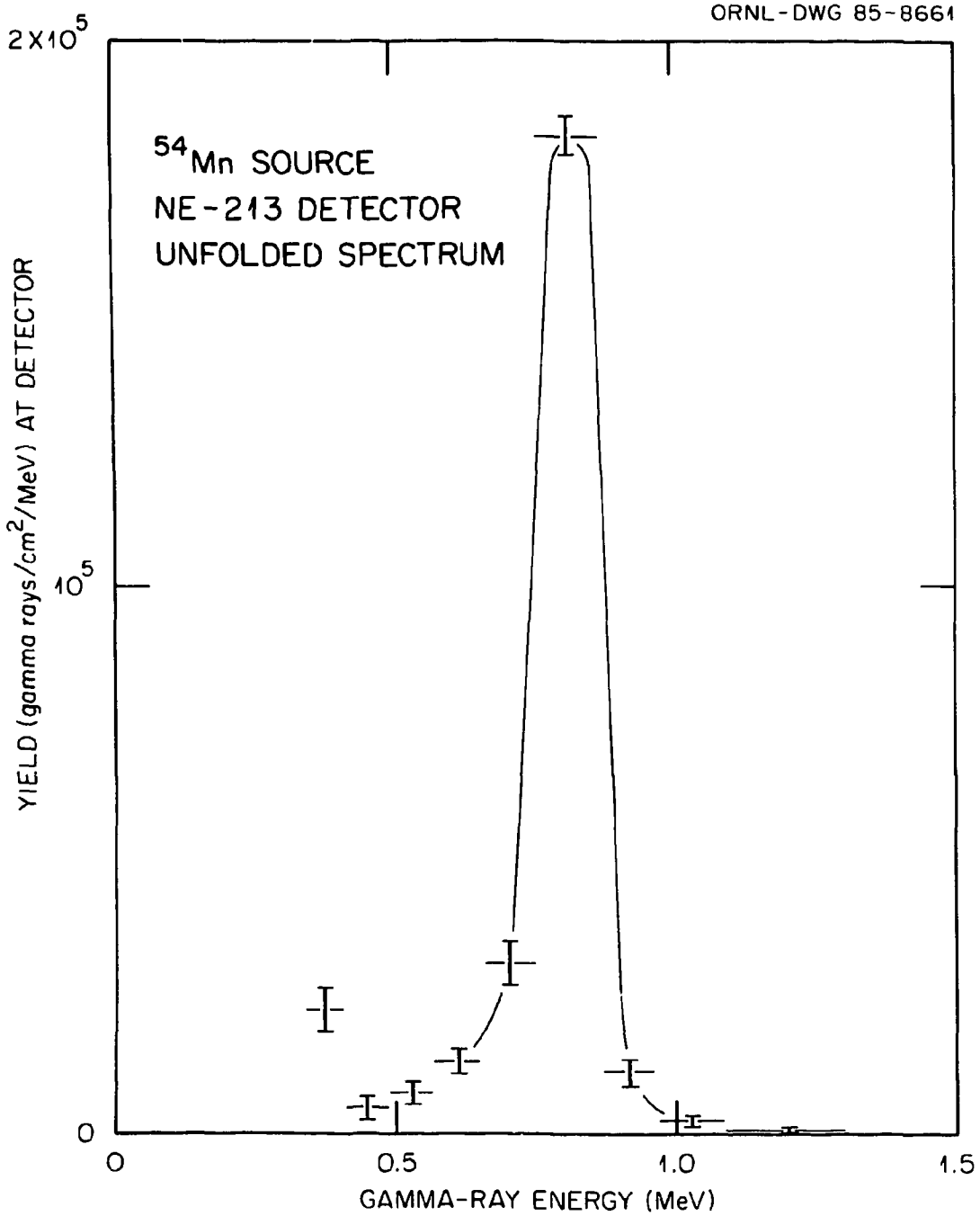

Fig. 9. Unfolded gamma-ray spectrum for a measurement using a source of ^{54}Mn. The source was placed 25 cm in front of, and on axis of the bare Medium detector. The lines delineating a "peak" are included only as guides.

One other aspect of data reduction needs attention. For most individual plasma shots, there accrue fewer counts in the detectors than one would like to have for the unfolding process. A separate program has been written to sum data of several individual runs. This program is interactive; one uses it by calling RUN NESUM (see Appendix D for details) and then following the prompts to specify the desired runs to be summed.

3.3 EXAMPLES OF DATA AND DATA REDUCTION

On December 11, 1984, there was a series of equivalent shots starting with shot No. 11777. Data were summed for 15 such shots. For these shots the medium-sized detector was mounted about 1 ft south of the north wall of the TCB, about 10.5 ft above the floor, about 6 ft west of the TFTR N-S centerline, and with the axis of the detector mounted horizontally pointing west along the E-W direction. The summed, unbinned pulse-height data for neutrons and for gamma rays are shown in Figs. 10 and 11, respectively. (At this point we make two observations: (1) to the untrained eye these data are very nearly featureless; and (2) without a knowledge of the channel-to-pulse-height calibration the data have little real meaning.) These data were processed at ORNL using the same unfolding-code program that was subsequently transferred to the CICADA at PPPL. The first step in this computation was to bin the raw spectral data by the appropriate bin grouping of Table 2; the result of this step for the neutron data is exhibited in Fig. 12. The final step in this computation was the unfolding, and the results of this step are exhibited in Figs. 13 and 14, respectively, for neutrons and gamma rays. The unfolded results exhibit "structure" and, more important, put the measurements on a firm, absolute-yield basis. One should resist the temptation to ascribe detailed meaning to each and every "peak" exhibited in these figures, since these details are rather dependent on the accuracy of the channel-to-pulse-height calibration. However, one may observe at least two meaningful peaks in Fig. 14, one near 0.51 MeV and the other near 0.84 MeV. The first is due to annihilation radiation, while the second is ascribed to $^{56}Fe(n,n'\gamma)^{56}Fe^*$ reactions leading to excitation of the first-excited state of ^{56}Fe. We speculate that these 0.84-MeV gamma rays are due to neutron interactions with the soft-iron magnetic shield surrounding the detector.

4. DETECTOR AND ELECTRONICS SETUP PROCEDURES

Equipment and materials needed to effect a setup of one of the detection systems includes (a) a fast oscilloscope (e.g., Tektronix Model No. 485), (b) a pulse-height analyzer (PHA), (c) radiation sources including a ^{22}Na gamma-ray source of several μCi or stronger and a ^{252}Cf (or a Pu-Be or similar) mixed neutron-gamma source, (d) an assortment of 50Ω cables (RG-58/U) of varying lengths, and (e) an assortment of small hand tools, including a "jewelers" screwdriver.

The process of setting up will follow generally along these lines:

1. Be sure that the HV to the detector (see Fig. 2) has been turned down to zero and that this HV unit and the NIM Bin 110-volt power are off. Then place the detector system at the desired place and connect the signal cables. BE SURE the ground wire is properly connected to the system to avoid a grounding problem before plugging into 110-volt power. Turn on power to the NIM Bin, then to the HV unit. Bring up the HV to, perhaps, −1900 V slowly; allow several seconds between each change of switch setting to allow the PA electronics to recover.

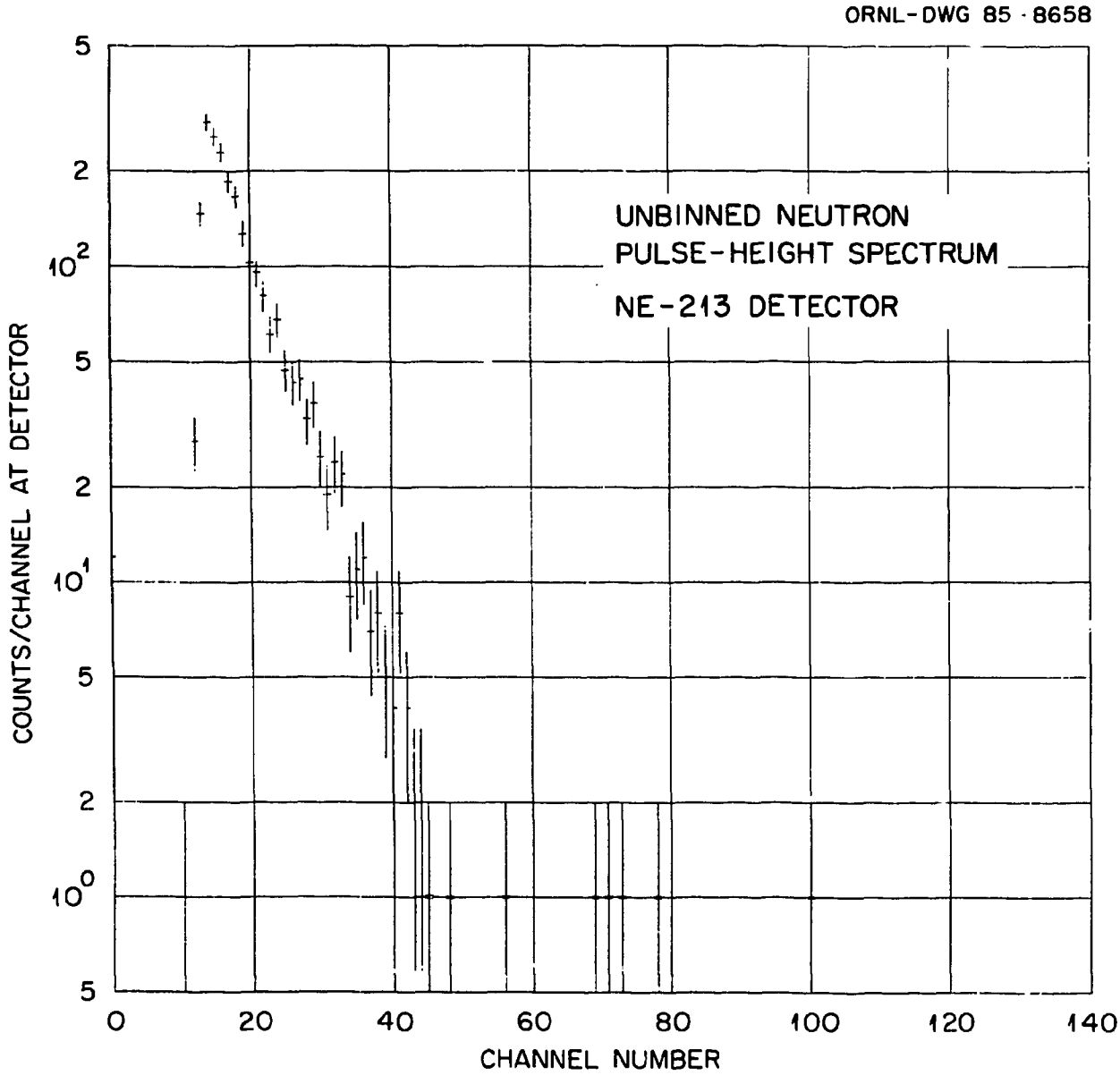

Fig. 10. Measured raw data at the TFTR TCB for neutron detection by the Medium detector. The data shown were obtained by summing spectra for 15 individual plasma shots.

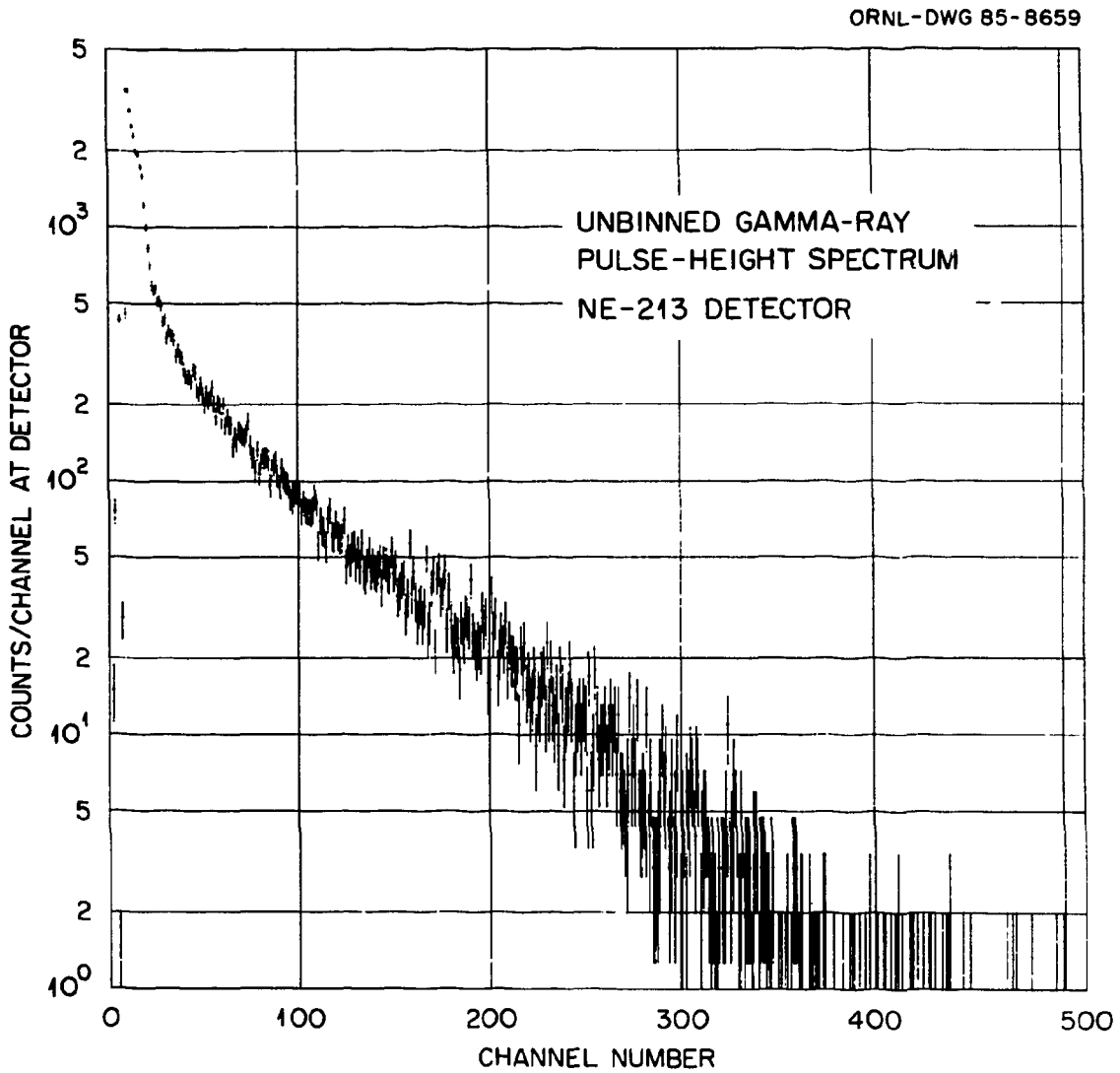

Fig. 11. Measured raw data for gamma-ray detection concurrent with the neutron measurement shown in Fig. 10.

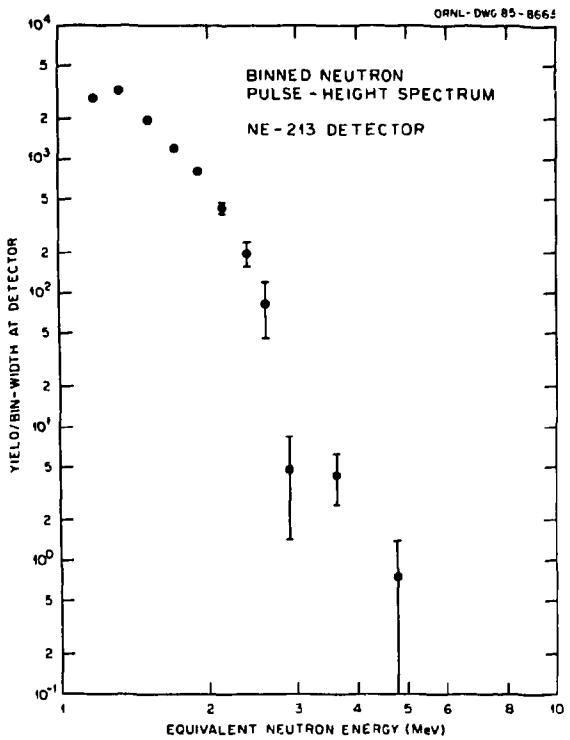

Fig. 12. Data of Fig. 10 binned prior to unfolding. There are, clearly, data for $E_n > 2.5$ MeV, the largest energy expected from just the D + D reactions in the plasma during the shot.

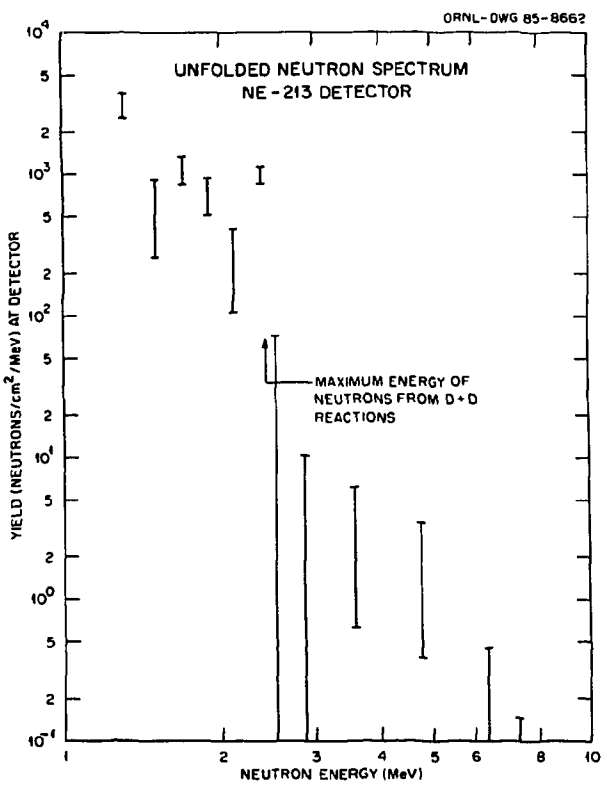

Fig. 13. Unfolded neutron spectrum for the data of Fig. 10. These results indicate the neutron fluence recorded by the NE-213 detector following moderation by the soft-iron magnetic shield.

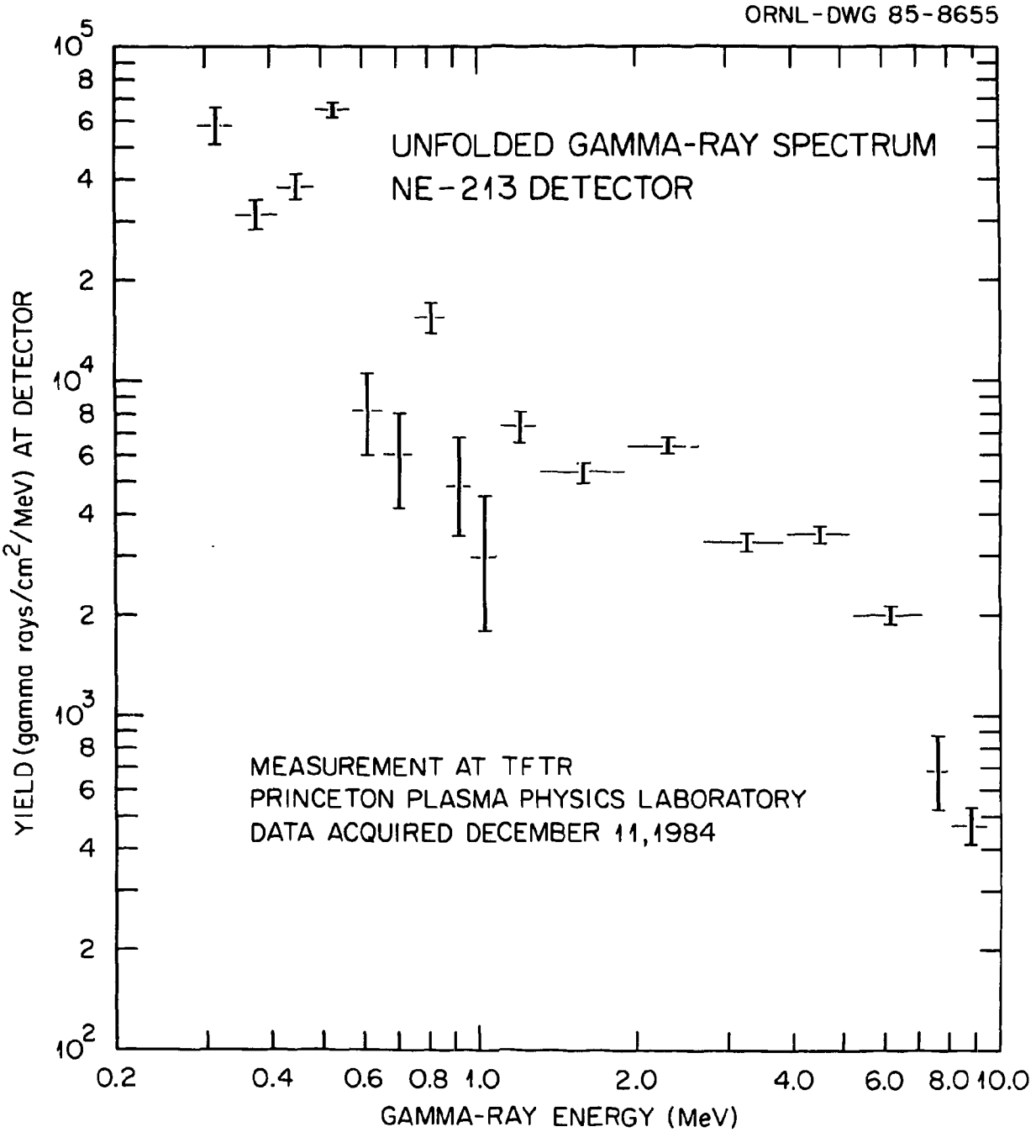

Fig. 14. Unfolded gamma-ray spectrum for the data of Fig. 11, following moderation by the soft-iron magnetic shield.

2. Place the ^{22}Na source on the iron magnetic shield. Then for the PSD electronics of Fig. 3, use the oscilloscope to be sure appropriate pulses are being transmitted over the long RG-59/U cables.

3. A decision must be made on the approximate incident-neutron energy span to be measured. The dynamic range of the system is ~ 15:1, so if measurements of 14-MeV neutrons are desired, the low-energy electronic cutoff will be ~1 MeV. On the other hand, the system should be capable of adequate PSD for E_n as small as 0.75 MeV, but a setting to measure these neutrons will limit the maximum E_n to about 6 MeV.

4. The overall gain setting is determined by observing the pulse-height spectrum of the ^{22}Na source in the PHA (the output at point *G* of Fig. 3). One estimates the "position" of the Compton distribution as the channel corresponding to the channel containing counts approximately equal to 50% of the average counts/channel over the approximately flat region of the Compton distribution as discussed on pages 9-11. The calibration thus consists of two such channels for display of a ^{22}Na source: one for E_γ = 511 keV and the other for E_γ = 1274 keV. An example is shown in Fig. 15. From Table 3, these two gamma rays are equivalent to pulse-height light units of 0.288 and 0.893, respectively. Linear extrapolation will yield the light-unit value corresponding to the maximum channel of the spectrum. Then by interpolating among values in Table 4 one may estimate the range of equivalent neutron energies spanned by the given gain setting. The desired gain is set by adjusting both the HV and the gain (amplification) of the Canberra Model No. 1411 amplifier. Generally, one wants the coarse gain switch on this unit at a small value and the fine gain potentiometer about mid range. The HV may be increased somewhat to adjust the final gain setting, but should not be increased beyond −2100 V.

5. Then the gain setting of the ORNL Q-5695 amplifier is approximately matched to that of the Canberra amplifier using the screwdriver adjustment on the front panel of the ORNL unit. It is better to have the gain on the ORNL unit less than (rather than greater than) that of the Canberra unit because of the ULD on the ORNL Q-5686 discriminator unit.

6. The next step is to make sure that the LLD on the Q-5686 crossover discriminator unit is set to be the defining LLD. The LLD of the CFD (of Fig. 2) should *not* be the defining LLD. One may observe the effect of varying the Q-5686 LLD on data accumulation for the ^{22}Na source.

7. The next step is to obtain a PHA spectrum similar to that exhibited in Fig. 4. A mixed neutron-gamma source is placed near the detector. The various pulses exhibited in Fig. 5 are displayed on the oscilloscope. The timing of these pulses with respect to each other may be observed by triggering the oscilloscope with the output of the EG&G T-105 discriminator unit (note that unused outputs on this unit are terminated in 50Ω). Coarse delay adjustments may be made using the ORNL Q-3073 delay unit, but fine tuning can be accomplished only by changing cable lengths of the "Start" and "Stop" signals on the TAC-and-SCA unit.

8. Finally, the LLD and ULD on the TAC-and-SCA unit are adjusted as indicated on Fig. 4.

We comment on several of the other available settings on the other electronic units. The LLD on the CFD of Fig. 2 is likely set as low as it will go. Pulses emanating from the output of this unit should go away when the source is removed from the detector.

The adjustment labelled "Walk" on the Q-5686 discriminator unit affects the details of the peak shapes of the PHA output of the TAC-and-SCA unit illustrated in Fig. 4. Generally an adjustment needs to be made only to improve an unsatisfactory peak-to-valley counts ratio, where the valley is the region between the two peaks of Fig. 4 corresponding to the ULD setting. Note that for the Q-5686 discriminator unit, also, unused connectors require termination of 50Ω on both front and rear panels.

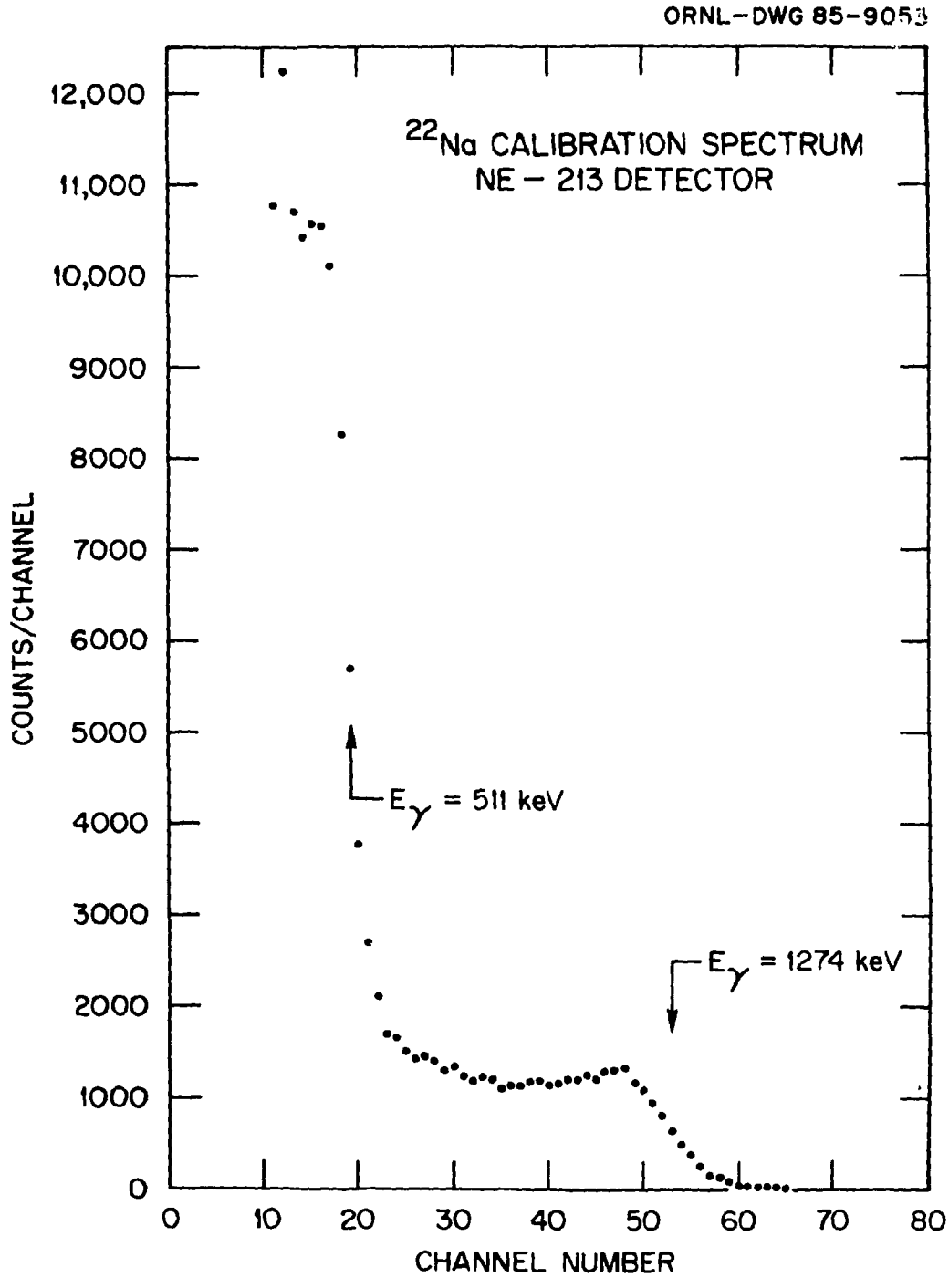

Fig. 15. Example of channel-to-pulse-height calibration using a ^{22}Na source. The chosen "channels" for the 511-keV and 1274-keV gamma rays emanating from the source are indicated in the figure.

Table 3. Light-unit equivalences

Gamma-ray source	Gamma-ray energy (keV)	Light unit	Equiv. neutron[a] energy (MeV)
^{241}Am	59.6	0.0095	0.14
^{57}Co	122.0[b]	0.0322	0.37
^{57}Co	136.4[b]	0.040	0.42
^{203}Hg	279	0.123	0.86
^{113}Sn	393	0.200	1.15
^{22}Na	511	0.288	1.45
^{137}Cs	662	0.400	1.8
^{54}Mn	834	0.537	2.2
^{88}Y	898	0.588	2.4
^{65}Zn	1115	0.764	2.8
^{60}Co	1173[c]	0.811	2.9
^{22}Na	1274	0.893	3.1
^{60}Co	1332[c]	0.942	3.2
^{24}Na	1368	0.97	3.3
^{40}K	1460	1.05	3.4
^{88}Y	1836	1.36	4.1
^{228}Th[d]	2614	2.00	5.4
^{24}Na	2754	2.12	5.6
$^{12}Na^{e}_{ex}$	4433	3.53	8.0
$^{16}O^{f}_{ex}$	6129	4.95	10.5

[a]Approximate.

[b]Usually unresolved. The 122-keV gamma ray has an 80% branching ratio, whereas the 136-keV gamma ray has an 11% branching ratio, so the lower-energy gamma ray may be used with some care.

[c]Often unresolved and taken as a single "peak" very equivalent to the 1274-keV gamma ray of ^{22}Na.

[d]Known as ThC".

[e]From a Pu-Be, a Po-Be, or an Am-Be neutron source.

[f]From ^{16}N decay, $^{16}O(n,n'\gamma)$, or a ^{244}Cm-^{13}C source.

Table 4. Light units as a function of neutron energy in MeV (after Verbinski et al., ref. 5)

Neutron energy	Light unit	Neutron energy	Light unit
0.10	0.00671[a]	2.4	0.625
0.13	0.00886	3.0	0.866
0.17	0.01207	3.4	1.042
0.20	0.01465	4.0	1.327
0.24	0.01838	4.8	1.718
0.30	0.0246	6.0	2.31
0.34	0.0290	7.2	2.95
0.40	0.0365	8.4	3.62
0.48	0.0483	10.0	4.55
0.60	0.0678	13.0	6.36
0.72	0.0910	17.0	8.83
0.84	0.1175	20.0	10.8
1.0	0.1562	24.0	13.5
1.3	0.2385	30.0	17.7
1.7	0.3660	34.0	20.5
2.0	0.4725	40.0	24.8

[a]Estimated errors are 2% for $0.2 \leqslant E_n \leqslant 20$ MeV and 5% otherwise.

5. COMPUTATIONAL PROCEDURES

As mentioned in the text, the data-taking code runs automatically. The accumulated pulse-height data are transferred via floppy disk to another PDP-11/23 machine for unfolding the spectrum. About 180 sets of data can be transferred via one floppy disk. After data are restored onto the analysis PDP 11/23 computer, one may RUN NESCN to obtain a quick summary of the data contents. This program (NESCN) generates a one-line summary for each set of data.

The first step in the data reduction is to RUN NESUM to prepare data for the unfolding routine. Follow the prompts (on the CRT) generated by this program to complete this portion of the task.

Then one may RUN UNFOLD for the final part of the data reduction. The first prompts request information on the source of the raw data to unfold. These are followed by two prompts to enter calibration information. Following each prompt, one enters in (a) a channel value, and (b) a light-unit value. After the second calibration prompt the computer goes to work, providing the desired information in about a minute as presently set up. More detailed output is recorded in a file labelled FOR001.DAT, which should be printed out. Note that the final results are output as Yield/cm^2 at the detector for each bin and are not a true *spectrum* in the usual sense. One may obtain a spectral distribution by dividing the Yield/cm^2 by the bin width as done for the results posted in Figs. 9, 13, and 14. Details of the computer programming for the unfolding analysis are given in Appendix C.

6. CONCLUDING REMARKS

We cannot too strongly stress the need for a regular schedule of checking electronic settings using the procedures discussed in Sect. 4. Although these electronic units are stable over a period of several days, they are operating in essentially state-of-the-art conditions. One should, therefore, regularly check the gain using a gamma-ray source. One should also check the PSD circuit using a mixed neutron-gamma source.

Very careful work requires careful calibration, and for these demands, calibrations using several sources should be done. In particular, if one wishes to extend E_n to 14 MeV, one needs a calibration using a high-energy gamma-ray source to reduce extrapolation errors. We provide a list of useful sources in Table 3.

Calibration of *both* LeCroy 3512 ADC units connected to each detector should be done, since these units do not necessarily have the same gains nor zero settings. This calibration can be carried out by removing the coincidence gate requirements on both ADC units and running the program NETST. (One must be certain to reset the coincidence gates following the calibration.)

ACKNOWLEDGMENTS

We express our appreciation to H. Conrads of PPPL and R. G. Alsmiller, Jr. of ORNL for providing the impetus to initiate this task and the patience to see it through, to C. E. Clifford of PPPL for careful attention to a myriad of administrative details and consultation on technical problems, to L. P. Ku of PPPL and his staff for providing information on experimental results most helpful to guide transport calculations, to J. Gulizio of PPPL for expeditious supervision of hardware installation in the TCB, to H. Hendel of PPPL and A. C. England of ORNL on temporary assignment to PPPL for providing information on the plasma-created neutron source term deduced from their experiments, to K. M. Chase of PPPL for technical assistance with the detector and electronic hardware, to N. M. Larson of ORNL for expert assistance on adapting the unfolding code to the specific problem, to D. E. Pierce of ORNL for design and fabrication of the Faraday shield, and to R. T. Santoro and J. M. Barnes of ORNL for calculations discussed in Appendix B. Projects such as this one cannot hope to succeed without the willing cooperation of capable people, and we are very pleased to acknowledge and to thank these individuals who contributed materially to the success of our project.

REFERENCES

1. N. M. Larson, *User's Guide for BAYES: A General-Purpose Computer Code for Fitting a Functional Form to Experimental Data,* ORNL/TM-8185 (August 1982).

2. R. E. Textor and V. V. Verbinski, *O5S: A Monte Carlo Code for Calculating Pulse Height Distributions Due to Monoenergetic Neutrons Incident on Organic Scintillators,* ORNL-4160 (1968); the particular version of this code is that described by M. A. Cleemput, *O5S - A Version Suitable for Use on the DEC System-10,* ORNL/CF-82/268/R1 (Nov. 15, 1982).

APPENDIX A. DETECTOR RESPONSES TO NEUTRONS AND PHOTONS

As mentioned in Sect. 3, to understand the raw spectral data one must know the detector responses. We used a combination of measurements and Monte Carlo calculations to deduce the neutron responses of each of the three detectors and a combination of measurements, interpolations, and extrapolations to deduce the photon responses of each detector. Responses for the large (of Table 1) and medium detectors are part of the unfolding code (see Appendix C) since these are the two detectors chosen for the first data accumulation. In the following tables we give the responses for all three detectors for both neutrons and gamma rays. If subsequent use is made of the small detector, it will not be difficult to incorporate its two responses to the current version of the unfolding software.

The data in the following six tables are ordered in the following manner: at the head of each column is an index number (1 through 18) corresponding to the incident particle energy bin, where these energies (neutron or gamma ray) are given in Table 2; the columnar data give the normalized yield per incident particle for each of the 19 pulse-height bins. Strictly speaking, these responses are valid only for the measurement geometry, namely radiation normally incident on the front face of the detector. However, experience[3] with detectors of the roughly "cubical" shapes of the large and small detectors indicates that the responses are quite insensitive to direction of incidence made by the impinging radiation. We tested this assumption for the large detector by taking measurements in two different geometries; the resulting response measurements appeared to be identical to within experimental uncertainties. We have made this assumption of directional independence for the small detector and also for the medium detector (although it is likely a less valid assumption), since any more detailed response analysis would substantially complicate the unfolding calculation, and it is not evident to us that the concomitant very moderate improvement in unfolded fluence is warranted in light of present-day transport-calculation capabilities. We also remind the reader that these responses do not include effects of the 1-cm-thick soft-iron shield of Fig. 1, although the (anticipated very small) perturbations due to the aluminum cell, photomultiplier tube, and μ-metal shielding are included.

Table A.I. Large detector neutron response

N-BIN =	1	2	3	4	5	6
1	7.589E-02	1.155E-01	1.103E-01	8.450E-02	5.946E-02	4.625E-02
2	1.481E-02	4.831E-02	7.258E-02	7.420E-02	5.700E-02	4.385E-02
3	2.060E-03	1.703E-02	5.359E-02	8.606E-02	8.384E-02	7.147E-02
4	0.000E-01	1.000E-03	1.174E-02	4.206E-02	6.506E-02	7.055E-02
5	0.000E-01	0.000E-01	9.810E-04	9.768E-03	3.329E-02	5.238E-02
6	0.000E-01	0.000E-01	4.920E-05	1.119E-03	9.653E-03	2.824E-02
7	0.000E-01	0.000E-01	0.000E-01	4.736E-05	1.349E-03	8.673E-03
8	0.000E-01	0.000E-01	0.000E-01	0.000E-01	1.059E-04	1.474E-03
9	0.000E-01	0.000E-01	0.000E-01	0.000E-01	0.000E-01	4.479E-05
10	0.000E-01	0.000E-01	0.000E-01	0.000E-01	0.000E-01	0.000E-01
11	0.000E-01	0.000E-01	0.000E-01	0.000E-01	0.000E-01	0.000E-01
12	0.000E-01	0.000E-01	0.000E-01	0.000E-01	0.000E-01	0.000E-01
13	0.000E-01	0.000E-01	0.000E-01	0.000E-01	0.000E-01	0.000E-01
14	0.000E-01	0.000E-01	0.000E-01	0.000E-01	0.000E-01	0.000E-01
15	0.000E-01	0.000E-01	0.000E-01	0.000E-01	0.000E-01	0.000E-01
16	0.000E-01	0.000E-01	0.000E-01	0.000E-01	0.000E-01	0.000E-01
17	0.000E-01	0.000E-01	0.000E-01	0.000E-01	0.000E-01	0.000E-01
18	0.000E-01	0.000E-01	0.000E-01	0.000E-01	0.000E-01	0.000E-01
19	0.000E-01	0.000E-01	0.000E-01	0.000E-01	0.000E-01	0.000E-01

N-BIN =	7	8	9	10	11	12
1	3.761E-02	2.903E-02	2.696E-02	2.273E-02	1.860E-02	1.350E-02
2	3.383E-02	2.635E-02	2.336E-02	1.977E-02	1.598E-02	1.146E-02
3	5.520E-02	4.310E-02	3.565E-02	3.050E-02	2.422E-02	1.722E-02
4	6.194E-02	4.985E-02	3.982E-02	3.250E-02	2.622E-02	1.820E-02
5	5.776E-02	5.307E-02	4.374E-02	3.477E-02	2.724E-02	1.820E-02
6	4.553E-02	5.141E-02	4.623E-02	3.838E-02	2.916E-02	1.947E-02
7	2.603E-02	4.090E-02	4.280E-02	4.000E-02	3.251E-02	2.115E-02
8	9.540E-03	2.723E-02	4.004E-02	4.456E-02	4.054E-02	2.717E-02
9	1.094E-03	7.187E-03	1.888E-02	2.833E-02	3.280E-02	2.480E-02
10	1.034E-04	1.605E-03	7.957E-03	1.957E-02	3.082E-02	2.842E-02
11	0.000E-01	1.433E-04	1.484E-03	1.120E-02	2.683E-02	4.205E-02
12	0.000E-01	0.000E-01	0.000E-01	7.000E-04	5.523E-03	4.966E-02
13	0.000E-01	0.000E-01	0.000E-01	0.000E-01	0.000E-01	2.083E-03
14	0.000E-01	0.000E-01	0.000E-01	0.000E-01	0.000E-01	0.000E-01
15	0.000E-01	0.000E-01	0.000E-01	0.000E-01	0.000E-01	0.000E-01
16	0.000E-01	0.000E-01	0.000E-01	0.000E-01	0.000E-01	0.000E-01
17	0.000E-01	0.000E-01	0.000E-01	0.000E-01	0.000E-01	0.000E-01
18	0.000E-01	0.000E-01	0.000E-01	0.000E-01	0.000E-01	0.000E-01
19	0.000E-01	0.000E-01	0.000E-01	0.000E-01	0.000E-01	0.000E-01

N-BIN =	13	14	15	16	17	18
1	8.602E-03	7.300E-03	9.260E-03	9.421E-03	9.302E-03	8.313E-03
2	7.357E-03	5.847E-03	4.847E-03	6.660E-03	8.264E-03	6.508E-03
3	1.076E-02	8.141E-03	5.152E-03	7.782E-03	1.022E-02	9.624E-03
4	1.119E-02	7.917E-03	5.037E-03	6.212E-03	7.688E-03	9.732E-03
5	1.130E-02	7.642E-03	5.110E-03	5.009E-03	5.985E-03	8.041E-03
6	1.172E-02	7.437E-03	5.176E-03	4.278E-03	5.381E-03	6.374E-03
7	1.214E-02	7.343E-03	5.184E-03	3.743E-03	5.010E-03	5.373E-03
8	1.535E-02	9.009E-03	6.313E-03	4.200E-03	4.990E-03	5.785E-03
9	1.319E-02	7.492E-03	5.189E-03	3.475E-03	3.134E-03	4.219E-03
10	1.631E-02	9.110E-03	6.104E-03	4.187E-03	3.164E-03	4.415E-03
11	2.802E-02	1.515E-02	9.797E-03	6.751E-03	4.911E-03	5.836E-03
12	7.569E-02	4.417E-02	2.667E-02	1.807E-02	1.318E-02	1.283E-02
13	3.827E-02	5.237E-02	3.180E-02	2.077E-02	1.512E-02	1.207E-02
14	1.871E-03	3.471E-02	5.003E-02	3.089E-02	2.276E-02	1.761E-02
15	0.000E-01	1.218E-03	2.256E-02	3.122E-02	2.241E-02	1.737E-02
16	0.000E-01	0.000E-01	2.500E-03	2.002E-02	3.135E-02	2.656E-02
17	0.000E-01	0.000E-01	6.000E-05	2.000E-03	6.203E-03	9.765E-03
18	0.000E-01	0.000E-01	0.000E-01	9.000E-05	3.000E-03	1.020E-02
19	0.000E-01	0.000E-01	0.000E-01	0.000E-01	3.600E-05	2.400E-03

Table A.2. Large detector photon response

G-BIN =	1	2	3	4	5	6
1	6.565E-02	8.203E-02	5.642E-02	4.115E-02	3.243E-02	2.555E-02
2	1.135E-02	3.750E-02	5.631E-02	3.734E-02	2.836E-02	2.169E-02
3	0.000E-01	1.777E-02	4.644E-02	6.587E-02	4.452E-02	3.191E-02
4	0.000E-01	0.000E-01	6.600E-03	3.757E-02	5.741E-02	3.715E-02
5	0.000E-01	0.000E-01	0.000E-01	8.970E-03	3.031E-02	4.770E-02
6	0.000E-01	0.000E-01	0.000E-01	9.000E-04	1.035E-02	2.620E-02
7	0.000E-01	0.000E-01	0.000E-01	0.000E-01	1.710E-03	7.710E-03
8	0.000E-01	0.000E-01	0.000E-01	0.000E-01	0.000E-01	2.320E-03
9	0.000E-01	0.000E-01	0.000E-01	0.000E-01	0.000E-01	3.000E-05
10	0.000E-01	0.000E-01	0.000E-01	0.000E-01	0.000E-01	0.000E-01
11	0.000E-01	0.000E-01	0.000E-01	0.000E-01	0.000E-01	0.000E-01
12	0.000E-01	0.000E-01	0.000E-01	0.000E-01	0.000E-01	0.000E-01
13	0.000E-01	0.000E-01	0.000E-01	0.000E-01	0.000E-01	0.000E-01
14	0.000E-01	0.000E-01	0.000E-01	0.000E-01	0.000E-01	0.000E-01
15	0.000E-01	0.000E-01	0.000E-01	0.000E-01	0.000E-01	0.000E-01
16	0.000E-01	0.000E-01	0.000E-01	0.000E-01	0.000E-01	0.000E-01
17	0.000E-01	0.000E-01	0.000E-01	0.000E-01	0.000E-01	0.000E-01
18	0.000E-01	0.000E-01	0.000E-01	0.000E-01	0.000E-01	0.000E-01
19	0.000E-01	0.000E-01	0.000E-01	0.000E-01	0.000E-01	0.000E-01

G-BIN =	7	8	9	10	11	12
1	2.144E-02	1.781E-02	1.471E-02	1.308E-02	1.047E-02	7.820E-03
2	1.892E-02	1.553E-02	1.264E-02	1.110E-02	9.043E-03	6.667E-03
3	2.840E-02	2.338E-02	1.918E-02	1.642E-02	1.383E-02	9.965E-03
4	2.906E-02	2.363E-02	2.000E-02	1.763E-02	1.440E-02	1.009E-02
5	3.606E-02	2.447E-02	2.051E-02	1.761E-02	1.442E-02	9.864E-03
6	4.248E-02	3.161E-02	2.281E-02	1.898E-02	1.509E-02	1.013E-02
7	2.330E-02	3.641E-02	2.620E-02	2.093E-02	1.613E-02	1.008E-02
8	8.320E-03	2.338E-02	4.082E-02	2.949E-02	2.083E-02	1.201E-02
9	1.990E-03	6.470E-03	1.765E-02	2.961E-02	1.924E-02	1.028E-02
10	5.400E-04	2.550E-03	9.170E-03	1.804E-02	2.832E-02	1.349E-02
11	0.000E-01	6.840E-04	2.130E-03	1.018E-02	2.467E-02	2.554E-02
12	0.000E-01	0.000E-01	0.000E-01	7.000E-05	7.130E-03	4.458E-02
13	0.000E-01	0.000E-01	0.000E-01	0.000E-01	0.000E-01	1.892E-03
14	0.000E-01	0.000E-01	0.000E-01	0.000E-01	0.000E-01	0.000E-01
15	0.000E-01	0.000E-01	0.000E-01	0.000E-01	0.000E-01	0.000E-01
16	0.000E-01	0.000E-01	0.000E-01	0.000E-01	0.000E-01	0.000E-01
17	0.000E-01	0.000E-01	0.000E-01	0.000E-01	0.000E-01	0.000E-01
18	0.000E-01	0.000E-01	0.000E-01	0.000E-01	0.000E-01	0.000E-01
19	0.000E-01	0.000E-01	0.000E-01	0.000E-01	0.000E-01	0.000E-01

G-BIN =	13	14	15	16	17	18
1	4.851E-03	2.873E-03	1.764E-03	1.163E-03	6.284E-04	6.953E-04
2	4.089E-03	2.510E-03	1.567E-03	1.029E-03	5.459E-04	6.238E-04
3	6.296E-03	3.877E-03	2.424E-03	1.585E-03	8.341E-04	9.804E-04
4	6.592E-03	4.016E-03	2.627E-03	1.705E-03	1.261E-03	1.081E-03
5	6.474E-03	4.107E-03	2.636E-03	1.754E-03	1.303E-03	1.114E-03
6	6.675E-03	4.268E-03	2.798E-03	1.855E-03	1.392E-03	1.188E-03
7	6.909E-03	4.356E-03	2.872E-03	1.923E-03	1.446E-03	1.239E-03
8	8.214E-03	5.201E-03	3.570E-03	2.354E-03	1.780E-03	1.522E-03
9	6.619E-03	4.305E-03	2.881E-03	1.965E-03	1.488E-03	1.260E-03
10	7.605E-03	4.939E-03	3.353E-03	2.295E-03	1.742E-03	1.502E-03
11	1.244E-02	8.075E-03	5.501E-03	3.773E-03	2.927E-03	2.527E-03
12	4.089E-02	2.117E-02	1.463E-02	9.712E-03	7.962E-03	6.849E-03
13	3.118E-02	2.870E-02	1.533E-02	1.068E-02	8.431E-03	7.355E-03
14	1.310E-03	2.803E-02	2.909E-02	1.524E-02	1.153E-02	1.025E-02
15	0.000E-01	1.578E-03	1.805E-02	1.966E-02	1.209E-02	9.896E-03
16	0.000E-01	0.000E-01	1.901E-03	1.694E-02	2.328E-02	1.674E-02
17	0.000E-01	0.000E-01	0.000E-01	1.625E-03	5.163E-03	8.411E-03
18	0.000E-01	0.000E-01	0.000E-01	5.360E-04	3.463E-03	7.370E-03
19	0.000E-01	0.000E-01	0.000E-01	0.000E-01	6.770E-04	2.094E-03

Table A.3. Medium detector neutron response

N-BIN =	1	2	3	4	5	6
1	4.561E-02	6.487E-02	6.093E-02	4.650E-02	3.355E-02	2.653E-02
2	9.574E-03	2.823E-02	4.171E-02	4.000E-02	3.007E-02	2.420E-02
3	9.000E-04	1.218E-02	3.179E-02	4.784E-02	4.498E-02	3.841E-02
4	0.000E-01	4.670E-03	7.000E-03	2.508E-02	3.689E-02	3.858E-02
5	0.000E-01	0.000E-01	3.548E-04	6.300E-03	1.991E-02	3.032E-02
6	0.000E-01	0.000E-01	0.000E-01	3.670E-04	5.875E-03	1.738E-02
7	0.000E-01	0.000E-01	0.000E-01	0.000E-01	4.330E-04	5.565E-03
8	0.000E-01	0.000E-01	0.000E-01	0.000E-01	0.000E-01	5.220E-04
9	0.000E-01	0.000E-01	0.000E-01	0.000E-01	0.000E-01	0.000E-01
10	0.000E-01	0.000E-01	0.000E-01	0.000E-01	0.000E-01	0.000E-01
11	0.000E-01	0.000E-01	0.000E-01	0.000E-01	0.000E-01	0.000E-01
12	0.000E-01	0.000E-01	0.000E-01	0.000E-01	0.000E-01	0.000E-01
13	0.000E-01	0.000E-01	0.000E-01	0.000E-01	0.000E-01	0.000E-01
14	0.000E-01	0.000E-01	0.000E-01	0.000E-01	0.000E-01	0.000E-01
15	0.000E-01	0.000E-01	0.000E-01	0.000E-01	0.000E-01	0.000E-01
16	0.000E-01	0.000E-01	0.000E-01	0.000E-01	0.000E-01	0.000E-01
17	0.000E-01	0.000E-01	0.000E-01	0.000E-01	0.000E-01	0.000E-01
18	0.000E-01	0.000E-01	0.000E-01	0.000E-01	0.000E-01	0.000E-01
19	0.000E-01	0.000E-01	0.000E-01	0.000E-01	0.000E-01	0.000E-01

N-BIN =	7	8	9	10	11	12
1	2.126E-02	1.801E-02	1.518E-02	1.354E-02	1.097E-02	7.866E-03
2	1.862E-02	1.555E-02	1.285E-02	1.155E-02	9.248E-03	6.602E-03
3	2.972E-02	2.399E-02	1.964E-02	1.716E-02	1.353E-02	9.726E-03
4	3.320E-02	2.644E-02	2.175E-02	1.800E-02	1.380E-02	1.018E-02
5	3.132E-02	2.730E-02	2.319E-02	1.849E-02	1.400E-02	1.020E-02
6	2.563E-02	2.659E-02	2.436E-02	2.064E-02	1.550E-02	1.053E-02
7	1.441E-02	2.191E-02	2.307E-02	2.139E-02	1.701E-02	1.102E-02
8	5.322E-03	1.604E-02	2.202E-02	2.408E-02	2.123E-02	1.408E-02
9	2.520E-04	4.279E-03	1.055E-02	1.568E-02	1.657E-02	1.214E-02
10	0.000E-01	4.400E-04	4.618E-03	1.107E-02	1.773E-02	1.468E-02
11	0.000E-01	0.000E-01	4.745E-04	5.000E-03	1.650E-02	2.429E-02
12	0.000E-01	0.000E-01	0.000E-01	1.000E-04	1.500E-03	2.779E-02
13	0.000E-01	0.000E-01	0.000E-01	0.000E-01	3.000E-05	5.600E-04
14	0.000E-01	0.000E-01	0.000E-01	0.000E-01	0.000E-01	0.000E-01
15	0.000E-01	0.000E-01	0.000E-01	0.000E-01	0.000E-01	0.000E-01
16	0.000E-01	0.000E-01	0.000E-01	0.000E-01	0.000E-01	0.000E-01
17	0.000E-01	0.000E-01	0.000E-01	0.000E-01	0.000E-01	0.000E-01
18	0.000E-01	0.000E-01	0.000E-01	0.000E-01	0.000E-01	0.000E-01
19	0.000E-01	0.000E-01	0.000E-01	0.000E-01	0.000E-01	0.000E-01

N-BIN =	13	14	15	16	17	18
1	4.782E-03	3.670E-03	5.031E-03	4.792E-03	4.888E-03	4.521E-03
2	4.040E-03	2.939E-03	2.492E-03	3.334E-03	4.328E-03	3.500E-03
3	5.953E-03	4.172E-03	2.718E-03	3.959E-03	5.170E-03	5.044E-03
4	6.204E-03	4.132E-03	2.634E-03	3.240E-03	3.896E-03	5.054E-03
5	6.223E-03	3.951E-03	2.677E-03	2.596E-03	3.075E-03	4.063E-03
6	6.437E-03	3.993E-03	2.781E-03	2.220E-03	2.778E-03	3.281E-03
7	6.600E-03	4.059E-03	2.803E-03	1.903E-03	2.521E-03	2.756E-03
8	8.139E-03	4.943E-03	3.408E-03	2.186E-03	2.496E-03	2.994E-03
9	6.897E-03	4.097E-03	2.809E-03	1.851E-03	1.646E-03	2.239E-03
10	8.416E-03	4.901E-03	3.289E-03	2.139E-03	1.651E-03	2.291E-03
11	1.418E-02	8.230E-03	5.162E-03	3.475E-03	2.458E-03	2.963E-03
12	3.950E-02	2.314E-02	1.368E-02	9.373E-03	6.882E-03	6.403E-03
13	2.222E-02	2.705E-02	1.651E-02	1.057E-02	8.048E-03	5.704E-03
14	6.000E-04	1.964E-02	2.553E-02	1.582E-02	1.186E-02	9.000E-03
15	0.000E-01	3.400E-04	1.189E-02	1.620E-02	1.147E-02	9.093E-03
16	0.000E-01	0.000E-01	2.820E-03	1.109E-02	1.607E-02	1.310E-02
17	0.000E-01	0.000E-01	0.000E-01	1.860E-04	3.418E-03	5.140E-03
18	0.000E-01	0.000E-01	0.000E-01	0.000E-01	5.330E-04	6.410E-03
19	0.000E-01	0.000E-01	0.000E-01	0.000E-01	0.000E-01	2.300E-04

Table A.4. Medium detector photon response

G-BIN =	1	2	3	4	5	6
1	3.967E-02	4.644E-02	2.963E-02	2.273E-02	1.843E-02	1.438E-02
2	1.934E-03	2.295E-02	3.099E-02	1.972E-02	1.537E-02	1.197E-02
3	0.000E-01	4.115E-03	2.617E-02	3.623E-02	2.376E-02	1.814E-02
4	0.000E-01	0.000E-01	1.097E-03	2.145E-02	3.082E-02	1.922E-02
5	0.000E-01	0.000E-01	0.000E-01	1.261E-03	1.736E-02	2.459E-02
6	0.000E-01	0.000E-01	0.000E-01	0.000E-01	2.170E-03	1.412E-02
7	0.000E-01	0.000E-01	0.000E-01	0.000E-01	0.000E-01	2.005E-03
8	0.000E-01	0.000E-01	0.000E-01	0.000E-01	0.000E-01	2.240E-04
9	0.000E-01	0.000E-01	0.000E-01	0.000E-01	0.000E-01	0.000E-01
10	0.000E-01	0.000E-01	0.000E-01	0.000E-01	0.000E-01	0.000E-01
11	0.000E-01	0.000E-01	0.000E-01	0.000E-01	0.000E-01	0.000E-01
12	0.000E-01	0.000E-01	0.000E-01	0.000E-01	0.000E-01	0.000E-01
13	0.000E-01	0.000E-01	0.000E-01	0.000E-01	0.000E-01	0.000E-01
14	0.000E-01	0.000E-01	0.000E-01	0.000E-01	0.000E-01	0.000E-01
15	0.000E-01	0.000E-01	0.000E-01	0.000E-01	0.000E-01	0.000E-01
16	0.000E-01	0.000E-01	0.000E-01	0.000E-01	0.000E-01	0.000E-01
17	0.000E-01	0.000E-01	0.000E-01	0.000E-01	0.000E-01	0.000E-01
18	0.000E-01	0.000E-01	0.000E-01	0.000E-01	0.000E-01	0.000E-01
19	0.000E-01	0.000E-01	0.000E-01	0.000E-01	0.000E-01	0.000E-01

G-BIN =	7	8	9	10	11	12
1	1.241E-02	1.000E-02	8.406E-03	7.236E-03	5.701E-03	4.237E-03
2	1.050E-02	8.607E-03	7.306E-03	6.271E-03	5.035E-03	3.561E-03
3	1.585E-02	1.286E-02	1.099E-02	9.536E-03	7.670E-03	5.324E-03
4	1.622E-02	1.322E-02	1.136E-02	9.787E-03	7.980E-03	5.372E-03
5	1.735E-02	1.313E-02	1.117E-02	9.870E-03	8.033E-03	5.218E-03
6	2.199E-02	1.498E-02	1.219E-02	1.024E-02	8.359E-03	5.343E-03
7	1.269E-02	1.865E-02	1.335E-02	1.101E-02	8.542E-03	5.256E-03
8	2.228E-03	1.244E-02	2.092E-02	1.463E-02	1.083E-02	6.371E-03
9	1.930E-04	1.883E-03	9.047E-03	1.510E-02	9.537E-03	5.481E-03
10	0.000E-01	3.090E-04	1.045E-03	9.155E-03	1.405E-02	6.681E-03
11	0.000E-01	0.000E-01	0.000E-01	4.560E-04	1.230E-02	1.170E-02
12	0.000E-01	0.000E-01	0.000E-01	0.000E-01	5.000E-05	2.231E-02
13	0.000E-01	0.000E-01	0.000E-01	0.000E-01	0.000E-01	4.000E-05
14	0.000E-01	0.000E-01	0.000E-01	0.000E-01	0.000E-01	0.000E-01
15	0.000E-01	0.000E-01	0.000E-01	0.000E-01	0.000E-01	0.000E-01
16	0.000E-01	0.000E-01	0.000E-01	0.000E-01	0.000E-01	0.000E-01
17	0.000E-01	0.000E-01	0.000E-01	0.000E-01	0.000E-01	0.000E-01
18	0.000E-01	0.000E-01	0.000E-01	0.000E-01	0.000E-01	0.000E-01
19	0.000E-01	0.000E-01	0.000E-01	0.000E-01	0.000E-01	0.000E-01

G-BIN =	13	14	15	16	17	18
1	2.786E-03	1.633E-03	1.002E-03	6.510E-04	4.908E-04	3.796E-04
2	2.286E-03	1.429E-03	8.884E-04	5.790E-04	4.359E-04	3.404E-04
3	3.435E-03	2.201E-03	1.350E-03	8.949E-04	6.854E-04	5.304E-04
4	3.467E-03	2.253E-03	1.428E-03	9.403E-04	7.275E-04	5.659E-04
5	3.461E-03	2.241E-03	1.446E-03	9.703E-04	7.355E-04	5.796E-04
6	3.487E-03	2.297E-03	1.497E-03	1.018E-03	7.812E-04	6.176E-04
7	3.566E-03	2.359E-03	1.527E-03	1.053E-03	8.164E-04	6.512E-04
8	4.191E-03	2.815E-03	1.848E-03	1.273E-03	9.933E-04	7.980E-04
9	3.396E-03	2.323E-03	1.517E-03	1.044E-03	8.149E-04	6.562E-04
10	3.939E-03	2.602E-03	1.767E-03	1.212E-03	9.524E-04	7.590E-04
11	6.519E-03	4.277E-03	2.861E-03	1.998E-03	1.556E-03	1.258E-03
12	2.042E-02	1.137E-02	7.538E-03	5.354E-03	4.250E-03	3.432E-03
13	1.405E-02	1.402E-02	8.051E-03	5.453E-03	4.418E-03	3.625E-03
14	2.000E-05	1.413E-02	1.299E-02	8.033E-03	6.404E-03	4.894E-03
15	0.000E-01	5.000E-05	8.857E-03	8.761E-03	6.287E-03	4.844E-03
16	0.000E-01	0.000E-01	5.000E-06	7.638E-03	1.038E-02	7.410E-03
17	0.000E-01	0.000E-01	0.000E-01	7.700E-05	2.362E-03	3.475E-03
18	0.000E-01	0.000E-01	0.000E-01	0.000E-01	3.682E-04	3.120E-03
19	0.000E-01	0.000E-01	0.000E-01	0.000E-01	0.000E-01	2.836E-04

Table A.5. Small detector photon response

N-BIN =	1	2	3	4	5	6
1	4.134E-02	6.083E-02	6.677E-02	3.150E-02	2.641E-02	2.143E-02
2	8.068E-03	2.744E-02	3.108E-02	2.650E-02	2.390E-02	1.780E-02
3	5.279E-03	1.773E-02	2.742E-02	4.084E-02	3.713E-02	2.713E-02
4	1.182E-03	3.372E-03	1.113E-02	3.219E-02	3.828E-02	3.093E-02
5	2.330E-04	5.680E-04	2.749E-03	1.733E-02	2.692E-02	2.952E-02
6	0.000E-01	7.800E-05	6.570E-04	6.971E-03	1.416E-02	2.340E-02
7	0.000E-01	0.000E-01	1.570E-04	2.060E-03	5.800E-03	1.303E-02
8	0.000E-01	0.000E-01	4.000E-05	4.960E-04	1.684E-03	6.118E-03
9	0.000E-01	0.000E-01	0.000E-01	8.500E-05	2.730E-04	1.383E-03
10	0.000E-01	0.000E-01	0.000E-01	2.900E-05	9.900E-05	3.870E-04
11	0.000E-01	0.000E-01	0.000E-01	0.000E-01	0.000E-01	1.110E-04
12	0.000E-01	0.000E-01	0.000E-01	0.000E-01	0.000E-01	0.000E-01
13	0.000E-01	0.000E-01	0.000E-01	0.000E-01	0.000E-01	0.000E-01
14	0.000E-01	0.000E-01	0.000E-01	0.000E-01	0.000E-01	0.000E-01
15	0.000E-01	0.000E-01	0.000E-01	0.000E-01	0.000E-01	0.000E-01
16	0.000E-01	0.000E-01	0.000E-01	0.000E-01	0.000E-01	0.000E-01
17	0.000E-01	0.000E-01	0.000E-01	0.000E-01	0.000E-01	0.000E-01
18	0.000E-01	0.000E-01	0.000E-01	0.000E-01	0.000E-01	0.000E-01
19	0.000E-01	0.000E-01	0.000E-01	0.000E-01	0.000E-01	0.000E-01

N-BIN =	7	8	9	10	11	12
1	1.731E-02	1.595E-02	1.027E-02	1.005E-02	8.212E-03	6.674E-03
2	1.444E-02	1.312E-02	8.990E-03	8.552E-03	6.990E-03	5.564E-03
3	2.219E-02	1.930E-02	1.425E-02	1.334E-02	1.114E-02	8.353E-03
4	2.555E-02	2.054E-02	1.657E-02	1.491E-02	1.253E-02	8.952E-03
5	2.737E-02	2.235E-02	1.842E-02	1.596E-02	1.316E-02	9.409E-03
6	2.585E-02	2.352E-02	1.944E-02	1.733E-02	1.416E-02	1.003E-02
7	2.018E-02	2.232E-02	2.046E-02	1.845E-02	1.481E-02	1.052E-02
8	1.250E-02	1.995E-02	2.324E-02	2.235E-02	1.841E-02	1.296E-02
9	4.254E-03	8.870E-03	1.499E-02	1.638E-02	1.510E-02	1.077E-02
10	1.632E-03	5.050E-03	1.013E-02	1.420E-02	1.674E-02	1.251E-02
11	4.450E-04	1.980E-03	6.009E-03	1.117E-02	1.983E-02	1.991E-02
12	3.000E-05	1.420E-04	4.910E-04	1.896E-03	9.823E-03	3.395E-02
13	0.000E-01	0.000E-01	0.000E-01	1.400E-05	1.010E-04	4.635E-03
14	0.000E-01	0.000E-01	0.000E-01	0.000E-01	0.000E-01	0.000E-01
15	0.000E-01	0.000E-01	0.000E-01	0.000E-01	0.000E-01	0.000E-01
16	0.000E-01	0.000E-01	0.000E-01	0.000E-01	0.000E-01	0.000E-01
17	0.000E-01	0.000E-01	0.000E-01	0.000E-01	0.000E-01	0.000E-01
18	0.000E-01	0.000E-01	0.000E-01	0.000E-01	0.000E-01	0.000E-01
19	0.000E-01	0.000E-01	0.000E-01	0.000E-01	0.000E-01	0.000E-01

N-BIN =	13	14	15	16	17	18
1	3.963E-03	2.950E-03	2.873E-03	2.887E-03	4.268E-03	2.693E-03
2	3.429E-03	2.452E-03	2.221E-03	2.240E-03	3.122E-03	2.212E-03
3	5.352E-03	3.713E-03	3.158E-03	3.228E-03	4.270E-03	3.415E-03
4	5.888E-03	3.887E-03	3.021E-03	3.192E-03	3.939E-03	3.816E-03
5	6.132E-03	3.950E-03	2.735E-03	2.855E-03	3.075E-03	3.870E-03
6	6.465E-03	4.138E-03	2.829E-03	2.609E-03	2.762E-03	3.690E-03
7	6.696E-03	4.211E-03	2.896E-03	2.406E-03	2.528E-03	3.229E-03
8	8.165E-03	5.103E-03	3.391E-03	2.590E-03	2.888E-03	3.271E-03
9	6.717E-03	4.107E-03	2.811E-03	1.964E-03	2.016E-03	2.160E-03
10	7.822E-03	4.831E-03	3.229E-03	2.233E-03	2.050E-03	2.278E-03
11	1.297E-02	7.899E-03	5.208E-03	3.533E-03	2.954E-03	2.893E-03
12	3.599E-02	2.142E-02	1.330E-02	9.150E-03	6.965E-03	6.786E-03
13	2.490E-02	2.326E-02	1.406E-02	9.401E-03	7.074E-03	6.017E-03
14	4.407E-03	2.213E-02	2.007E-02	1.329E-02	9.689E-03	8.098E-03
15	0.000E-01	3.675E-03	1.507E-02	1.267E-02	9.482E-03	7.886E-03
16	0.000E-01	6.300E-05	4.182E-03	1.266E-02	1.261E-02	1.065E-02
17	0.000E-01	0.000E-01	1.450E-04	1.880E-03	3.813E-03	4.158E-03
18	0.000E-01	0.000E-01	0.000E-01	3.450E-04	3.512E-03	5.734E-03
19	0.000E-01	0.000E-01	0.000E-01	0.000E-01	9.760E-04	2.052E-03

3. G. L. Morgan, T. A. Love, and F. G. Perey, *Nucl. Instrum. Meth.* **128**, 125 (1975).

4. W. W. Engle, Jr., *ANISN, A One-Dimensional Discrete Ordinate Transport Code,* ORNL/CCC-254 (1967, updated 1973).

5. V. V. Verbinski, W. R. Burrus, T. A. Love, W. Zobel, and N. W. Hill, *Nucl. Instrum. Meth.* **65**, 8 (1969).

GLOSSARY OF ACRONYMS

ADC	Analog-to-Digital Converter
ANISN	Designates a program to calculate effects of neutron and photon transport.
BNC	Designates a specific type of connector.
CAMAC	Computer Automatic Measurement And Control
CFD	Constant-Fraction Discriminator
CICADA	Central Instrumentation Control And Data Acquisition (Computer)
CRT	Cathode Ray Tube (designates the interactive computer terminal)
HV	High Voltage
I/O	Input-Output
LLD	Lower Level Discriminator
NIM	Nuclear Instrument Modules
ORELA	Oak Ridge Electron Linear Accelerator
ORNL	Oak Ridge National Laboratory
PA	Preamplifier
PHA	Pulse Height Analyzer
PPPL	Princeton Plasma Physics Laboratory
PSD	Pulse-Shape Discrimination
SCA	Single-Channel Analyzer
TAC	Time-to-Amplitude Converter
TCB	Test Cell Basement
TFTR	Tokamak Fusion Test Reactor
ULD	Upper Level Discriminator

Table A.6. Small detector photon response

G-BIN =	1	2	3	4	5	6
1	3.484E-02	4.390E-02	3.360E-02	2.400E-02	1.840E-02	1.600E-02
2	6.790E-03	1.930E-02	2.790E-02	2.140E-02	1.640E-02	1.280E-02
3	0.000E-01	9.800E-03	2.260E-02	3.330E-02	2.580E-02	1.830E-02
4	0.000E-01	8.000E-04	3.760E-03	1.760E-03	2.710E-02	1.970E-02
5	0.000E-01	0.000E-01	0.000E-01	4.470E-03	1.420E-02	2.090E-02
6	0.000E-01	0.000E-01	0.000E-01	6.300E-04	4.900E-03	1.190E-02
7	0.000E-01	0.000E-01	0.000E-01	0.000E-01	1.100E-03	4.040E-03
8	0.000E-01	0.000E-01	0.000E-01	0.000E-01	0.000E-01	9.100E-04
9	0.000E-01	0.000E-01	0.000E-01	0.000E-01	0.000E-01	4.300E-05
10	0.000E-01	0.000E-01	0.000E-01	0.000E-01	0.000E-01	0.000E-01
11	0.000E-01	0.000E-01	0.000E-01	0.000E-01	0.000E-01	0.000E-01
12	0.000E-01	0.000E-01	0.000E-01	0.000E-01	0.000E-01	0.000E-01
13	0.000E-01	0.000E-01	0.000E-01	0.000E-01	0.000E-01	0.000E-01
14	0.000E-01	0.000E-01	0.000E-01	0.000E-01	0.000E-01	0.000E-01
15	0.000E-01	0.000E-01	0.000E-01	0.000E-01	0.000E-01	0.000E-01
16	0.000E-01	0.000E-01	0.000E-01	0.000E-01	0.000E-01	0.000E-01
17	0.000E-01	0.000E-01	0.000E-01	0.000E-01	0.000E-01	0.000E-01
18	0.000E-01	0.000E-01	0.000E-01	0.000E-01	0.000E-01	0.000E-01
19	0.000E-01	0.000E-01	0.000E-01	0.000E-01	0.000E-01	0.000E-01

G-BIN =	7	8	9	10	11	12
1	1.420E-02	1.170E-02	8.960E-03	7.450E-03	6.210E-03	4.127E-03
2	1.160E-02	9.590E-03	7.510E-03	6.300E-03	5.250E-03	3.349E-03
3	1.640E-02	1.380E-02	1.130E-02	9.080E-03	7.870E-03	4.904E-03
4	1.620E-02	1.320E-02	1.150E-02	9.690E-03	8.030E-03	4.844E-03
5	1.750E-02	1.320E-02	1.181E-02	9.770E-03	8.030E-03	4.691E-03
6	1.780E-02	1.490E-02	1.290E-02	1.050E-02	8.400E-03	4.921E-03
7	1.050E-02	1.480E-02	1.388E-02	1.129E-02	8.940E-03	5.267E-03
8	4.400E-03	1.030E-02	1.688E-02	1.407E-02	1.134E-02	6.720E-03
9	8.400E-04	3.250E-03	5.070E-03	1.160E-02	9.580E-03	5.810E-03
10	9.000E-05	1.210E-03	4.690E-03	8.420E-03	1.141E-02	7.045E-03
11	0.000E-01	1.900E-04	1.280E-03	4.840E-03	1.154E-02	1.227E-02
12	0.000E-01	0.000E-01	0.000E-01	3.000E-04	1.440E-03	2.104E-02
13	0.000E-01	0.000E-01	0.000E-01	0.000E-01	0.000E-01	1.871E-03
14	0.000E-01	0.000E-01	0.000E-01	0.000E-01	0.000E-01	0.000E-01
15	0.000E-01	0.000E-01	0.000E-01	0.000E-01	0.000E-01	0.000E-01
16	0.000E-01	0.000E-01	0.000E-01	0.000E-01	0.000E-01	0.000E-01
17	0.000E-01	0.000E-01	0.000E-01	0.000E-01	0.000E-01	0.000E-01
18	0.000E-01	0.000E-01	0.000E-01	0.000E-01	0.000E-01	0.000E-01
19	0.000E-01	0.000E-01	0.000E-01	0.000E-01	0.000E-01	0.000E-01

G-BIN =	13	14	15	16	17	18
1	3.038E-03	1.829E-03	1.138E-03	7.177E-04	5.185E-04	4.075E-04
2	2.648E-03	1.592E-03	9.950E-04	6.395E-04	4.624E-04	3.606E-04
3	3.988E-03	2.454E-03	1.543E-03	9.930E-04	7.184E-04	5.651E-04
4	4.175E-03	2.549E-03	1.629E-03	1.066E-03	7.790E-04	6.100E-04
5	4.090E-03	2.558E-03	1.662E-03	1.093E-03	8.044E-04	6.359E-04
6	4.209E-03	2.681E-03	1.727E-03	1.157E-03	8.544E-04	6.794E-04
7	4.277E-03	2.748E-03	1.788E-03	1.204E-03	8.858E-04	7.080E-04
8	5.176E-03	3.278E-03	2.193E-03	1.466E-03	1.096E-03	8.721E-04
9	4.243E-03	2.672E-03	1.793E-03	1.213E-03	9.093E-04	7.316E-04
10	4.939E-03	3.127E-03	2.066E-03	1.424E-03	1.060E-03	8.526E-04
11	8.265E-03	5.126E-03	3.362E-03	2.329E-03	1.769E-03	1.412E-03
12	2.011E-02	1.410E-02	9.199E-03	6.240E-03	4.772E-03	3.873E-03
13	5.736E-03	1.364E-02	9.998E-03	6.730E-03	5.033E-03	4.103E-03
14	1.030E-04	5.168E-03	1.211E-02	9.640E-03	7.310E-03	5.883E-03
15	0.000E-01	2.100E-05	3.297E-03	7.887E-03	7.042E-03	5.936E-03
16	0.000E-01	0.000E-01	2.800E-05	3.070E-03	6.973E-03	6.817E-03
17	0.000E-01	0.000E-01	0.000E-01	7.200E-05	9.181E-04	1.959E-03
18	0.000E-01	0.000E-01	0.000E-01	8.000E-06	1.078E-03	1.217E-03
19	0.000E-01	0.000E-01	0.000E-01	0.000E-01	1.170E-04	6.010E-04

APPENDIX B. EFFECTS OF THE SOFT-IRON MAGNETIC SHIELD

Because of the substantial uncertainty in magnetic field strengths in the TCB, we chose a quite conservative approach to magnetic shielding since our experience with photomultiplier tubes has led us to be cautious with these devices even in the presence of very modest ($\sim 10^{-3}$ Tesla) magnetic fields. The operational magnetic field inside the TFTR is expected to exceed 5 Tesla; the combination of toroidal and poloidal sources leads to a nontrivial computation of magnetic fields in the TCB. During the design phase of the present detection systems, "definitive" information on magnetic fields near the floor of the TCB varied by five orders of magnitude, depending on the source of information. It was not until Dec. 10, 1984, or well after the detectors were in place in the TCB undergoing final tests (and preliminary data taking), that we were informed of a *measurement* of the magnetic field in the TCB. The then-reported measurement indicated a magnetic field strength of ~0.02 Tesla 5 ft above the TCB floor (the magnetic field direction was not reported). We expect our configuration to be a satisfactory shield for at least 0.5 Tesla, perhaps as much as 1 Tesla, and so seems very adequate to protect the photomultiplier tube at least for measurements planned for the current campaign.

It is of some concern, however, to determine the effect of this iron shield on the detector responses of Appendix A. For neutrons normal to the surface of this shield (to first order), the neutron attenuation is given by

$$N/N_o = e^{-\sigma \rho t A/56} \quad , \tag{A.1}$$

where σ is the total Fe + n cross section and ranges between about 2.6×10^{-24} cm^2 and about 4×10^{-24} cm^2, ρ(Fe) = 7.86 g/cm^3, A = Avogadro's number = 6.023×10^{23}, the number 56 is the mass, in grams of the major isotope of elemental Fe, and t = 1 cm. Then N/N_o is the fraction of non-attenuated neutrons. Thus, this fraction varies between about 0.8 and 0.7 for the σ_{tot}(Fe) limits of interest. However, the detector will register some of the "attenuated" neutrons anyway, as pulses corresponding to apparent lower-energy neutrons, and also a few percent as gamma rays. Indeed, the incident neutron attenuation will be somewhat compensated for by detector registration of neutrons that were not originally headed in the direction of the detector but that impinge obliquely on the iron and are subsequently scattered into the detector. Some idea of the overall spectral effect on the neutron fluence incident on the iron shield was obtained from an ANISN calculation. (We are indebted to R. T. Santoro and J. M. Barnes for performing this calculation.) As this calculation is a one-dimensional calculation, the experimental configuration (of Fig. 1) had to be "modeled" for the calculation. The model chosen was an iron sphere having a 4.76-cm outside diameter and a wall thickness of 1 cm. A spherical "detector" was located at the center of the (iron) sphere, with the "detector" radius being deduced from the volume of the actual detector. These dimensions put the model "detector" at approximately the same average distance from the inside surface of the iron sphere as in the actual configuration of Fig. 1. The air space between the "detector" and the iron sphere was treated as a void. The C:H ratio of the scintillator was taken as 1:1.22.

For the purpose of the calculation, the incident neutron source was essentially monoenergetic and was assumed to be spatially isotropic and uniformly distributed over the outer surface of the iron sphere. More specifically, the neutrons impinging on a point on the surface of the iron sphere could be normal to the surface, tangential to the surface, or have any in-between orientation to the surface. The computation then determined the *energy* distribution of those neutrons deduced to be at the surface of the model "detector," without, however, deducing the directional orientation of these neutrons. The overall secondary neutron energy ranged between thermal and the energy of the incident neutrons. In addition, the *energy* distribution of gamma rays produced by neutron interactions with the three elements (Fe, C, and H) was also deduced.

These computations were done for incident neutron energies between 0.75 and 14 MeV, and for three different models corresponding to the three different detectors. In addition, some of these computations were carried out by replacing the Fe with Void, and others by replacing the model "detector" with Void. The characteristics of the calculations are very similar for all incident neutron energies. In Tables B.1 and B.2 we give the results of the model corresponding to ~2.5-MeV neutrons and the medium detector, and for the three model configurations [i.e., (1) full model, (2) no Fe, and (3) no "detector"]. In Table B.1 the calculated neutron energy distributions are given, and in Table B.2 the resulting photon energy distributions are given.

Table B.1. Neutron energy distributions of 2.5-MeV neutrons for the model corresponding to the medium detector: three different configurations. Units are in % of incident neutron flux.

Energy bin (MeV)	Full model	No iron	No detector
2.36 - 2.72	44.87	50.83	50.64
2.31 - 2.36	0.95	0.23	0.86
2.23 - 2.31	0.70	0.27	0.54
1.65 - 2.23	3.35	2.17	1.53
1.35 - 1.65	2.65	0.59	2.41
0.86 - 1.35	1.44	0.93	0.47
0.82 - 0.86	0.11	0.08	0.03
0.74 - 0.82	0.21	0.16	0.04
0.61 - 0.74	0.41	0.27	0.13
0.00 - 0.61	2.49	1.80	0.46
Total	57.18	57.33	57.11

Table B.2. Photon energy distributions of 2.5-MeV neutrons for the model corresponding to the medium detector: three different configurations. Units are in % of incident neutron flux.

Energy bin (MeV)	Full model	No iron	No detector
>2.0	0.04	0.00	0.04
1.5 - 2.0	0.13	0.00	0.13
1.0 - 1.5	0.42	0.00	0.44
0.6 - 1.0	4.21	0.00	4.42
0.2 - 0.6	2.19	0.00	2.12
0.1 - 0.2	0.88	0.00	0.83
Total	7.87	0.00	7.98

APPENDIX C. THE UNFOLDING COMPUTER PROGRAM

As discussed in Sect. 3, the obtained raw data (e.g., as shown in Figs. 10 and 11) must be processed to obtain meaningful results; the manner of processing is called "unfolding" as a contradistinction to the "folding" process, of Eq. (2), that is inherent in the experiment.

There are a number of programs written to unfold data such as we obtain. One major family of codes depends (essentially) on matrix inversion and iteration. Another family, based upon the FERD (or FERDOR) concept,[C1] does not use matrix inversion, but depends upon a technique of expanding a postulated ideal instrument response in terms of the actual instrument response; the output of the codes is in terms of a "confidence interval," which is often, mistakenly, interpreted as a specific value ± one-standard-deviation error. A third family, the oldest process, is essentially peak stripping. We have developed a somewhat different method which depends upon solving what are called "Bayes' equations" which, in turn, are based upon definitions of probability. We do not here give derivations; these are provided in the report by Larson[1] which also documents the general-purpose code developed on these principles. The primary advantages of adopting the Bayes' methodology are threefold: (1) a complete description of covariances among the input data as well as among the output values can be effected; (2) the calculation is rapid, as no iteration is involved; and (3) the (hardware) memory requirements may be minimized so that the program written in FORTRAN can be fitted on the CICADA PDP-11/23 microprocessor at our disposal.

A complete description and a complete listing of the general-purpose program BAYES is given in ref. 1. We have taken only some portions of this general-purpose package. We have added routines necessary to prepare the input to the package. Listings of all of these routines are given. Not included, however, are "standard" subroutines to do matrix inversion, matrix manipulation, etc., as the LINPACK package that we used is copyright protected.[C2]

In principle, one may start with no *a priori* estimates of fluence magnitudes; however, experience dictates that one reduces substantially the overall required computer time by first providing a finite zero-order set. We do this by reading in the raw data and then use a very crude peak-stripping method (family no. 3) to provide these initial guesses. Since these initial estimates were deduced from the *same* data to which they will be subject for adjustment, we are not, strictly speaking, using the Bayes' methodology as a "no-iteration" technique, but rather as a "one-iteration" computation. However, unlike standard iterative techniques which rely on goodness-of-fit parameters to deduce the adequacy of the computation, we instead depend upon the correctness of the methodology to provide the answer following a single pass through the routine. (Although the code allows a second iteration, in principle the second iteration should never be exercised. If it is, one ought to check for errors prior to entering the BAYES routine.)

A flow chart of the overall process is given in Fig. C.1. The only operator entries that are required correspond to the oval of this figure and are the results of prompts issued by the code of the CRT. The final results are presented in a graphics display and are in a file labelled "FOR001.DAT" which should be printed for archival reasons if no other.

We will now discuss the purposes of the specific routines in this program.

The main routine performs the tasks in the oval of Fig. C.1, then calls subroutines to set up the calculation, and then finally presents the computed results.

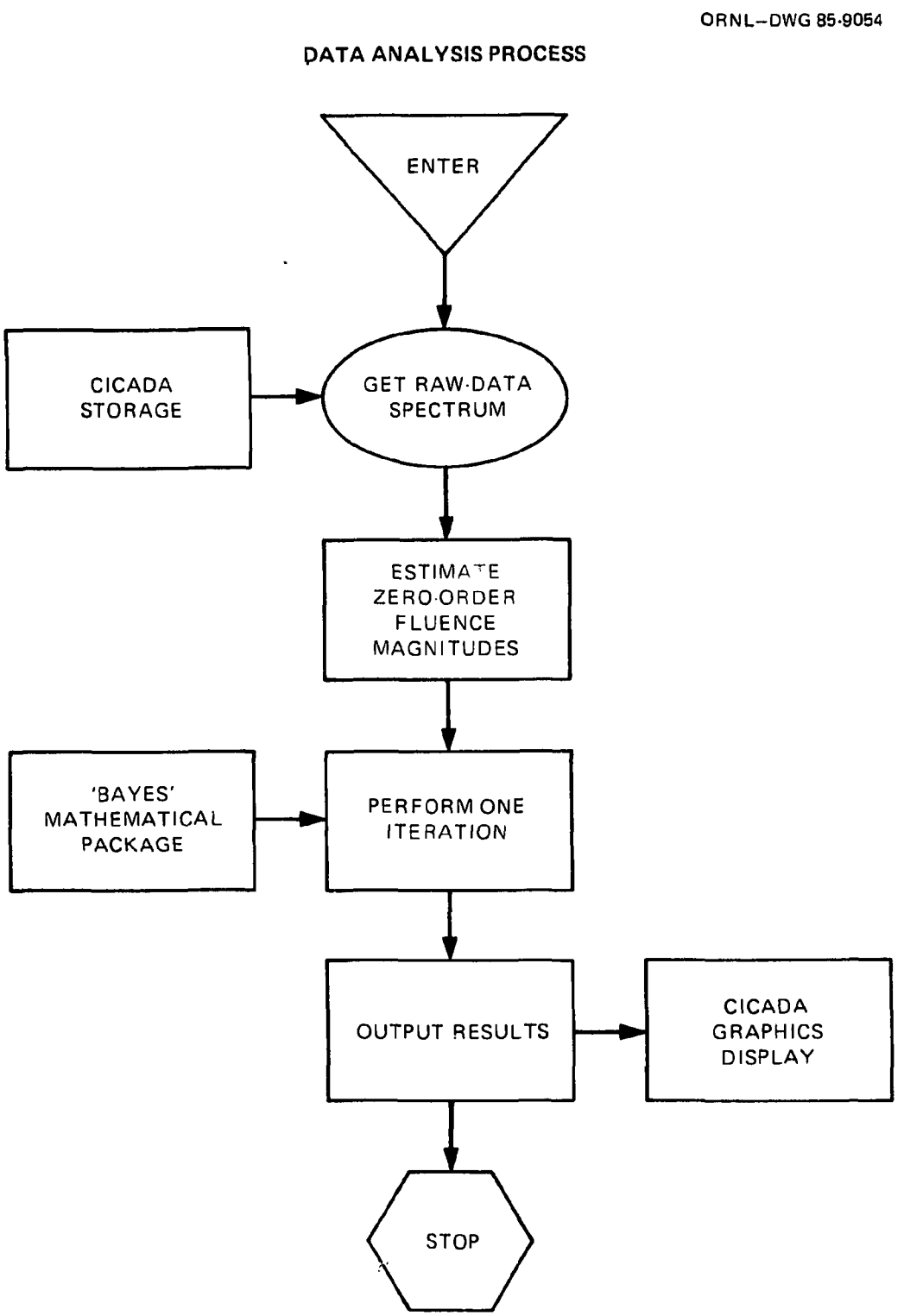

Fig. C.1. Flow chart of the unfolding computation. User interaction occurs in the oval portion.

The subroutine CALIBR accepts the operator-supplied calibration information, and then computes the (linear) calibration coefficients for (pulse-height) light units vs channel. (Note that a neutron energy may be used instead of a light-unit value as the second parameter of each input.)

The subroutine BINSUM provides the binning of the raw spectral data into bins of predetermined light-unit values. The algorithm, incidently, is very simple. One computes a running-sum array of the 240 channels of raw data along with a 240-element array of monotonically increasing pulse-height values corresponding to the calibration. One uses simple interpolation to determine a summed-data value corresponding to a specific pulse-height value which corresponds to, most likely, a fractional value of channel number. The difference in summed-data values for the lower and upper pulse-height bin limits gives the yield for that bin. The algorithm is fast since it depends on a minimal number of interpolations, and it preserves overall integral yields.

The subroutine UNFOLD decouples the main routine and its subroutines from the BAYES package. It also provides nondiagonal covariance elements for the binned pulse-height data with values chosen to correspond to small uncertainties in calibration parameters. As noted in comments, the -4% off-diagonal elements were deduced somewhat empirically by simply trying different calibrations and observing the effects of these tests.

The subroutine PBAYES is the main routine of the BAYES package. We have made several alterations, the most important of which is to remove all DOUBLE PRECISION statements and to set the dimensions exactly for our computation (and to eliminate statements checking on these dimensions). One space-saving "trick" is to condense the symmetric data covariance matrix VARDAT into just the upper (or lower) triangle for storage, and thus its dimension is 190 instead of 19×19. This condensation takes place in subroutine FIXV. Subroutine THEORY is a simple general routine to prepare calculated data and partial derivative arrays from user-supplied functions THEO and DERIV. Function THEO provides the deduced bin yield expected from the postulated or deduced fluence, parameters $n(E_k)$, for Eq. (2). Function DERIV provides the partial derivative of this deduced bin yield with respect to a particular E_k parameter; in our case it is just the appropriate element of the detector response.

Four response functions, two each for the large detector and medium detector, are tabulated in function RESPON(I,J,K). The index K designates which of the four responses is chosen. The index I corresponds to the (input) energy parameter, and the index J corresponds to the pulse-height bin. Although the response arrays are two dimensional, the DATA arrays are one dimensional; to accommodate the standard FORTRAN compiler, the responses are entered first in terms of increasing I, then in terms of increasing J. To accommodate the compiler on our particular computer, we have had to resort to designating several vector arrays for each response matrix and to use EQUIVALENCE statements to enter all of the data.

The subroutines SETPAR and QUICK perform essentially the tasks in the box under the oval of Fig. C.1. In addition, estimates are given for the parameter covariance matrix PARCOV, and then these covariances are condensed into the triangular version array VARPAR. In these routines to deduce the zero-order fluence estimates, we have observed the physics constraint that none may be negative.

The function ETOL is used to equate pulse height (in light units) to neutron, or photon, energy (in MeV). The functions XTERP and AA are simple interpolation functions.

The subroutine NEWPAR sets up and solves Bayes' equations and returns with the first-order set of fluence parameters $n_1(E_k)$. It calls three services routines, *viz.* SCALE, MUL and MUL2. The last two routines calculate pieces of the Bayes' equations, while SCALE (a) checks for accidental singularities in the matrix given in its calling sequence and (b) performs a scaling operation to maintain numerical magnitudes of the matrix elements in a mid range so that subsequent matrix manipulations avoid operations among matrix elements differing by many orders of magnitude with concomitant relatively large round-off errors.

The subroutines OUTPAR, OUTTH, OUTPI, OUTP2, and OUTV prepare the output and transmit to it unit 1, resulting in a file labelled FOR001.DAT. Moderate changes from Larson's original package[1] were made to accommodate the present task. The subroutine SETDAT is essentially a dummy subroutine in the present use. The subroutine RAWDAT retrieves the NE-213 raw data from the data file NESUM.DAT. The subroutine PUTDAT puts the unfolded results into file NEPLOT.DAT for graphics plotting. The subroutine DPPCO called in NEWPAR is part of the LINPACK package[C2] mentioned above, as is the subroutine DPPSL. The original subroutines are completely in double precision; we have redone them to single precision but keeping the same structure. These subroutines taken together perform the matrix solution

$$A \times C = B \quad . \tag{C.1}$$

The subroutine DPPCO tests the "condition" of the triangular two-dimensional matrix array EN prior to the operation given in Eq. (C.1). If the EN array passes this test, the subroutine DPPSL performs the task of Eq. (C.1) where our input arrays are EN $\rightarrow A$ and DUM $\rightarrow B$. The solution vector C of Eq. (C.1) is returned as vector B at the exit of DPPSL.

SUPPLEMENTARY REFERENCES

C1. B. W. Rust, D. T. Ingersoll and W. R. Burrus, *A User's Manual for the FERDO and FERD Unfolding Codes,* ORNL/TM-8720 (1983); B. W. Rust, "Mathematical Foundations of the Burrus Techniques for Spectral Unfolding," A Review of Radiation Energy Spectra Unfolding Proc. of a Seminar Workshop April 12-13, 1976, ORNL/RSIC-40 (1976), p. 23; W. R. Burrus, *Utilization of a priori Information by Means of Mathematical Programming in the Statistical Interpretation of Measured Distributions,* ORNL-3743 (1965).

C2. J. J. Dongarra, C. B. Moler, J. R. Bunch, and G. W. Stewart, *LINPACK User's Guide,* SIAM (1979).

```
C   FILE 'UNFOLD.FTN'
C   UNFOLD NE-213 DETECTOR DATA OF 1984-1985
C
      BYTE      SUMID(64)
      DIMENSION IDAT(250),SDAT(19),DDAT(19),AN(6)
      COMMON /BLOWER/ MINBIN,TXX
      COMMON /RESP/ MM
      COMMON /JKD/ UNC(19)
      COMMON /NORM/ ANORM
      COMMON /RESULT/ EM(18),DEM(18),AA(18),DAA(18)
      DATA AN/0.06, 0.06, 0.06, 0.06, 0.29, 0.29/
C
   79 TYPE 80
   80 FORMAT(//,'  TYPE N=1 FOR LARGE DETECTOR, NEUTRON'
     1       /,'  TYPE N=2 FOR LARGE DETECTOR, GAMMA'
     2       /,'  TYPE N=3 FOR MONITOR DETECTOR, NEUTRON'
     3       /,'  TYPE N=4 FOR MONITOR DETECTOR, GAMMA'
     4       /,'$ ENTER N >> ')
      READ(5,81)MM
81    FORMAT(I2)
C
      MO=MM/2
      MP=MM-2*MO
      IF (MP.EQ.1) WRITE(1,94)
      IF (MP.EQ.0) WRITE(1,95)
   94 FORMAT(/21H    NEUTRON UNFOLDING)
   95 FORMAT(/19H    GAMMA UNFOLDING )
C
C   GET APPROPRIATE NORMALIZATION FOR RESULTS IN -PER CM**2 -
      ANORM=AN(MM)
C
C  GET DATA NOW
C
      CALL RAWDAT(MM,IDAT,NSLOT,SUMID)        \RETURN THE SLOT NUMBER
      IMX=250
C
C  NOW, INPUT PULSE-HEIGHT CALIBRATION
      CALL CALIBR
C
C   NOW BIN THE PULSE-HEIGHT DATA INTO ARRAYS 'SDAT' 'AND 'DDAT
C  DDAT ARE THE UNCERTAINTIES FOR SDAT
      CALL BINSUM(IMX,IDAT,SDAT,DDAT,NBINS)
C
C  THERE WILL BE 'NBINS' VALUES OF 'SDAT' AND 'DDAT',
C       FOR THIS PPPL VERSION NBINS = 19 .. .. 2/4/85
C
C   NOW OUTPUT THE RESULTS
      WRITE(6,120)
      WRITE(1,120)
  120 FORMAT('    BINNED DATA'/T12,'COUNTS',T26,'UNC.')
      DO 10 J=1,NBINS
      UNC(J)=DDAT(J)
      WRITE(6,140) J,SDAT(J),DDAT(J)
      WRITE(1,140) J,SDAT(J),DDAT(J)
  140 FORMAT(I7,0P2F11.1)
   10 CONTINUE
C
C  NEXT STEP, UNFOLDING
      CALL UNFOLD(NBINS,SDAT,DDAT,NP)
C
      IF (MP.EQ.1) WRITE (6,94)
      IF (MP.EQ.0) WRITE (6,95)
C
C  'EM'  NEUTRON ENERGY
C  'DEM' NEUTRON ENERGY BIN WIDTH
```

```
C  'AA'  YIELD/CMSQ
C  'DAA' UNCERTAINTY ON AA
C
      DO 2Ø I=MINBIN,NP
      EL=EM(I)-Ø.5*DEM(I)
      EU=EM(I)+Ø.5*DEM(I)
      XAA=AA(I)/DEM(I)
      XDAA=DAA(I)/DEM(I)
      WRITE(6,15Ø) I,EL,EU,AA(I),DAA(I),XAA,XDAA
 15Ø  FORMAT(' ',I3,3F6.2,1P4E12.3)
  2Ø  CONTINUE
C
C  CALL ROUTINE PUTDAT TO WRITE DATA INTO FILE 'NEPLOT.DAT',
C  AND THEN INVOKE THE PLOTTING ROUTINE
      CALL PUTDAT(MINBIN,NP,MM,NSLOT,SUMID)
      CALL EXIT
      END
CC
CC
CC
      SUBROUTINE UNFOLD(N,DATA,UNC,NP)
C  PURPOSE IS TO SET UP TO 'UNFOLD' THE 'DATA' ARRAY CONTAINING
C  'N' ELEMENTS.  THE 'UNC' ARRAY CONTAINS THE UNCERTAINTIES RELATED
C  TO THE 'DATA'. THE 'NP' DATUM WILL RETURN WITH THE NUMBER OF
C  FINAL VALUES OF THE UNFOLD DATA, WHICH WILL BE FOUND IN THE
C  'AA' AND 'DAA' ARRAYS OF THE /RESULT/ COMMON
      COMMON /NUMBER/ NDAT,NPAR,ITER,ITMAX,CONVER
      COMMON /DAT/D1(19),D2(19),DAT(19),VARDAT(190),D3(190),D4(19),
     X   D5(19),D6(19)
      DIMENSION DATA(1),UNC(1),DATCOV(19,19)
      EQUIVALENCE (DATCOV(1,1),VARDAT(1))
C
      NDAT=N
      DO 1Ø I=1,NDAT
      DAT(I)=DATA(I)
      DO 5 J=1,N
   5  DATCOV(J,I)=Ø.Ø
      DATCOV(I,I)=UNC(I)*UNC(I)
  1Ø  CONTINUE
C
C   WE PUT IN A SMALL OFF-DIAGONAL COVARIANCE TERM TO
C     ACCOUNT FOR A MODEST ERROR IN THE CALIBRATION,
C     AMOUNT CHOSEN TO BE 4% BASED ON EMPIRICAL TRIES
C
      DO 15 I=2,NDAT
      DD=-Ø.Ø4*UNC(I)*UNC(I-1)
      DATCOV(I,I-1)=DD
  15  DATCOV(I-1,I)=DD
C
      CALL PBAYES
C
C  SUBROUTINE IN PBAYES WILL
C  (1). MAKE AN ESTIMATE OF THE UNFOLDED SPECTRUM
C  (2). DO ONE ITERATION (ONE ONLY) TO GET THE FINAL RESULTS
C       USING THE BAYES THEOREM IN THE MATHEMATICAL PROBLEM SET-UP
C
      NP=NPAR
      RETURN
      END
```

```
      SUBROUTINE PBAYES
C  THIS IS NMLARSON'S GBAYES, STRIPPED DOWN FOR THIS APPLICATION
C
      COMMON/NUMBER NDAT,NPAR,ITER,ITMAX,CONVER
C
      ITMAX=2
      CONVER=Ø.ØØ5
1Ø    CALL SETPAR
      CALL OUTPAR
2Ø    CALL SETDAT(KGO)
      IF (KGO.GE.ITMAX) RETURN
C  LAST ADDED 1/2/85 TO RETURN CONTROL TO MAIN PROGRAM
C
      CALL FIXV
      ITER=Ø
3Ø    CALL THEORY
      CALL OUTTH
      CALL NEWPAR
C  OUTPUT FROM THIS ROUTINE ARE THE ADJUSTED PARAMETER VALUES
C
      IF (ITER.LT.ITMAX) CALL OUTP1
      IF (ITER.EQ.ITMAX) CALL OUTP2
      ITER=ITER+1
      IF (ITER.LE.ITMAX) GOTO 3Ø
      GOTO 2Ø
C
      END
C
C
CC
      SUBROUTINE FIXV
C
C  PURPOSE--- REARRANGE DATCOV TO BE VARDAT, IE.. KEEP ONLY LOWER
C  TRIANGULAR PORTION OF DATA COVARIANCE MATRIX
C
      COMMON /NUMBER/ NDAT,NPAR,ITER,ITMAX,CONVER
      COMMON /DAT/ E(19),E2(19),DATA(19),VARDAT(19Ø),EN(19Ø),
     1   TH(19),DUM(19),SIG(19)
      DIMENSION DATCOV(19,19)
      EQUIVALENCE (DATCOV(1,1),VARDAT(1))
C
      IL=Ø
      DO 2Ø I=1,NDAT
      DO 1Ø L=1,I
      IL=IL+1
      VARDAT(IL)=DATCOV(I,L)
1Ø    CONTINUE
2Ø    CONTINUE
      RETURN
      END
CC
CC
      SUBROUTINE THEORY
C
C  PURPOSE--- GENERATE TH(EORY) CALCULATION AT EACH POINT AND THE
C  DERIVATIVE MATRIX G(DATA,PARAMETER)
C
      COMMON /NUMBER/ NDAT,NPAR,ITER,ITMAX,CONVER
      COMMON /DAT/ E(19),E2(19),DATA(19),VARDAT(19Ø),EN(19Ø),TH(19),
     X   DUM(19),SIG(19)
      COMMON /BOTH/ G(19,18), EMG(19,18)
C
      DO 5Ø I=1,NDAT
      KDAT=IDAT
      TH(IDAT)=THEO(KDAT)
      DO 1Ø I=1,NPAR
      II=I
      G(KDAT,II)=DERIV(KDAT,II)
1Ø    CONTINUE
5Ø    CONTINUE
      RETURN
      END
```

```
      SUBROUTINE NEWPAR
C
C  PURPOSE TO SET UP AND SOLVE BAYES' EQUATIONS
C
      COMMON /NUMBER/ NDAT,NPAR,ITER,ITMAX,CONVER
      COMMON /PAR/ POLD(18),PARM(18),PDUM(18),VARPAR(171),
     1   VARNEW(171),IDUM(18)
      COMMON /DAT/ E(19),E2(19),DATA(19),VARDAT(190),EN(190),TH(19),
     1   DUM(19),SIG(19)
      COMMON /BOTH/ G(19,18), EMG(19,18)
C
      DO 10 I=1,NDAT
      TH(I)=DATA(I)-TH(I)
10    CONTINUE
C
      IF(ITER.EQ.0)GOTO 110
      DO 100 IPAR=1,NPAR
      DO 90 I=1,NDAT
      TH(I)=TH(I)-G(I,IPAR)*(POLD(IPAR)-PARM(IPAR))
90    CONTINUE
100   CONTINUE
110   CONTINUE
      CALL MUL
      CALL MUL2
      CALL SCALE(EN,SIG,NDAT,IFDIAG)
      IF (IFDAIG.EQ.0) GOTO 120
      IIIII=0
      CALL DPPCO(EN,NDAT,RCOND,DUM,IIIII)
      IF(1.0+RCOND.EQ. 1.0) GOTO 300
120   CONTINUE
      DO 130 I=1,NDAT
      DUM(I)=TH(I)*SIG(I)
130   CONTINUE
      IF(IFDIAG.EQ.1) CALL DPPSL(EN,NDAT,DUM)
      DO 140 I=1,NDAT
      DUM(I)=DUM(I)*SIG(I)
140   CONTINUE
C
C  *** NOW, CALCULATE M*G*EN**-1*TH
      DO 170 I=1,NPAR
      PDUM(I)=0.0
170   CONTINUE
      DO 190 I=1,NPAR
      DO 180 J=1,NDAT
      PDUM(I)=PDUM(I)+EMG(J,I)*DUM(J)
180   CONTINUE
190   CONTINUE
      ICONV=0
      IL=0
      DO 210 I=1,NPAR
      A=PDUM(I)+POLD(I)
      IF( CONVER.LE.0.0) GOTO 200
      IL=IL+I
      PDN=VARPAR(IL)
      PDN=SQRT(PDN)
      IF (PDN.EQ.0.0) GO TO 200
      B=ABS(A-PARM(I))
      IF (B.LE.CONVER*PDN)  ICONV=ICONV+1
200   PARM(I)=A
210   CONTINUE
      IF( ICONV.EQ.NPAR ) ITER=ITMAX
      IF( ITER.NE.ITMAX ) GOTO 290
      IJ=0
      DO 230 I=1,NPAR
      DO 220 J=1,I
      IJ=IJ+1
      VARNEW(IJ)=VARPAR(IJ)
220   CONTINUE
230   CONTINUE
```

```
      IJ=0
      DO 280 I=1,NPAR
      DO 240 J=1,NDAT
      DUM(J)=EMG(J,I)*SIG(J)
240   CONTINUE
      IF (IFDIAG.EQ.1) CALL DPPSL(EN,NDAT,DUM)
      DO 250 IDAT=1,NDAT
      DUM(IDAT)=DUM(IDAT)*SIG(IDAT)
250   CONTINUE
      DO 270 J=1,I
      IJ=IJ+1
      DO 260 K=1,NDAT
      VARNEW(IJ)=VARNEW(IJ)-EMG(K,J)*DUM(K)
260   CONTINUE
270   CONTINUE
280   CONTINUE
290   RETURN
C
300   WRITE(5,99) RCOND
      GOTO 120
C
99    FORMAT(/,'   ***** ERROR IN NEWPAR, RCOND=',1PE12.5)
      END
CC
CC
      SUBROUTINE SCALE(A,SIG,N,IFDIAG)
C
      DIMENSION  A(1),SIG(N)
      IL=0
      DO 20 I=1,N
      IL=IL+I
      SI=A(IL)
      IF( SI.LE.0.0) GOTO 10
      SIG(I)=1.0/SQRT(SI)
      GOTO 20
10    SIG(I)=1.0/SQRT(-SI)
20    CONTINUE
C
      IFDIAG=0
      IL=0
      DO 40 I=1,N
      SI=SIG(I)
      DO 30 K=1,I
      IL=IL+1
      IF (I.NE.L.AND.A(IL).NE.0.0) IFDIAG=1
      A(IL)=A(IL)*SI*SIG(L)
30    CONTINUE
40    CONTINUE
      RETURN
      END
CC
CC
```

```
      SUBROUTINE MUL
      COMMON /NUMBER/ NDAT,NPAR,ITER,ITMAX,CONVER
      COMMON /PAR/ POLD(18),PARM(18),PDUM(18),VARPAR(171),
     1  VARNEW(171),IDUM(18)
      COMMON /BOTH/ G(19,18), EMG(19,18)
C
      JK=0
      DO 60 J=1,NPAR
      DO 10 L=1,NDAT
      EMG(L,J)=0.0
10    CONTINUE
      DO 50 K=1,NPAR
      IF (J.GE.K) GOTO 20
      KJ=J+(K*(K-1))/2
      EM=VARPAR(KJ)
      GOTO 30
20    JK=JK+1
      EM=VARPAR(JK)
30    CONTINUE
      IF( EM.EQ.0.0) GOTO 50
      DO 40 L=1,NDAT
      EMG(L,J)=EMG(L,J)+EM*G(L,K)
40    CONTINUE
50    CONTINUE
60    CONTINUE
      RETURN
      END
CC
CC
CC
      SUBROUTINE MUL2
C
      COMMON /NUMBER/ NDAT,NPAR,ITER,ITMAX,CONVER
      COMMON /DAT/ E(19),E2(19),DATA(19),VARDAT(190),EN(190),TH(19),
     1  DUM(19),SIG(19)
      COMMON /BOTH/ G(19,18) EMG(19,18)
C
      IL=NDAT*(NDAT+1)
      IL=IL/2
      DO 20 I=1,IL
      EN(I)=VARDAT(I)
20    CONTINUE
C
      DO 50 J=1,NPAR
      IL=0
      DO 40 I=1,NDAT
      DO 30 L=1,I
      IL=IL+1
      EN(IL)=G(I,J)*EMG(L,J)+EN(IL)
30    CONTINUE
40    CONTINUE
50    CONTINUE
      RETURN
      END
CC
```

```
C  FILE 'DATSET.FTN'
C
      SUBROUTINE SETDAT(KBAR)
C  THIS (EFFECTIVELY) IS A DUMMY ROUTINE
      DATA KB/0/
      KB=KB+1
      WRITE (1,1) KB
    1 FORMAT(/10(4H*   ), 'N-TIME THRU SETDAT ='I2/)
      KBAR=KB
      RETURN
      END
CC
CC
      FUNCTION THEO(KDAT)
C   GENERATE CALCULATED VALUE OF THE YIELD FOR THE DATA POINT 'KDAT'
C   AND THE PARAMETERS 'PARAM' AND THE GIVEN RESPONSES
C
      COMMON /NUMBER/ NDAT,NPAR,ITER,ITMAX,CONV
      COMMON /PAR/ P0(18),P(18),PD(18),V(171),V1(171),ID(18)
C   THE 'P' ARRAY IN THIS COMMON STATEMENT HAS THE
C      AMPLITUDES OF THE BIN YIELDS.
      COMMON /RESP/ KR
C
      K=KDAT
      T=0.0
      DO 10 I=1,NPAR
      I1=I
      S=RESPON(I1,K,KR)
      T=T+S*P(I1)
   10 CONTINUE
      THEO=T
      RETURN
      END
CC
CC
      FUNCTION DERIV(KDAT,KPAR)
C  GENERATE PARTIAL DERIVATIVES  DEL(DATA(KDAT))/DEL(PARAM(KPAR))
C
CCCCCCCCCCCCCCCCCCCCCCCCCCCCCCCCCCCCCCCCCCCCCCCCCCCCCCCCCCCCCCCC
C                                                               C
C     FOR THIS PARTICULAR APPLICATION THE PARTIAL                C
C       DERIVATIVE IS JUST THE APPROPRIATE                      C
C       ELEMENT OF THE RESPONSE ARRAY.                          C
C                                                               C
CCCCCCCCCCCCCCCCCCCCCCCCCCCCCCCCCCCCCCCCCCCCCCCCCCCCCCCCCCCCCCCC
C
      COMMON /RESP/ KR
      DERIV=RESPON(KPAR,KDAT,KR)
      RETURN
      END
```

```
      SUBROUTINE SETPAR
C++
C  GET GOOD INITIAL GUESS FOR PULSE HEIGHT BIN MAGNITUDES
C  FOR 'PBAYES' TO ITERATE ON
C++
      COMMON /NUMBER/ NDAT,NPAR,ITER,ITMAX,CONVER
      COMMON /PAR/ POLD(18),PARM(18),PDUM(18),VARPAR(171),
     1   VARNEW(171),IDUM(18)
      COMMON /DAT/ E1(19),E22(19),DATA(19),VARDAT(190),DUM3(190),
     1   DUM4(19),DUM5(19),DUM6(19)
      COMMON /BLOWER/ MINBIN,TMAX
      COMMON /RESP/ MZ
      COMMON /JKD/ UNC(19)
      DIMENSION D(19),V(19),A(19),DA(19),AT(19),DATCOV(19,19)
      DIMENSION PARCOV(18,18)
      EQUIVALENCE (PARCOV(1,1),VARPAR(1))
      EQUIVALENCE (DATCOV(1,1),VARDAT(1))
      DATA FIVEP/0.05/,TENP/0.1/
C
      NPAR=NDAT-1
C  THIS IS DEFINITION OF 'NPAR' FOR THE TFTR UNFOLDING PACKAGE
C       THAT IS -- THE NUMBER OF 'UNFOLDED' DATA IS ALWAYS
C       ONE LESS THAN THE NUMBER OF RAW DATA BINS.  THIS
C       ALLOWS FOR THE FACT THAT THE DETECTOR RESPONSE
C       APPEARS TO INCLUDE FINITE VALUES FOR PULSE-HEIGHT
C       BINS THAT SCALE OUT TO NEUTRON (OR PHOTON) ENERGIES
C       GREATER THAN THE ENERGY OF THE DETECTED NEUTRON (OR PHOTON)
C
      SSM=0.0
      DO 4, J=1,NDAT
      D(J)=DATA(J)
   4  SSM=SSM+D(J)
      WRITE(6,95) SSM
      WRITE(1,95) SSM
C
C  FILL IN 'HOLES', IF POSSIBLE
      K=NDAT
      DO 5 I=1,NDAT
      IF (D(K).GT.0.0) GOTO 6
   5  K=K-1
   6  IS=NDAT-K+2
      DO 7 I=IS,NDAT
      K=NDAT-IS+1
      IF (D(K).GT.0.0) GO TO 7
      D(K)=1.0
      IF (D(K).GT.0.5*D(K+1)) D(K)=0.5*D(K+1)
      D(K+1)=D(K+1)-D(K)
C  LAST STATEMENT TO PRESERVE INTEGRAL YIELD
   7  CONTINUE
C
      K=NPAR
      A(NDAT)=0.0
      DA(NDAT)=0.0
      CALL QUICK(MZ,D,AT,V)
      DO 1 I=1,NPAR
      A(I)=AT(I)
      IF (A(I).LT.0.0) A(I)=0.0
      IF (V(I).LT.1.0)  V(I)=1.0
   1  CONTINUE
C
      SSM=0.0
      DSUMM=0.0
      DO 9 J=MINBIN,NDAT
      SSM=SSM+DATA(J)
   9  DSUMM=DSUMM+D(J)
C
      RINC=1.0 + DSUMM/SSM
      WRITE(6,92) RINC
      WRITE(1,92) RINC
      DO 11 I=1,NPAR
  11  A(I)=RINC*A(I)
C
```

```
      IF (MINBIN.EQ.1) GO TO 16
      MB=MINBIN-1
      DO 14 I=1,MB
      AR=TMAX*FLOAT(MINBIN-I)
      UNC(I)=AR
14    DATCOV(I,I)=AR*AR
C
16    DO 20 I=1,NPAR
      DSS=FIVEP*A(I)
      DA(I)=SQRT(DSS*DSS+V(I)**2)
20    CONTINUE
C
      DO 30 I=1,NPAR
      IF (AT(I).LE.0.0) GO TO 30
      IF (DA(I) .LT. TENP*A(I)) DA(I)=TENP*A(I)
30    CONTINUE
C
C  NOW WE SHOULD HAVE SUITABLE FIRST GUESS PARAMETERS
C  AND UNCERTAINTIES
      WRITE(6,99)
      ASUM=0.0
      DO 35 I=1,NPAR
      WRITE(6,98) I,A(I),DA(I)
35    ASUM=ASUM+A(I)
      WRITE(6,97) ASUM
C
      DO 38 I=1,NPAR
      DO 36 J=1,NPAR
36    PARCOV(I,J)=0.0
      PARM(I)=A(I)
      PARCOV(I,I)=DA(I)*DA(I)
38    CONTINUE
C
C    NOW PUT SOMETHING IN OFF-DIAGONAL COVARIANCE ELEMENTS OF
C   THE FIRST GUESS PARAMETERS.  THE IMPORTANT POINT IS THAT IF
C   SOME 'PARM(N)' INCREASES, THEN 'PARM(N-1)' HAS TO HAVE A
C   RELATIVE DECREASE TO COMPENSATE.
C
      DO 42 I=3,NPAR
      PBAR = -0.36*DA(I)*DA(I-1)
      PARCOV(I,I-1)=PBAR
42    PARCOV(I-1,I)=PBAR
C
      DO 44 I=3,NPAR
      PBAR=-0.04*DA(I)*DA(I-2)
      PARCOV(I,I-2)=PBAR
44    PARCOV(I-2,I)=PBAR
C
      PBAR=-0.4*DA(2)*DA(1)
      PARCOV(1,2)=PBAR
      PARCOV(2,1)=PBAR
C
      PBAR=-0.4*DA(NPAR)*DA(NPAR-1)
      PARCOV(NPAR,NPAR-1)=PBAR
      PARCOV(NPAR-1,NPAR)=PBAR
C
C  NOW WE REARRANGE COVARIANCE TO STORE IN VARPAR AS A VECTOR
C
      IL=0
      DO 60 I=1,NPAR
      POLD(I)=PARM(I)
      DO 55 L=1,I
      IL=IL+1
55    VARPAR(IL)=PARCOV(L,I)
60    CONTINUE
C
      RETURN
92    FORMAT(/4X,12HR-INCREASE =,1PE12.4/)
95    FORMAT(8H  TOTAL=,0PF10.1)
97    FORMAT(0PF16.1,23H = SUM OF FIRST GUESSES)
98    FORMAT(I4,0P2F12.1)
99    FORMAT(//20H  FIRST PASS RESULTS/5X,
     1   25HFIRST-GUESS   UNCERTAINTY)
      END
```

```
      SUBROUTINE QUICK(M,D,T,V)
      COMMON /NUMBER/  NDAT,NPAR,ITER,ITMAX,CONVER
      COMMON /BLOWER/ MINBIN,TX
      DIMENSION D(1),T(1),DD(19),V(1)
C   SIMPLE "STRIPPING" ROUTINE FROM HIGH-ENERGY END TO LOW-ENERGY END.
C
      DO 4 I=1,NDAT
      DD(I)=D(I)
      IF (D(I),LE,Ø,Ø ,AND, I,GT,1) DD(I)=Ø,1*DD(I-1)
   4  CONTINUE
C
      MM=M
      K=NPAR
      DO 1Ø I=1,NPAR
      L=K+1
      IF (L,GT,NDAT) L=NDAT
   2  S=RESPON(K,L,MM)
      IF (S,GT,Ø,Ø) GOTO 3
      L=L-1
      GOTO 2
C
3     DOFL=D(L)
      IF (DOFL,LE,Ø,Ø) DOFL=Ø,1* DD(L)
 5    AK=DOFL/S
      Q=SQRT(DD(L))/S
      IF (D(L) ,LE, Ø,Ø) Q=Ø,32* Q
      LL=L-1
      IF (LL,LT,MINBIN) GOTO 6
      DO 1 J=MINBIN,LL
      J1=J
      S=RESPON(K,J1,MM)
      AK1=D(J1)/S
      QK1=SQRT(DD(J1))/S
      IF (AK,GT,AK1) AK=AK1
      IF (Q ,GT, QK1) Q=QK1
   1  CONTINUE
C
 6    FRAC=Ø,8 + Ø,ØØ54*FLOAT(K)
C  COEFFICIENTS IN LAST STATEMENT DETERMINED MORE OR LESS
C  EMPIRICALLY, BY TRIAL AND ERROR
      AK=FRAC*AK
      Q=Q*SQRT(FRAC)
      IF (AK,LT,Ø,Ø) AK=Ø,Ø
      T(K)=AK
      V(K)=Q
      DO 8 J=1,L
      J1=J
      S=RESPON(K,J1,MM)
      DSUB=AK*S
      ESUB=(Q*S)**2
      D(J)=D(J)-DSUB
      DD(J)=DD(J)+5,D-1 * (DSUB+ESUB)
C  LAST IS A COMPROMISE, NOT A TRUE ERROR PROPAGATION
 8    CONTINUE
 1Ø   K=K-1
      MB=MINBIN-1
      IF (MB,LE,Ø) GOTO 14
      DO 12 I=1,MB
 12   T(I)=Ø,Ø
 14   DO 15 I=2,NPAR
      VNM=Ø,Ø1*T(I-1)
      IF (V(I),LE,VNM)  V(I)=VNM
 15   CONTINUE
C
      RETURN
      END
```

```
      FUNCTION ETOL(N,A)
C  FUNCTION TO GET A NEUTRON ENERGY (MEV) FOR A (PROTON) LIGHT-UNIT
C  VALUE OF 'A', IF N=1
C  OR, GET A (PROTON) LIGHT-UNIT VALUE FOR A NEUTRON ENERGY VALUE OF
C  'A', IF N=2
C  OR, PHOTON ENERGY FOR A LIGHT-UNIT VALUE OF A, IF N=3
C  OR, LIGHT-UNIT VALUE FOR A PHOTON ENERGY OF A (MEV), IF N=4
C
      DIMENSION ALU(35),ALG(35),E(35)
      DATA NN/35/
      DATA ALU/ 0.001,  0.003,  0.005,  0.00671,0.00886,0.01207,
     1          0.01465,0.01838,0.0246, 0.029,  0.0365, 0.0483,
     2          0.0678, 0.091,  0.1175, 0.1562, 0.2385, 0.366,
     3          0.4725, 0.625,  0.866,  1.042,  1.327,  1.718,
     4          2.31,   2.95,   3.62,   4.55,   6.36,   8.83,
     5         10.8,   13.5,   17.7,   20.5,   24.8/
C
C
      DATA E/ 0.01,  0.043, 0.075, 0.1,   0.13,  0.17,  0.2,
     1        0.24,  0.3,   0.34,  0.4,   0.48,  0.6,   0.72,
     2        0.84,  1.0,   1.3,   1.7,   2.0,   2.4,   3.0,
     3        3.4,   4.0,   4.8,   6.0,   7.2,   8.4,  10.0,
     4       13.0,  17.0,  20.0,  24.0,  30.0,  34.0,  40.0/
C
      DATA ALG/ 0.0003, 0.0052, 0.0143, 0.0237, 0.0369, 0.0572,
     1          0.0739, 0.0979, 0.1364, 0.1634, 0.2055, 0.2637,
     2          0.354,  0.447,  0.542,  0.67,   0.915,  1.244,
     3          1.493,  1.826,  2.327,  2.662,  3.16,   3.84,
     4          4.84,   5.85,   6.86,   8.21,  10.73,  14.1,
     5         16.62,  20.0,   25.0,   28.4,   33.5/
C
      AA=A
      B=0.0
      IF (N.LE.0.OR.N.GE.5) WRITE(5,1) N
1     FORMAT(/37H   ????? ERROR IN FUNCTION ETOL --N =,I10/)
      IF (N.EQ.1) B=XTERP(ALU,E,AA,NN)
      IF (N.EQ.2) B=XTERP(E,ALU,AA,NN)
      IF (N.EQ.3) B=XTERP(ALG,E,AA,NN)
      IF (N.EQ.4) B=1.6835*AA*AA/(0.511+2.0*AA)
      ETOL=B
      RETURN
      END
CC
CC
      FUNCTION XTERP(A,B,C,N)
C  LINEAR INTERPOLATION IN LOG-LOG OF ARRAYS A,B FOR VALUE C
      DIMENSION A(1),B(1)
      IF (C.LE.A(1)) GO TO 3
      IF (C.GE.A(N)) GO TO 4
      DO 1 I=2,N
      IF (C.LT.A(I)) GO TO 2
1     CONTINUE
C
2     J=I
      I=I-1
      AE=ALOG(A(I))
      D=(ALOG(C)-AE)/(ALOG(A(J))-AE)
      X=ALOG(B(I))
      Y=X+D*(ALOG(B(J))-X)
      XTERP=EXP(Y)
      RETURN
3     XTERP=B(I)
      RETURN
4     XTERP=B(N)
      RETURN
      END
```

```
CC
      FUNCTION RESPON(I,J,K)
      DIMENSION RN1(18,19),RD1(342),RD2(125),RD3(125)
      DIMENSION RD4(62),RN2(18,19),RE1(342),RE2(130)
      DIMENSION RE3(140),RE4(62),RG1(18,19),RB1(342)
      DIMENSION RB2(130),RB3(140),RB4(62),RG2(18,19)
      DIMENSION RC1(342),RC2(130),RC3(140),RC4(62)
      DIMENSION RD22(30),RC22(10),RB22(10),RE22(10)
C  (THE REASON FOR ALL THIS EXTRA DIMENSIONING AND
C   EQUIVALENCING IS THE LOCAL COMPILER -- IT ACCEPTS
C   ONLY SO MUCH CONTINUATION, AND I HAVEN'T FIGURED
C   OUT QUITE HOW MUCH THAT IS.)
C
      EQUIVALENCE (RN1(1,1),RD1(1))
      EQUIVALENCE (RD1(1),RD2(1))
      EQUIVALENCE (RD1(156),RD3(1))
      EQUIVALENCE (RD1(281),RD4(1))
      EQUIVALENCE (RN2(1,1),RE1(1))
      EQUIVALENCE (RE1(1),RE2(1))
      EQUIVALENCE (RE1(141),RE3(1))
      EQUIVALENCE (RE1(281),RE4(1))
      EQUIVALENCE (RG1(1,1),RB1(1))
      EQUIVALENCE (RB1(1),RB2(1))
      EQUIVALENCE (RB1(141),RB3(1))
      EQUIVALENCE (RB1(281),RB4(1))
      EQUIVALENCE (RG2(1,1),RC1(1))
      EQUIVALENCE (RC1(1),RC2(1))
      EQUIVALENCE (RC1(141),RC3(1))
      EQUIVALENCE (RC1(281),RC4(1))
      EQUIVALENCE (RD1(126),RD22(1))
      EQUIVALENCE (RB1(131),RB22(1))
      EQUIVALENCE (RC1(131),RC22(1))
      EQUIVALENCE (RE1(131),RE22(1))
C
CC  I=INDEX CORRESPONDING TO NEUTRON (GAMMA-RAY) ENERGY
CC  J=INDEX CORRESPONDING TO PULSE-HEIGHT BIN OF RESPONSE
CC  K=INDEX TELLING WHICH RESPONSE TO USE
CC
CC  THE FIRST ARRAYS CONTAIN THE LARGE DETECTOR NEUTRON RESPONSE
C
      DATA RD2/  Ø.Ø7589,  Ø.1155,   Ø.1103,   Ø.Ø845,   Ø.Ø5946,
     1   Ø.Ø4625,  Ø.Ø3761,  Ø.Ø2903,  Ø.Ø2696,  Ø.Ø2273,  Ø.Ø186,
     2   Ø.Ø135Ø,  Ø.ØØ86Ø2, Ø.ØØ73,   Ø.Ø926,
     2   Ø.ØØ9421, Ø.ØØ93Ø2, Ø.ØØ8313, Ø.Ø1481,  Ø.Ø4831,  Ø.Ø7258,
     3   Ø.Ø742,   Ø.Ø57,    Ø.Ø4385,  Ø.Ø3383,  Ø.Ø2635,  Ø.Ø2336,
     4   Ø.Ø1977,  Ø.Ø1598,  Ø.Ø1146,  Ø.ØØ7357, Ø.ØØ5847, Ø.ØØ4847,
     4   Ø.ØØ666,  Ø.ØØ8264, Ø.ØØ65Ø8,                    Ø.ØØ2Ø6,
     5   Ø.Ø17Ø3,  Ø.Ø5359,  Ø.Ø8606,  Ø.Ø8384,  Ø.Ø7147,  Ø.Ø552,
     6   Ø.Ø431,   Ø.Ø3565,  Ø.Ø3Ø5,   Ø.Ø2422,  Ø.Ø1722,  Ø.Ø1Ø76,
     7   Ø.ØØ8141, Ø.ØØ5152, Ø.ØØ7782, Ø.Ø1Ø22,  Ø.ØØ9624,
     7   Ø.Ø,      Ø.ØØ1,    Ø.Ø1174,  Ø.Ø42Ø6,  Ø.Ø65Ø6,
     8   Ø.Ø7Ø55,  Ø.Ø6194,  Ø.Ø4985,  Ø.Ø3982,  Ø.Ø3293,  Ø.Ø2622,
     9   Ø.Ø182Ø,  Ø.Ø1119,  Ø.ØØ7917, Ø.ØØ5Ø37, Ø.ØØ6212, Ø.ØØ7688,
     9   Ø.ØØ9732,                     Ø.Ø,      Ø.Ø,      Ø.ØØØ981,
     A   Ø.ØØ9768, Ø.Ø3329,  Ø.5238,   Ø.Ø5776,  Ø.Ø53Ø7,  Ø.Ø4374,
     B   Ø.Ø3477,  Ø.Ø2724,  Ø.Ø182Ø,  Ø.Ø113,   Ø.ØØ7642, Ø.ØØ511,
     B   Ø.ØØ5ØØ9, Ø.ØØ5985, Ø.ØØ8Ø41,                    Ø.Ø,
     C   Ø.Ø,      Ø.ØØØØ492,Ø.ØØ1119, Ø.ØØ9633, Ø.Ø2824,  Ø.Ø4553,
     D   Ø.Ø5141,  Ø.Ø4623,  Ø.Ø3838,  Ø.Ø2916,  Ø.Ø1947,  Ø.Ø1172,
     E   Ø.ØØ7437, Ø.ØØ5176, Ø.ØØ4278, Ø.ØØ5381, Ø.ØØ6374,
     E   Ø.Ø,      Ø.Ø,      Ø.Ø,      Ø.ØØØØ4736,Ø.ØØ1349,
     F   Ø.ØØ8673, Ø.Ø2603,  Ø.Ø4Ø9,   Ø.Ø428,   Ø.Ø4Ø,    Ø.Ø3251,
     G   Ø.Ø2115,  Ø.Ø1214,  Ø.ØØ7343, Ø.ØØ5184, Ø.ØØ3743, Ø.ØØ5Ø1/
C
      DATA RD22/ Ø.ØØ5373,                Ø.Ø,      Ø.Ø,      Ø.Ø,
     H   Ø.Ø,      Ø.ØØØ1Ø59,Ø.ØØ1474,  Ø.ØØ954,  Ø.Ø2723,  Ø.Ø4ØØ4,
     I   Ø.Ø4456,  Ø.Ø4Ø54,  Ø.Ø2717,  Ø.Ø1535,  Ø.ØØ9ØØ9,
     I   Ø.ØØ6313, Ø.ØØ42,   Ø.ØØ499,  Ø.ØØ5795, Ø.Ø,
     J   Ø.Ø,      Ø.Ø,      Ø.Ø,      Ø.Ø,      Ø.ØØØØ4479,Ø.ØØ1Ø94,
     K   Ø.ØØ7187, Ø.Ø1888,  Ø.Ø2833,  Ø.Ø328/
C
```

```
      DATA RD3/  Ø.Ø248,   Ø.Ø1319,
     L  Ø.ØØ7492, Ø.ØØ5189, Ø.ØØ3475, Ø.ØØ3134, Ø.ØØ4219,
     L  Ø.Ø,      Ø.Ø,      Ø.Ø,      Ø.Ø,      Ø.Ø,
     M  Ø.Ø,      Ø.ØØØ1Ø34,Ø.ØØ1605, Ø.ØØ7952, Ø.Ø1957,  Ø.Ø3Ø82,
     N  Ø.Ø2842,  Ø.Ø1631,  Ø.ØØ911,  Ø.ØØ6Ø14, Ø.ØØ4187, Ø.ØØ3164,
     N  Ø.ØØ4415, Ø.Ø,      Ø.Ø,      Ø.Ø,      Ø.Ø,      Ø.Ø,
     1  Ø.Ø,      Ø.Ø,      Ø.ØØØ1433,Ø.ØØ1484, Ø.Ø112,  Ø.Ø2683,
     2  Ø.Ø42Ø5,  Ø.Ø2802,  Ø.Ø1515,  Ø.ØØ9797, Ø.ØØ6751, Ø.ØØ4911,
     2  Ø.ØØ5836,                     Ø.Ø,      Ø.Ø,      Ø.Ø,
     3  Ø.Ø,      Ø.Ø,      Ø.Ø,      Ø.Ø,      Ø.Ø,      Ø.Ø,
     4  Ø.ØØØ7,   Ø.ØØ5523, Ø.Ø4966,  Ø.Ø7569,  Ø.Ø4417,  Ø.Ø2667,
     4  Ø.Ø1807,  Ø.Ø1318,  Ø.Ø1283,                      Ø.Ø,
     5  Ø.Ø,      Ø.Ø,      Ø.Ø,      Ø.Ø,      Ø.Ø,      Ø.Ø,
     6  Ø.Ø,      Ø.Ø,      Ø.Ø,      Ø.Ø,      Ø.ØØ2Ø83, Ø.Ø3827,
     7  Ø.Ø5237,  Ø.Ø318,   Ø.Ø2Ø77,  Ø.Ø1512,  Ø.Ø12Ø7,
     7  Ø.Ø,      Ø.Ø,      Ø.Ø,      Ø.Ø,      Ø.Ø,
     8  Ø.Ø,      Ø.Ø,      Ø.Ø,      Ø.Ø,      Ø.Ø,      Ø.Ø,
     9  Ø.Ø,      Ø.ØØ1871, Ø.Ø3471,  Ø.Ø5ØØ3,  Ø.Ø3Ø89,  Ø.Ø2276,
     9  Ø.Ø1761,                      Ø.Ø,      Ø.Ø,      Ø.Ø,
     A  Ø.Ø,      Ø.Ø,      Ø.Ø,      Ø.Ø,      Ø.Ø,      Ø.Ø,
     B  Ø.Ø,      Ø.Ø,      Ø.Ø,      Ø.Ø,      Ø.ØØ1218, Ø.Ø2256,
     C  Ø.Ø3122,  Ø.Ø2241,  Ø.Ø1737,                      Ø.,
     C  Ø.,       Ø.,       Ø.,       Ø.,       Ø.,       Ø.,
     C  Ø.,       Ø.,       Ø.Ø/
C
      DATA RD4/  Ø.Ø,      Ø.Ø,      Ø.Ø.      Ø.Ø,      Ø.ØØ25,
     1  Ø.Ø2ØØ2,  Ø.Ø3135,  Ø.Ø2656,  Ø.,       Ø.,       Ø.,
     2  Ø.,       Ø.,       Ø.,       Ø.,       Ø.,       Ø.,
     3  Ø.,       Ø.,       Ø.,       Ø.,       Ø.,       Ø.ØØØØ6,
     4  Ø.ØØ2,    Ø.ØØ62Ø3, Ø.ØØ9765. Ø.,       Ø.,       Ø.,
     5  Ø.,       Ø.,       Ø.,       Ø.,       Ø.,       Ø.,
     6  Ø.,       Ø.,       Ø.,       Ø.,       Ø.,       Ø.,
     7  Ø.ØØØØ9,  Ø.Ø3,     Ø.Ø1Ø2,   Ø.,       Ø.,       Ø.,
     8  Ø.,       Ø.,       Ø.,       Ø.,       Ø.,       Ø.,
     9  Ø.,       Ø.,       Ø.,       Ø.,       Ø.,       Ø.,
     A  Ø.,       Ø.ØØØØ36, Ø.ØØ24/
C
C
C  NEXT IS LARGE DETECTOR PHOTON RESPONSE
C
       DATA RB2/  Ø.Ø6565,  Ø.Ø8203,  Ø.Ø5642,  Ø.Ø4115,  Ø.Ø3243,
     A Ø.Ø2555,   Ø.Ø2144,  Ø.Ø2782,  Ø.Ø1471,  Ø.Ø1Ø8,   Ø.Ø1Ø47,
     B Ø.ØØ782,   Ø.ØØ4851, Ø.ØØ2873, Ø.ØØ1764, Ø.ØØ1163, Ø.ØØØ6284,
     C Ø.ØØØ6953,Ø.Ø1135,   Ø.Ø375,   Ø.Ø5631,  Ø.Ø3734,  Ø.Ø2836,
     D Ø.Ø2169,   Ø.Ø1892,  Ø.Ø1553,  Ø.Ø1264,  Ø.Ø111,   Ø.ØØ9Ø43,
     E Ø.ØØ6667,  Ø.ØØ4Ø89, Ø.ØØ251,  Ø.ØØ1567, Ø.ØØ1Ø29, Ø.ØØØ5459,
     F Ø.ØØØ6238,Ø.,        Ø.Ø1777,  Ø.Ø4644,  Ø.Ø6587,  Ø.Ø4452,
     G Ø.Ø3191,   Ø.Ø284,   Ø.Ø2338,  Ø.Ø1918,  Ø.Ø1642,  Ø.Ø1383,
     H Ø.ØØ9965,  Ø.ØØ6296, Ø.ØØ3877, Ø.ØØ2424, Ø.ØØ1585, Ø.ØØØ8341,
     I Ø.ØØØ98Ø4,Ø.Ø,       Ø.Ø,      Ø.ØØ66,   Ø.Ø3757,  Ø.Ø5741,
     J Ø.Ø3715,   Ø.Ø2906,  Ø.Ø2363,  Ø.Ø2,     Ø.Ø1763,  Ø.Ø144,
     K Ø.Ø1ØØ93,  Ø.ØØ6592, Ø.ØØ4Ø16, Ø.ØØ2627, Ø.ØØ1705, Ø.ØØ1261,
     L Ø.ØØ1Ø81,  Ø.,       Ø.,       Ø.,       Ø.ØØ897,  Ø.Ø3Ø31,
     M Ø.Ø477,    Ø.Ø3606,  Ø.Ø2447,  Ø.Ø2Ø51,  Ø.Ø1761,  Ø.Ø1442,
     N Ø.ØØ9864,  Ø.ØØ6474, Ø.ØØ41Ø7, Ø.ØØ2636, Ø.ØØ1754, Ø.ØØ13Ø3,
     O Ø.ØØ1114,  Ø.,       Ø.,       Ø.,       Ø.ØØØ9,   Ø.Ø1Ø35,
     P Ø.Ø262,    Ø.Ø4248,  Ø.Ø3161,  Ø.Ø2281,  Ø.Ø1898,  Ø.Ø1509,
     Q Ø.Ø1Ø13,  Ø.ØØ6675,  Ø.ØØ4268, Ø.ØØ2798, Ø.ØØ1855, Ø.ØØ1392,
     R Ø.ØØ1188, Ø.,        Ø.,       Ø.,       Ø.,       Ø.ØØ171,
     S Ø.ØØ771,   Ø.Ø233,   Ø.Ø3641,  Ø.Ø262,   Ø.Ø2Ø93,  Ø.Ø1613,
     T Ø.Ø1ØØ8,   Ø.ØØ69Ø9, Ø.ØØ4356, Ø.ØØ2872, Ø.ØØ1923, Ø.ØØ1446,
     U Ø.ØØ1239, Ø.,        Ø.,       Ø.,       Ø.Ø/
C
       DATA RB22/ Ø.,
     V Ø.ØØ232,   Ø.ØØ832,  Ø.Ø2338,  Ø.Ø4Ø82,  Ø.Ø2949,  Ø.Ø2Ø83,
     W Ø.Ø12Ø1,   Ø.ØØ8214, Ø.ØØ52Ø1/
C
```

```
      DATA RB3/  0.00357,  0.002354, 0.00178,  0.001522,
     A 0.,       0.,       0.,       0.,       0.00003,
     B 0.00199,  0.00647,  0.01765,  0.02961,  0.01924,  0.01028,
     C 0.006619, 0.004305, 0.002881, 0.001965, 0.001488, 0.00126,
     D 0.,       0.,       0.,       0.,       0.,
     E 0.00054,  0.00255,  0.00917,  0.01804,  0.02832,  0.01349,
     F 0.007605, 0.004939, 0.003353, 0.002295, 0.001742, 0.001502,
     G 0.,       0.,       0.,       0.,       0.,
     H 0.,       0.000684, 0.00213,  0.01018,  0.02467,  0.02554,
     I 0.01244,  0.008075, 0.005501, 0.003773, 0.002927, 0.002527,
     J 0.,       0.,       0.,       0.,       0.,
     K 0.,       0.,       0.,       0.00007,  0.00713,  0.04458,
     L 0.04089,  0.02117,  0.01463,  0.009712, 0.007962, 0.006849,
     M 0.,       0.,       0.,       0.,       0.,       0.,
     N 0.,       0.,       0.,       0.,       0.,       0.001892,
     O 0.03118,  0.0287,   0.01533,  0.01068,  0.00843,  0.007355,
     P 0.,       0.,       0.,       0.,       0.,       0.,
     Q 0.,       0.,       0.,       0.,       0.,       0.,
     R 0.00131,  0.02803,  0.02909,  0.01524,  0.01153,  0.01025,
     S 0.,       0.,       0.,       0.,       0.,       0.,
     T 0.,       0.,       0.,       0.,       0.,       0.,
     U 0.,       0.001578, 0.01805,  0.01966,  0.01209,  0.009896,
     V 0.,       0.,       0.,       0.,       0.,       0.,
     W 0.,       0.,       0.,       0.0/
C
      DATA RB4/  0.,       0.,
     A 0.,       0.,       0.001901, 0.01694,  0.02328,  0.01674,
     B 0.,       0.,       0.,       0.,       0.,       0.,
     C 0.,       0.,       0.,       0.,       0.,       0.,
     D 0.,       0.,       0.,       0.001625, 0.005163, 0.008411,
     E 0.,       0.,       0.,       0.,       0.,       0.,
     F 0.,       0.,       0.,       0.,       0.,       0.,
     G 0.,       0.,       0.,       0.000536, 0.003463, 0.00737,
     H 0.,       0.,       0.,       0.,       0.,       0.,
     I 0.,       0.,       0.,       0.,       0.,       0.,
     J 0.,       0.,       0.,       0.,       0.000677, 0.002094/
C
CC  NEXT IS NEUTRON RESPONSE OF MEDIUM DETECTOR
C
      DATA RE2/  0.04561,  0.06487,  0.06093,  0.0465,   0.03355,
     B 0.02653,  0.02126,  0.01801,  0.01518,  0.01354,  0.01097,
     C 0.007866, 0.004782, 0.00367,  0.005031, 0.004792, 0.004888,
     C 0.004521, 0.009574, 0.02823,  0.04171,  0.040,    0.03007,
     D 0.0242,   0.01862,  0.01555,  0.01285,  0.01155,  0.009248,
     E 0.006602, 0.00404,  0.002939, 0.002492, 0.003334, 0.004328,
     F 0.0035,   0.0009,   0.01218,  0.03179,  0.04784,  0.04498,
     G 0.03841,  0.02972,  0.02399,  0.01964,  0.01716,  0.01353,
     H 0.009726, 0.005953, 0.004172, 0.002718, 0.002959, 0.00517,
     I 0.005044, 0.,       0.00467,  0.0070,   0.02508,  0.03689,
     J 0.03858,  0.0332,   0.02644,  0.02175,  0.018,    0.0138,
     K 0.01018,  0.006204, 0.004132, 0.002634, 0.00324,  0.003896
     L 0.005054, 0.,       0.,       0.0003548,0.0063,   0.01991,
     M 0.03032,  0.03132,  0.0273,   0.02319,  0.01849,  0.014,
     N 0.0102,   0.006223, 0.003951, 0.002677, 0.002596, 0.003075,
     O 0.004063, 0.,       0.,       0.,       0.000367, 0.005875,
     P 0.01738,  0.02563,  0.02659,  0.02436,  0.02064,  0.0155,
     Q 0.01053,  0.006437, 0.003993, 0.002781, 0.00222,  0.002778,
     R 0.003281, 0.,       0.,       0.,       0.,       0.000433,
     S 0.005565, 0.01441,  0.02191,  0.02307,  0.02139,  0.01701,
     T 0.01102,  0.0066,   0.004059, 0.002803, 0.001803, 0.002521,
     U 0.002756, 0.,       0.,       0.,       0.0/
C
      DATA RE22/ 0.,
     V 0.000522, 0.005322, 0.01604,  0.02202,  0.02408,  0.02123,
     W 0.01408,  0.008139, 0.004943/
C
```

```
      DATA RE3/  0.003408,  0.002186,  0.002496,  0.002994,
     A 0.,       0.,        0.,        0.,        0.,
     B 0.000252, 0.004279,  0.01055,   0.01568,   0.01657,   0.01214,
     C 0.006897, 0.004097,  0.002809,  0.001851,  0.001646,  0.002239,
     D 0.,       0.,        0.,        0.,        0.,
     E 0.,       0.00044,   0.004618,  0.01107,   0.01773,   0.01468,
     F 0.008416, 0.004901,  0.003289,  0.002139,  0.001651,  0.002291,
     G 0.,       0.,        0.,        0.,        0.,
     H 0.,       0.,        0.0004745, 0.0050,    0.0165,    0.02429,
     I 0.01418,  0.00823,   0.005162,  0.003475,  0.002458,  0.002963,
     J 0.,       0.,        0.,        0.,        0.,
     K 0.,       0.,        0.,        0.0001,    0.0015,    0.02779,
     L 0.0395,   0.02314,   0.01368,   0.009373,  0.006882,  0.006403,
     M 0.,       0.,        0.,        0.,        0.,
     N 0.,       0.,        0.,        0.,        0.00003,   0.00056,
     O 0.02222,  0.02705,   0.01651,   0.01057,   0.008048,  0.005704,
     P 0.,       0.,        0.,        0.,        0.,        0.,
     Q 0.,       0.,        0.,        0.,        0.,        0.,
     R 0.0006,   0.01964,   0.02553,   0.01582,   0.01186,   0.0090,
     S 0.,       0.,        0.,        0.,        0.,        0.,
     T 0.,       0.,        0.,        0.,        0.,        0.,
     U 0.,       0.00034,   0.01189,   0.0162,    0.01147,   0.009093,
     V 0.,       0.,        0.,        0.,        0.,        0.,
     W 0.,       0.,        0.,        0.0/
C
      DATA RE4/  0.,        0.,
     A 0.,       0.,        0.00282,   0.01109,   0.01607,   0.0131,
     B 0.,       0.,        0.,        0.,        0.,        0.,
     C 0.,       0.,        0.,        0.,        0.,        0.,
     D 0.,       0.,        0.,        0.000186,  0.003418,  0.00514,
     E 0.,       0.,        0.,        0.,        0.,        0.,
     F 0.,       0.,        0.,        0.,        0.,        0.,
     G 0.,       0.,        0.,        0.,        0.000533,  0.00641,
     H 0.,       0.,        0.,        0.,        0.,        0.,
     I 0.,       0.,        0.,        0.,        0.,        0.,
     J 0.,       0.,        0.,        0.,        0.,        0.00023/
C
CC    NEXT IS PHOTON RESPONSE OF MEDIUM DETECTOR
C
      DATA RC2/  0.03967,   0.04644,   0.02963,   0.02273,   0.01843,
     A 0.01438,  0.01241,   0.010,     0.008406,  0.007236,  0.005701,
     B 0.004237, 0.002786,  0.001633,  0.001002,  0.000651,  0.0004908,
     C 0.0003796,0.001934,  0.02295,   0.03099,   0.01972,   0.01537,
     D 0.01197,  0.0105,    0.008607,  0.007306,  0.006271,  0.005035,
     E 0.003561, 0.002286,  0.001429,  0.0008884, 0.000579,  0.0004359,
     F 0.0003404,0.0,       0.004115,  0.02617,   0.03623,   0.02376,
     G 0.01814,  0.01583,   0.01286,   0.01099,   0.009536,  0.00767,
     H 0.005324, 0.003435,  0.002201,  0.00135,   0.0008949, 0.0006854,
     I 0.0005304,0.0,       0.,        0.001097,  0.02145,   0.03082,
     J 0.01922,  0.01622,   0.01322,   0.01136,   0.009787,  0.00798,
     K 0.005372, 0.003467,  0.002253,  0.001428,  0.0009403, 0.0007275,
     L 0.0005659,0.0,       0.,        0.,        0.001261,  0.01736,
     M 0.02459,  0.01735,   0.01313,   0.01117,   0.00987,   0.008033,
     N 0.005218, 0.003461,  0.002241,  0.001446,  0.0009703, 0.0007355,
     O 0.0005796,0.0,       0.,        0.,        0.,        0.00217,
     P 0.01412,  0.02199,   0.01498,   0.01219,   0.01024,   0.008359,
     Q 0.005343, 0.003487,  0.002297,  0.001497,  0.001018,  0.0007812,
     R 0.0006176,0.0,       0.,        0.,        0.,        0.,
     S 0.002005, 0.01269,   0.01865,   0.01335,   0.01101,   0.008542,
     T 0.005256, 0.003566,  0.002359,  0.001527,  0.001053,  0.0008164,
     U 0.0006512,0.0,       0.,        0.,        0.0/
C
      DATA RC22/ 0.,
     V 0.0000224,0.002228,  0.01244,   0.02092,   0.01463,   0.01083,
     W 0.006371, 0.004191,  0.002815/
C
```

```
      DATA RC3/  0.001848, 0.001273, 0.0009933,0.000798,
     A 0.,       0.,       0.,       0.,       0.,
     B 0.000193, 0.001883, 0.009049, 0.0151,   0.009537, 0.005481,
     C 0.003396, 0.002323, 0.001517, 0.001044, 0.0008149,0.0006562,
     D 0.,       0.,       0.,       0.,       0.,
     E 0.,       0.000309, 0.001045, 0.009155, 0.01405,  0.006681,
     F 0.003939, 0.002602, 0.001767, 0.001212, 0.0009524,0.000759,
     G 0.,       0.,       0.,       0.,       0.,
     H 0.,       0.,       0.,       0.000456, 0.0123,   0.0117,
     I 0.006519, 0.004277, 0.002861, 0.001998, 0.001556, 0.001258,
     J 0.,       0.,       0.,       0.,       0.,
     K 0.,       0.,       0.,       0.,       0.00005,  0.02231,
     L 0.02042,  0.01137,  0.007538, 0.005354, 0.00425,  0.003432,
     M 0.,       0.,       0.,       0.,       0.,       0.,
     N 0.,       0.,       0.,       0.,       0.,       0.00004,
     O 0.01405,  0.01402,  0.008051, 0.005453, 0.004418, 0.003625,
     P 0.,       0.,       0.,       0.,       0.,       0.,
     Q 0.,       0.,       0.,       0.,       0.,       0.,
     R 0.00002,  0.01413,  0.01299,  0.008033, 0.006404, 0.004894,
     S 0.,       0.,       0.,       0.,       0.,       0.,
     T 0.,       0.,       0.,       0.,       0.,       0.,
     U 0.,       0.00005,  0.008857, 0.008761, 0.006287, 0.004844,
     V 0.,       0.,       0.,       0.,       0.,       0.,
     W 0.,       0.,       0.,       0.0/
C
      DATA RC4/  0.,       0.,
     A 0.,       0.,       0.000005, 0.007638, 0.01038,  0.00741,
     B 0.,       0.,       0.,       0.,       0.,       0.,
     C 0.,       0.,       0.,       0.,       0.,       0.,
     D 0.,       0.,       0.,       0.000077, 0.002362, 0.003475,
     E 0.,       0.,       0.,       0.,       0.,       0.,
     F 0.,       0.,       0.,       0.,       0.,       0.,
     G 0.,       0.,       0.,       0.,       0.0003682,0.00312
     H 0.,       0.,       0.,       0.,       0.,       0.,
     I 0.,       0.,       0.,       0.,       0.,       0.,
     J 0.,       0.,       0.,       0.,       0.,       0.0002836/
CC
CC    (IF THERE ARE ANY DISCREPANCIES BETWEEN THESE TABULATED
CC       RESULTS AND DATA IN APPENDIX A, THE APPENDIX A DATA ARE
CC       THE CORRECT VALUES.)
C
      KK=K
      RESPON=1.E+20
      IF (I.LE.0.OR.J.LE.0) RETURN
      IF (I.GT.18 .OR. J.GT.19) RETURN
      IF (KK.EQ.1) RESPON=RN1(I,J)
      IF (KK.EQ.2) RESPON=RG1(I,J)
      IF (KK.EQ.3) RESPON=RN2(I,J)
      IF (KK.EQ.4) RESPON=RG2(I,J)
      RETURN
      END
CC
CC
```

```
      SUBROUTINE CALIBR
      COMMON /CALIB/ XZERO,SLOPE
      DIMENSION C(2),P(2)
      WRITE(5,80)
   80 FORMAT(/,'  ENTER CALIBRATION DATA'$)
C
C  INPUT P(J)> Ø  THEN IN LIGHT UNITS
C  INPUT P(J)< Ø  THEN IN E(NEUTRON) IN MEV
      DO 1 J=1,2
      WRITE(5,81)J
81    FORMAT('$ FOR J=',I2,', ENTER CHANNEL & P.H. IN 2FIØ.4 FORMAT >>')
      READ(5,82) C(J),P(J)
   82 FORMAT(2FIØ.4)
1     CONTINUE
C
      DO 6 J=1,2
      PP=-P(J)
      IF (P(J).LT.Ø.Ø) P(J)=ETOL(2,PP)
6     CONTINUE
C
      SL=(P(2)-P(1))/(C(2)-C(1))
      SLOPE=SL
      XZERO=P(1)-C(1)*SL
      WRITE (6,83) XZERO,SL
      WRITE(5,83) XZERO,SL
      WRITE(1,83) XZERO,SL
   83 FORMAT('   P.H. (L-U) =',1PEIØ.3,'  + CHAN-NO * ',E11.4/)
      RETURN
      END
```

```
C     THIS IS FILE BINSUM.FTN
      SUBROUTINE BINSUM(IMAX,IDAT,SDAT,DDAT,JB)
C++
C  PURPOSE IS TO BIN (OR CRUNCH) THE RAW DATA INTO YIELDS-
C  PER-PREDETERMINED PULSE-HEIGHT BINS.  THE BINNED DATA ARE
C  RETURNED IN 'SDAT' WITH UNCERTAINTIES IN 'DDAT'.  THERE ARE
C  'JB' SUCH ELEMENTS IN 'SDAT'
C++
      DIMENSION IDAT(1),SDAT(1),DDAT(1),BLIMS(20),DSUM(250)
      DIMENSION PH(250)
      COMMON /DAT/ ELOW(19),EHIGH(19),DM1(19),DM2(190),DM3(190),
     1   DM4(19),DM5(19),DM6(19)
      COMMON /BLOWER/ MINBIN,TX
      COMMON /CALIB/ XZERO,SLOPE
      COMMON /RESP/ MS
      DATA JBINS/19/
      DATA BLIMS/.097,.132,.164,.215,.272,.333,.4,.4725,.565,
     X   .645,.742,.911,1.424,2.05,3.06,4.15,5.8,6.5,7.7,8.5/
C
C  FIRST STEP IS TO DETERMINE PH<LOWER> AND PH<HIGHER> OF THE
C  HISTOGRAM CHANNELS, AND TO GET A RUNNING SUM OF THE DATA
C
      DSUM(1)=FLOAT(IDAT(1))
      IF(DSUM(1).LT.0.0) DSUM(1)=DSUM(1)+65536.0
      PH(1)=XZERO-0.5*SLOPE
      DO 4 I=2,IMAX
      FIDAT=FLOAT(IDAT(I))
      IF(FIDAT.LT.0.0) FIDAT=FIDAT+65536.0
      DSUM(I)=DSUM(I-1) + FIDAT
 4    PH(I)=PH(I-1) + SLOPE
C
C  MAIN LOOP FOLLLOWS
      SUMLOW=AA(BLIMS(1),PH,DSUM,IMAX)
      JJJ=JBINS+1
      DO 7 J=2,JJJ
      BHI=BLIMS(J)
      SUMHI=AA(BHI,PH,DSUM,IMAX)
      SDAT(J-1)=SUMHI-SUMLOW
      DDAT(J-1)=SQRT(SDAT(J-1))
      IF (DDAT(J-1).GT.0.0) GO TO 6
      DDAT(J-1)=1.0
      IF (BHI.LT.PH(1)) DDAT(J-1)=0.0001
      IF (BHI.GT.PH(IMAX)) DDAT(J-1)=0.0001
C   LAST 2 CASES OUTSIDE OF RANGE OF RAW DATA
 6    SUMLOW=SUMHI
 7    CONTINUE
C
C  GET NEUTRON OR PHOTON ENERGIES AT BIN LIMITS
      MP=MS/2
      MQ=MS-2*MP
      IF (MQ.EQ.0) MQ=3
      ELOW(1)=ETOL(MQ,BLIMS(1))
      EHIGH(1)=ETOL(MQ,BLIMS(2))
      DO 20 J=2,JBINS
      ELOW(J)=EHIGH(J-1)
      EHIGH(J)=ETOL(MQ,BLIMS(J+1))
20    CONTINUE
C
C  FIND BIN WITH LARGEST YIELD PER BIN-WIDTH
C  ITS INDEX WILL BE THE VARIABLE 'MINBIN'
C  ITS YIELD WILL BE THE VARIABLE 'TX'
C
      DE=EHIGH(1)-ELOW(1)
      T=SDAT(1)/DE
      J=1
      DO 25 I=2,JBINS
      DE=EHIGH(I)-ELOW(I)
      TB=SDAT(I)/DE
      IF (TB.LT.T .AND. I.EQ.2) GO TO 25
      IF (TB.GT.T) GO TO 23
      IF (I.GT.2) GO TO 27
23    J=I
      T=TB
      TX=SDAT(I)
25    CONTINUE
27    MINBIN=J
```

```
C
C    NOW WE TEST FOR POSSIBLY HIGHEST ENERGY BINS
C       HAVING ENERGIES CORRESPONDING TO CHANNELS > 250
          JB=0
          DO 30 J=1,JBINS
          IF (BLIMS(J).GT.PH(IMAX)) GOTO 50
  30      JB=JB+1
C    IF SO WE REDUCE THE NUMBER OF ACTIVE BINS IN
C       THE CALCULATION
          JB=JBINS
  50      RETURN
          END
CC
CC
CC
      FUNCTION AA(A,B,C,N)
C++
C  LINEAR INTERPOLATION
C++
      DIMENSION B(1),C(1)
      AA=C(1)
      IF(A.LE.B(1)) RETURN
      AA=C(N)
      NM=N-1
      DO 1 I=2,NM
      IF( A.LT. B(I+1)) GOTO 7
  1   CONTINUE
      RETURN
  7   R=(A-B(I))/(B(I+1)-B(I))
      S=C(I-1)+R*(C(I)-C(I-1))
      AA=S
      RETURN
      END
```

```
      SUBROUTINE RAWDAT(M,IDAT,NSLOT,PLOTID)
C++
C  THIS PROGRAM READS NE-213 RAW DATA AND RETURNS IT TO THE CALLER
C  M=1 FOR LARGE DETECTOR, NEUTRON
C  M=2 FOR LARGE DETECTOR, GAMMA
C  M=3 FOR MONITOR DETECTOR, NEUTRON
C  M=4 FOR MONITOR DETECTOR, GAMMA
C  IDAT IS THE ARRAY TO RETURN DATA
C++
      INCLUDE  'NECOM.FTN'
C
C          (SEE APPENDIX 'D' FOR FILE 'NECOM.FTN')
C
      INTEGER   IDAT(1)
      BYTE      PLOTID(1)
C
C  ASK FOR SLOT NUMBER
5     WRITE(5,90)
90    FORMAT('$ ENTER DATA SLOT NUMBER, 1-5 >> ')
      READ(5,910) NSLOT
910   FORMAT(I2)
      IF (NSLOT.LT.1.OR.NSLOT.GT.5) THEN
        WRITE(5,920)
120     FORMAT('  ERROR??? SLOT 1 TO 5 ONLY, TRY AGAIN')
        GOTO 5
      ENDIF
C
C  READ FILE 'NESUM.DAT' FOR THE RAW DATA
      OPEN(UNIT=4,FILE='NESUM.DAT',STATUS='OLD',READONLY,
     1 FORM='UNFORMATTED',BUFFERCOUNT=1,ACCESS='DIRECT',
     2 RECORDTYPE='FIXED',RECL=512)
      READ(UNIT=4,REC=NSLOT) NEREC
      CLOSE(UNIT=4)
C
C  GET THE USER'S RAW DATA,
C  ADC1(I) IS MONITOR DETECTOR, NEUTRON
C  ADC2(I) IS LARGE DETECTOR, NEUTRON
C  ADC3(I) IS LARGE DETECTOR, GAMMA
C  ADC4(I) IS MONITOR DETECTOR, GAMMA
      GOTO (10,20,30,40) M      \GET DIFFERENT DATA ARRAY
C
10    DO 15, I=1,240
      IDAT(I)=ADC2(I)
15    CONTINUE
      GOTO 50
20    DO 25, I=1,240
      IDAT(I)=ADC3(I)
25    CONTINUE
      GOTO 50
C
30    DO 35, I=1,240
      IDAT(I)=ADC1(I)
35    CONTINUE
      GOTO 50
C
40    DO 45, I=1,240
      IDAT(I)=ADC4(I)
45    CONTINUE
C
50    DO 55,I=240,250
      IDAT(I)=0
55    CONTINUE
C
C  RETURN THE RECORD DESCRIPTION
      DO 60, I=1,64
      PLOTID(I)=SUMID(I)
60    CONTINUE
      RETURN
      END
```

```
      SUBROUTINE PUTDAT(MINBIN,NP,MM,NSLOT,SUMID)
C++
C  THIS ROUTINE PUTS DATA INTO FILE 'NEPLOT.DAT', THE INVOKES
C  TASK 'NEPLOT' TO DO THE PLOTTING
C++
      COMMON /RESULT/ EM(18),DEM(18),AA(18),DAA(18)
      BYTE    SUMID(64)
      REAL    NEPLOT
      DATA    NEPLOT/6RNEPLOT/
      INTEGER IBUF(13)
C
C  OPEN FILE 'NEPLOT.DAT'
      OPEN(UNIT=4,FILE='NEPLOT.DAT',STATUS='OLD',
     1 FORM='UNFORMATTED',BUFFERCOUNT=2,RECORDTYPE='FIXED',
     2 RECL=90,ACCESS='DIRECT')
C
C  GET RECORD NUMBER FROM THE SLOT NUMBER AND DETECTOR SELECTED
      RECNO=(NSLOT-1)*4+MM       \EACH SLOT HAS 4 GRAPHICS DATASET
      WRITE(UNIT=4,REC=RECNO) EM,DEM,AA,DAA,SUMID,NIMBIN,NP,MM,NSLOT
      CLOSE(UNIT=4)
C
C  INVOKE TASK 'NEPLOT.TSK' TO DO THE PLOTTING
C  PASS THE RECORD NUMBER
      IBUF(1)=RECNO
      CALL SDRC(NEPLOT,IBUF )
C
      RETURN
      END
```

```
C   THIS IS FILE SHOWG.FTN
C       ADAPTED FROM N M LARSON VERSION
C
      SUBROUTINE OUTPAR
      COMMON /NUMBER/ NDAT,NPAR,ITER, ITMAX, CONVER
      COMMON /PAR/ POLD(18),PARM(18),PDUM(18),VARPAR(171),
     X  VARNEW(171),IDUM(18)
C
      WRITE (1,99)
      II = 0
      DO 10 I=1,NPAR
      II=II+I
      PDUM(I)=SQRT(VARPAR(II))
   10 CONTINUE
      WRITE (1,98)
        DO 15 I=1,NPAR
        ZPARM=PARM(I)
        ZPDUM=PDUM(I)
        IF (ZPARM.NE.0.0) GO TO 13
        IF (ZPDUM.NE.0.0) GO TO 12
        WRITE(1,94) I
        GO TO 15
   12   WRITE(1,95) I,ZPDUM
        GO TO 15
   13   IF (ZPDUM.NE.0.0) GO TO 14
        WRITE(1,93) I,ZPARM
        GO TO 15
   14   WRITE (1,97) I,ZPARM,ZPDUM
    15  CONTINUE
      CALL OUTV(VARPAR,PDUM,IDUM,NPAR)
       RETURN
C
   99 FORMAT (/29H ******INPUT PARAMETER VALUES)
   98 FORMAT(34H          PARAMETER     UNCERTAINTY)
   97 FORMAT(I5,1P2E14.5)
   95   FORMAT(I5,3X,3H0.0,8X,1PE14.5)
   94   FORMAT(I5,3X,3H0.0,14X,3H0.0)
   93   FORMAT(I5,1PE14.5,3X,3H0.0)
      END
C
C
C
      SUBROUTINE OUTTH
      COMMON /BLOWER/ MIN,TDUM
      COMMON /NUMBER/ NDAT,NPAR,ITER,ITMAX,CONVER
      COMMON /PAR/ POLD(18),PARM(18),PDUM(18),
     X VARPAR(171),VARNEW(171),IDUM(18)
      COMMON /DAT/ E(19),E2(19),DATA(19),VARDAT(190),EN(190),
     X TH(19),DUM(19),SIG(19)
      COMMON /JKD/ UNC(19)
      COMMON /RESP/ MNG
C
        IF (MIN.LE.0) MIN=1
        CHISQ=0.0
      WRITE (1,99)
      IF (MNG.EQ.1 .OR. MNG.EQ.3) WRITE (1,98)
      IF (MNG.EQ.2 .OR. MNG.EQ.4) WRITE (1,92)
        DO 1 I=1,NDAT
        CHI=(DATA(I)-TH(I))/UNC(I)
        IF (I.GE.MIN) CHISQ=CHISQ+CHI*CHI
        ZDATA=DATA(I)
        ZTH=TH(I)
        EDELTA=E2(I)-E(I)
        ZDD1=ZDATA/EDELTA
        ZDD2=ZTH/EDELTA
        ZCHI=CHI
        IF(I.LT.MIN) WRITE(1,95)I,E(I),E2(I),ZDATA,ZTH,ZCHI,ZDD1,ZDD2
        IF(I.GE.MIN) WRITE(1,97)I,E(I),E2(I),ZDATA,ZTH,ZCHI,ZDD1,ZDD2
    1   CONTINUE
        IF (MIN.EQ.1) WRITE(1,96) CHISQ
        MINN=MIN-1
        IF (MIN.EQ.2) WRITE(1,93) CHISQ
        IF (MIN.GT.2) WRITE(1,94) CHISQ,MINN
      RETURN
```

```
C
  99  FORMAT (/30H ***** THEORETICAL CALCULATION,36X,5HDATA/,
     S   6X,7HTHEORY/)
  98  FORMAT(55H       E-NEUTRON BIN       DATA       THEORY     (EXP-TH)/U
     X    2HNC,2X,2(4X,9HBIN-WIDTH) )
  97  FORMAT(I5,0PF6.2,2H -,F6.2,2F12.1,1PE14.4,4X,2E13.5)
  96  FORMAT(40X,6HCHISQ=,1PE11.4)
  95    FORMAT(I5,0PF6.2,2H -,F6.2,2F12.1,1PE14.4,4H**  ,1P2E13.5)
  94  FORMAT(40X'CHISQ='1PE11.4,8H EXCEPT ,I2,21H' DATA HAVING ** IDENT
     X   /)
  93  FORMAT(40X'CHISQ='1PE11.4,31H EXCEPT 1 DATUM HAVING ** IDENT/)
  92  FORMAT(8X,46HE-GAMMA BIN       DATA       THEORY     (EXP-TH)/
     X   3HUNC,2X,2(4X,9HBIN-WIDTH))
      END
C
CC
C
      SUBROUTINE OUTP1
      COMMON /NUMBER/ NDAT,NPAR,ITER,ITMAX,CONVER
      COMMON /PAR/ POLD(18),PARM(18),PDUM(18),VARPAR(171),
     X  VARNEW(171),IDUM(18)
      COMMON /DAT/ E(19),E2(19),DATA(19),VARDAT(190),EN(190),
     X   TH(19),DUM(19),SIG(19)
      COMMON /BLOWER/ MINBIN,TXX
C
      WRITE(1,99)
      WRITE(1,98)
C
        ZOLDT=0.0
        ZNEWT=0.0
      DO 10 I=1,NPAR
        ZPOLD=POLD(I)
        ZPARM=PARM(I)
        ZOLDT=ZOLDT+ZPOLD
        IF (I.GE.MINBIN) ZNEWT=ZNEWT+ZPARM
        ZD=E2(I)-E(I)
        ZZ=ZPARM/ZD
      WRITE(1,97) I,ZPOLD,ZPARM,ZZ
      IF (I.EQ. MINBIN-1) WRITE(1,90)
   10 CONTINUE
      WRITE(1,91) ZOLDT,ZNEWT
      RETURN
C
  99  FORMAT(/27H ***** INTERMEDIATE RESULTS )
  98  FORMAT(49H              OLD PARAM      NEW PARAM       NEW/BIN)
  97  FORMAT(I7,0P3F14.2)
  91  FORMAT(' TOTALS='F13.2,F14.2,24H FOR DATA BELOW THE LINE)
  90  FORMAT(3X,24(2H- ))
      END
C
C
C
      SUBROUTINE OUTP2
      COMMON /NUMBER/ NDAT,NPAR,ITER,ITMAX,CONVER
      COMMON /PAR/ POLD(18),PARM(18),PDUM(18),VARPAR(171),
     X VARNEW(171),IDUM(18)
      COMMON /DAT/ E(19),E2(19),DATA(19),VARDAT(190),EN(190),
     X  TH(19),DUM(19), SIG(19)
      COMMON /NORM/ ANORM
      COMMON /RESULT/ EMED(18),DEMED(18),PMED(18),DPMED(18)
C
      WRITE (1,99)
C
      II=0
      DO 10 I=1,NPAR
      II=II+I
      PDUM(I)=SQRT(VARNEW(II))
   10 CONTINUE
```

```
C
      WRITE(1,98)
        DO 15 I=1,NPAR
        DE=E2(I)-E(I)
        DEMED(I)=DE
        EMED(I)=E(I)+Ø.5*DE
        X=PARM(I)*ANORM
        Y=PDUM(I)*ANORM
        PMED(I)=X
        DPMED(I)=Y
        Z1=1.ØD+Ø
        Z2=1.ØD+Ø
        IF (DE.LE.Ø.Ø) GO TO 14
        Z1=X/DE
        Z2=Y/DE
  14    ZL=Z1-Z2
        ZU=Z1+Z2
      WRITE(1,97) I,E(I),E2(I),POLD(I),PARM(I),PDUM(I),X,Y,Z1,Z2
     X   ,ZU,ZL,I
  15    CONTINUE
C
      CALL OUTV(VARNEW,PDUM,IDUM,NPAR)
      RETURN
C
  99  FORMAT(/34H ******* NEW VALUES FOR PARAMETERS)
  98  FORMAT(6X,13HE-NEUTRON BIN,5X,4HPOLD,7X,18HPNEW    UNCERTAINTY
     T  7X,8H-NORMED-,12X,9H-PER MED-,11X,5HUPPER,6X,5HLOWER)
  97  FORMAT(I5,F6.2,2H -,F6.2,1PE9.1,3,I5)
      END
C
C
      SUBROUTINE OUTV(V,S,IC,N)
      DIMENSION V(1),S(N),IC(N)
C
          WRITE (1,99)
C
C        SHORTENED VERSION OF N.M.L. ORIGINAL SINCE WE KNOW N < 25
C
        NN=N
        WRITE (1,98) (I,I=1,NN)
        MAX=Ø
        DO 3Ø I=1,NN
         MIN=MAX+1
         MAX=MAX+I
         JMAX=I
         SI = S(I)
         IL=MIN-1
         DO 1Ø L=1,JMAX
          IL=IL+1
          D=V(IL)*1ØØ.Ø/(S(L)*SI)
          IF (D.GT.Ø.Ø) D=D+Ø.5
          IF (D.LT.Ø.Ø) D=D-Ø.5
          IC(L)=D
   1Ø    CONTINUE
   3Ø   WRITE(1,97) I,SI,(IC(L),L=1,JMAX)
      RETURN
C
  99  FORMAT(32H ***    STD. DEV.    CORRELATION)
  98  FORMAT(18X,25I4)
  97  FORMAT(I5,1PE13.6,25I4)
      END
```

APPENDIX D. THE DATA-TAKING PROGRAM

The system is configured as shown in Fig. D-1. The interface hardware for the NE-213 detector signals consists of four LeCroy Research Systems Model 3512 peak-detector ADC modules plus one 3588 histogramming memory module. A 50-pin conductor cable connects these modules via front panel matching connectors. This cable is the common bus for exchanging data between the histogramming memory ("histogrammer") and the ADC modules. It works as follows:

1. The detector electronics send 1-μs pulses, with different pulse heights, to the peak detector ADC modules. These pulses are digitized into "channels" ranging from 1 to 240. This range was chosen to minimize the load on computer processing without compromising the accuracy needed for the intended use.
2. For each pulse, an ADC module sends the "channel" value to the histogrammer via the common bus. The histogrammer uses this datum as an address pointer, and the content of that memory location is increased by one (1). A total counts-per-channel data set is thus accumulated in the histogrammer. Each ADC is programmed to use a different memory partition within the histogrammer.

To communicate with to the Remote CAMAC crate, which is located inside the experimental building in the TCB (2000 ft away from the Local CAMAC crate), a Kinetics 3992-bit serial highway driver module is installed in the Local CAMAC crate. Through this 5 MHz, optical-fiber CAMAC link, the microcomputer programs and controls the CAMAC-resident modules in the Remote crate for data taking. The CAMAC driver software for this configuration was developed by the CICADA group. The PDP-11/23 is a standard package from Digital Equipment Corporation. It has a 10Mb Winchester drive disk and two floppy disk drivers, each of which can hold a 400Kb floppy disk. Currently this machine has 256Kb of memory; the operating system is micro-RSX. The CAMAC interface is Kinetics 3912/2912 plus the Q-bus auxiliary crate controller set. This pair allows the PDP-11/23 to access any of the modules in the Local communication crate, such as the graphics modules. The graphics capability is based on CICADA module types 205 and 208. A microcomputer sends down (via 3912/2912 auxiliary crate controller) high-level commands such as MOVE CURSOR, DRAW VECTOR, pixel-to-pixel addressing and bit-map manipulation. A composite video signal is output from the 205/208 hardware to an Electrohome 9-in. CRT, where the display is shown.

The data taking is started at one second before TFTR plasma pulse discharge (t_o) and it is stopped at 5 seconds after t_o, for a total duration of 6 seconds. Ideally, the start/stop should be triggered by hardware timing signals that are synchronized with the TFTR machine cycle. However, the LeCroy modules do not have an appropriate hardware control input. Currently, the data-taking start/stop is done by the software, and all the timing marks are accurate to $\sim \pm 0.25$ sec. At the end of the 6-sec period, data accumulation is stopped and the data are unloaded from the histogrammer and put onto the computer's hard disk.

Two data files store the raw data: NE-213.DAT and NE-213.IDX. The file NE-213.DAT contains records of fixed size (2Kb each), one for each shot. Data stored here are the raw counts/channel for every detector signal, data and time, shot number, and a 16-character description for each detector's characteristic parameters. The file NE-213.IDX is the index file for the NE-213.DAT file. These two files constitute an index-sequential organization, with two search keys in the index file: the date and time stamp; and the shot number. A user accesses the stored data by specifying a key value (a shot number) or a range of key values (starting/ending dates and times).

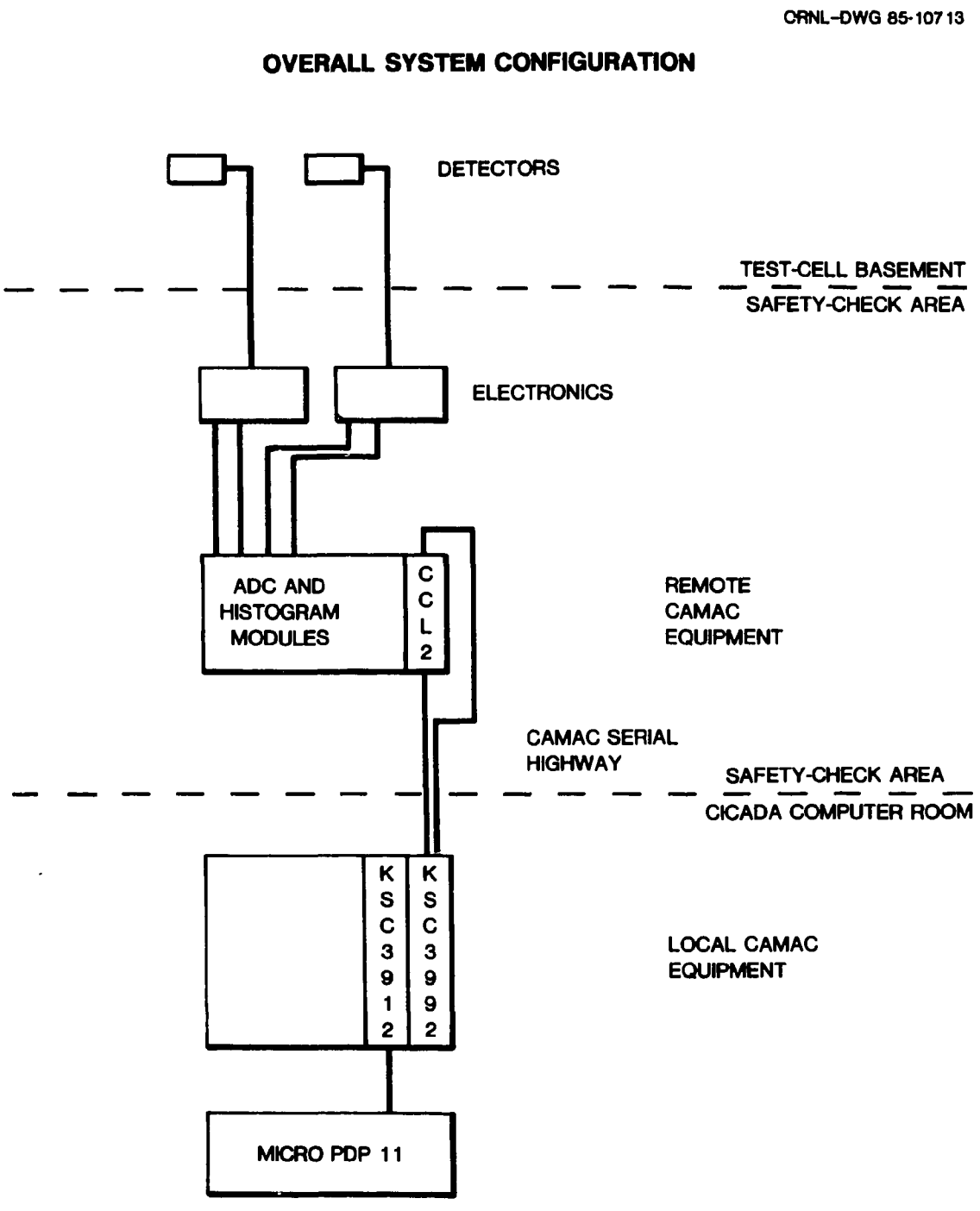

Fig. D.1. Overall system configuration exhibiting the relationships among the detectors, the CAMAC equipment, and the controlling computer.

The hard disk in the microcomputer system (10Mb) is shared among several users. Each user is limited to no more than 1Mb disk space. With this limitation, the on-line system can store data for ~450 TFTR plasma shots.

Once the data have been archived, there are utility programs to scan through the data records, or to sum up several records for better unfolding analysis. A software data-flow diagram, Fig. D.2, is included here to show the general software structure. Two of the programs, NEMAIN and NESUM, are listed on the following pages. There are brief descriptions from CICADA entitled "NE-213 Detector Diagnostics Overview Design" and "NE-213 Detector Diagnostics User's Guide" which provide detailed step-by-step illustrations of how to use the software utility programs.

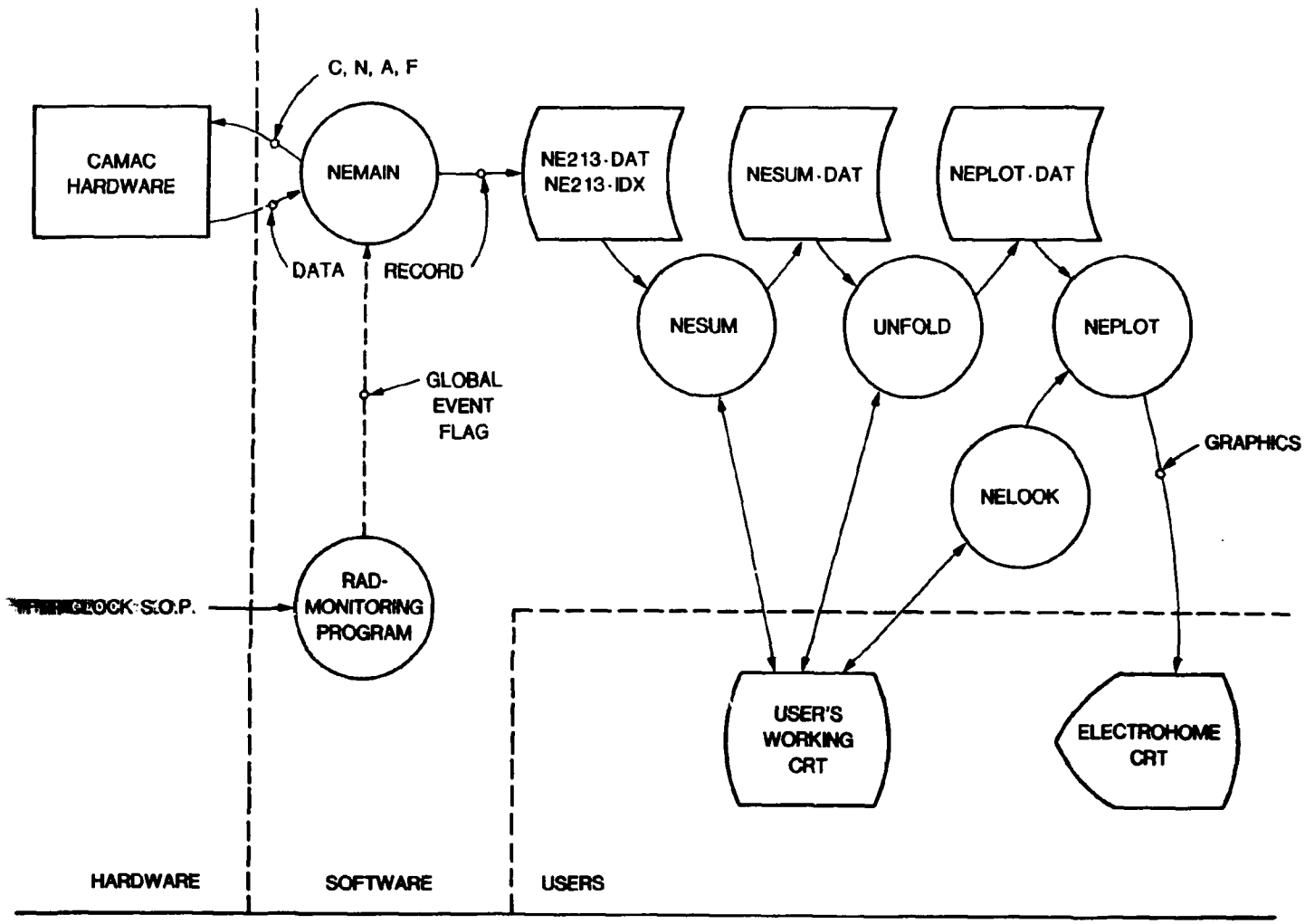

Fig. D.2. Flow diagram for the software for this experiment. The item labelled "Rad. Monitoring Program" is a system program which provides a flag, or signal, which is synchronized with the TFTR plasma shot.

```
      PROGRAM NEMAIN
C
C    THIS PROGRAM SERVES THE NE-213 DETECTORS.  THE ARMING IS
C    AT 1 SECOND BEFORE T ZERO.  DATA COLLECTION IS STOPPED AT
C    5 SECONDS AFTER T ZERO.
C
      IMPLICIT INTEGER (A-Z)
      REAL     SECNDS,NERPT
      DATA     NERPT/6RNERPT /          \ONLINE REPORT TASK
      INTEGER  IBUF(13)                 \USED FOR SDRC CALL TO PASS DATA
C
      INCLUDE 'NECOM.FTN'
C
C  READ FILE 'NEID.DAT' FOR THE 16 CHARACTERS DESCRIPTION FOR
C  EACH DETECTOR SIGNAL
      OPEN(UNIT=1,FILE='NEID.DAT',READONLY,STATUS='OLD',
     1   FORM='UNFORMATTED',BUFFERCOUNT=2,RECL=16,
     2   RECORDTYPE='FIXED')
      READ (UNIT=1) ADC1ID,ADC2ID,ADC3ID,ADC4ID
      CLOSE (UNIT=1)
C
C  PROGRAM THE ADC'S TO START THE DATA ACQUISITION, F(16)A(Ø)
      CALL TRANO(CRATE,NADC1,Ø,16,Ø,'Ø6ØØ'X,Ø,IERR)    \OFFSET Ø
      CALL TRANO(CRATE,NADC2,Ø,16,Ø,'Ø6Ø1'X,Ø,IERR)    \OFFSET 256
      CALL TRANO(CRATE,NADC3,Ø,16,Ø,'Ø6Ø2'X,Ø,IERR)    \OFFSET 512
      CALL TRANO(CRATE,NADC4,Ø,16,Ø,'Ø6Ø3'X,Ø,IERR)    \OFFSET 768
C
C  WAIT FOR THE EVENT FLAG FROM THE MASTER CONTROL TASK
1Ø    CALL WAITER(64,IDS)
C
C  A SHOT IS COMING,,,GET THE INSTRUMENT READY
C  DISABLE THE EXTERNAL PORT OF THE HISTOGRAMMER, F(19)A(Ø)
      CALL TRANO(CRATE,N3588,Ø,19,Ø,Ø,IERR)
C
C  CLEAR THE HISTOGRAMMER, F(9)A(Ø)
      CALL TRANI(CRATE,N3588,Ø,9,Ø,IERR)
C
C  GET THE SHOT NUMBER
      CALL GTSHOT(HSHOT)
C
C  RECORD THE DATE AND TIME FOR THIS SHOT
      CALL RCDATE(HDATE)
      CALL RCTIME(SECNDS(Ø.Ø),HTIME)
      LENGTH=6.Ø                        \DATA COLLECTION DURATION
C
C  WAIT FOR 1Ø SECONDS, TARGETING AT T MINUS 1
      CALL WAIT(6ØØ,Ø)
C
C  IT IS TIME TO ARM THE INSTRUMENT, RESET LAM AND ENABLE THE EXTERNAL
C  PORT.  F(1Ø)A(Ø) TO RESET LAM,  F(11)A(Ø) TO ENABLE PORT
C++   CALL TRANI(CRATE,N3588,Ø,1Ø,Ø,IERR)     \DO NOT NEED THIS
      CALL TRANI(CRATE,N3588,Ø,11,Ø,IERR)
C
C  WAIT FOR 6 SECONDS, WHILE INSTRUMENT IS COLLECTING DATA
      CALL WAIT(36Ø,Ø)
C
C  IT'S TIME TO STOP HISTOGRAMMER AND READ DATA.  F(19)A(Ø) TO
C  STOP THE HISTOGRAMMER, DISABLE ITS EXTERNAL PORT
      CALL TRANO(CRATE,N3588,Ø,19,Ø,Ø,Ø,IERR)
C
C  READ THE DATA INTO THE DATA RECORD
      CALL RDDATA(  Ø,24Ø,ADC1,TOTCNT(1))          \1ST ADC
      CALL RDDATA(256,24Ø,ADC2,TOTCNT(2))          \2ND ADC
      CALL RDDATA(512,24Ø,ADC3,TOTCNT(3))          \3RD ADC
      CALL RDDATA(768,24Ø,ADC4,TOTCNT(4))          \4TH ADC
```

```
C
C  WRITE DATA RECORD INTO NE213 DATA BASE.
C  FIRST OPEN INDEX FILE 'NE213.IDX', FIND OUT THE LAST RECORD NO.
       OPEN (UNIT=1,FILE='NE213.IDX', ACCESS='DIRECT',
     1   FORM='UNFORMATTED',BUFFERCOUNT=2,STATUS='OLD',
     2   RECORDTYPE='FIXED',RECL=3)
       READ (UNIT=1, REC=1) IDXREC                \FIRST RECORD THERE POINTS TO
C                                                 \THE LAST RECORD NUMBER USED.
       RECNO=IDXREC(1)+1                          \BUMP THE POINTER
       IDXREC(1)=RECNO                            \RECORD NUMBER
       IDXREC(2)=HDATE(4)                  \DAY-OF-THE-YEAR
       IDXREC(3)=HTIME(4)                  \TICKS-OF-THE-DAY
       IXSHOT=HSHOT                        \SHOT NUMBER
C
C  WRITE TO INDEX FILE, APPEND TO THE LAST RECORD
       WRITE (UNIT=1, REC=RECNO) IDXREC
C
C  WRITE TO THE FIRST RECORD.  (THE FIRST RECORD POINTS TO THE MOST
C  RECENT DATA RECORD)
       WRITE (UNIT=1, REC=1) IDXREC
C
C  CLOSE INDEX FILE
       CLOSE (UNIT=1)
C
C  OPEN FILE 'NE213.DAT' IN DIRECT MODE, WRITE DATA RECORD INTO
C  THE SLOT POINTED BY RECNO
       OPEN(UNIT=1,FILE='NE213.DAT',ACCESS='DIRECT',
     1   FORM='UNFORMATTED',BUFFERCOUNT=2,STATUS='OLD',
     2   RECORDTYPE='FIXED',RECL=512)
C
       WRITE (UNIT=1,REC=RECNO) NEREC
       CLOSE (UNIT=1)
C
C  SEND A REQUEST FOR THE ONLINE DISPLAY TASK
       IBUF(1)=RECNO              \PASS THE RECORD NO. AS A GIFT
       CALL SDRC(NERPT, IBUF)
C
C  RESET THE EVENT FLAG
       CALL CLREF(64,IDS)
C
C  GOTO STARTING POINT, WAIT FOR NEXT ROUND
       GOTO 10
       END
```

```
      SUBROUTINE RDDATA(STADDR,COUNT,ARRAY,SUM)
C
C  THIS ROUTINE READS DATA FROM THE LECROY 3588 HISTOGRAMMER
C  STADDR IS THE STARTING ADDRESS IN THE HISTOGRAMMER.  COUNT
C  IS THE NUMBER OF WORDS TO BE READ.  ARRAY IS THE PLACE THAT
C  DATA GOES.  SUM IS THE SUMMATION OF THE DATA.
C+
      IMPLICIT INTEGER (A-Z)
      INCLUDE  'NECOM.FTN'
      INTEGER  ARRAY(1)                \DUMMY ARRAY TO RETURN DATA
      INTEGER*4 SUM
C
C  ENABLE ADDRESS AUTO INCREMENT MODE. F(25)A(0)
      CALL TRANI(CRATE,N3588,0,25,0,IERR)
C
C  LOAD MEMORY ADDRESS REG WITH STARTING ADDRESS, F(18)A(1)
      CALL TRANO(CRATE,N3588,1,18,0,STADDR,0,IERR)
C
C  READ BACK DATA, SUM THEM UP, F(2)A(0) IN REPEAT MODE.
      SUM=0
      CALL TRANI(CRATE,N3588,0,2,1,IERR)      \REPEAT MODE
      DO 10,I=1,COUNT
      CALL CAMI(NHIWAY,0,0,DATALO,DUMMY,Q,IERR)
      IF (DATALO.GE.16384) DATALO=DATALO-16384        \SOFTWARE PATCH
      SUM=SUM+DATALO
      ARRAY(I)=DATALO
10    CONTINUE
C
      RETURN
      END
C
C
C
      SUBROUTINE GTSHOT(SHOTNO)
      IMPLICIT INTEGER (A-Z)
      INCLUDE  'NECOM.FTN'
      INTEGER*4 SHOTNO
C
C  GET LOW 4 DIGITS, F(0)A(0)
      CALL CAMI(NSHOT,0,0,DATALO,DUMMY,Q,IERR)
C
C  GET HIGH 2 DIGITS, F(0)A(0)
      CALL CAMI(NSHOT+1,0,0,DATAHI,DUMMY,Q,IERR)
      DATAHI=IIAND('00FF'X,DATAHI)
C
C  CONVERT THE HIGH 2 DIGITS INTO INTEGER*4 VARIABLE. THEN
C  PROCEED TO GET THE RESULT.
      SHOTNO=BCDBIN(DATAHI)
      SHOTNO=10000*SHOTNO+BCDBIN(DATALO)
C
      RETURN
      END
C
C
C
      INTEGER FUNCTION BCDBIN(DATA)
      IMPLICIT INTEGER(A-Z)
      TEMP=0
      DO 10,I=1,4                \4 DIGITS TO CONVERT
      TEMP=10*TEMP+IIAND('000F'X,(IIAND('F000'X,DATA)/4096))
      DATA=IISHFT(DATA,4)        \SHIFT BY 4
10    CONTINUE
      BCDBIN=TEMP
      RETURN
      END
```

```
C   NECOM.FTN DEFINES THE DATA RECORD FOR THE FAST NEUTRON
C    NE-213 DETECTOR SYSTEM
C
        PARAMETER (CRATE=2)      \CRATE NUMBER
        PARAMETER (NADC1=11)     \1ST ADC SLOT
        PARAMETER (NADC2=13)     \2ND ADC SLOT
        PARAMETER (NADC3=15)     \3RD ADC SLOT
        PARAMETER (NADC4=17)     \4TH ADC SLOT
        PARAMETER (N3588=19)     \HISTOGRAMMER SLOT NO.
        PARAMETER (NHIWAY=17)    \HIGHWAY DRIVER SLOT
        PARAMETER (NSHOT=4)      \SHOT COUNT SLOT NUMBER
        PARAMETER (N208=10)      \208 FIFO FOR THE GRAPHICS
C
        INTEGER NEREC(1024)      \BIG ARRAY OF ALL
        INTEGER HDATE(5),HTIME(4)        \DATE, TIME
        INTEGER*4 HSHOT          \HPP SHOT NUMBER
        INTEGER*4 TOTCNT(4)      \TOTAL COUNT
        INTEGER ADC1(240)        \1ST ADC DATA
        INTEGER ADC2(240)        \2ND ADC DATA
        INTEGER ADC3(240)        \3RD ADC DATA
        INTEGER ADC4(240)        \4TH ADC DATA
        REAL    LENGTH           \DATA COLLECTION LENGTH, IN SECONDS
C
        BYTE    ADC1ID(16)       \16 CHARACTER ID.
        BYTE    ADC2ID(16)
        BYTE    ADC3ID(16)
        BYTE    ADC4ID(16)
        BYTE    SUMID(64)        \64 CHARACTER FOR SUMMATION RECORD
C
        EQUIVALENCE (NEREC(1),HDATE(1))
        EQUIVALENCE (NEREC(6),HTIME(1))
        EQUIVALENCE (NEREC(10),HSHOT)
        EQUIVALENCE (NEREC(12),TOTCNT(1))
        EQUIVALENCE (NEREC(20),SUMID(1))         \THE SAME SPACE
        EQUIVALENCE (NEREC(20),ADC1ID(1))        \ FOR ID'S
        EQUIVALENCE (NEREC(28),ADC2ID(1))
        EQUIVALENCE (NEREC(36),ADC3ID(1))
        EQUIVALENCE (NEREC(44),ADC4ID(1))
        EQUIVALENCE (NEREC(52),LENGTH)
C
C    SOME SPARE WORDS RESERVED HERE...,NEREC(54) TO NEREC(63)
C
        EQUIVALENCE (NEREC(64),ADC1(1))
        EQUIVALENCE (NEREC(304),ADC2(1))
        EQUIVALENCE (NEREC(544),ADC3(1))
        EQUIVALENCE (NEREC(784),ADC4(1))
C
        COMMON /NEDAT/ NEREC             \PUT EVERYTHING INTO COMMON
C
C   DECLARE THE INDEX FILE RECORDS NEXT
        INTEGER   IDXREC(6)
        INTEGER*4 IXSHOT
        EQUIVALENCE (IDXREC(4),IXSHOT)
C   IDXREC(1)     RECORD NUMBER
C   IDXREC(2)     DAY-OF-YEAR INTEGER
C   IDXREC(3)     TICKS-OF-THE-DAY
C   IDXREC(4,5)   SHOT NUMBER
C   IDXREC(6)     SPARE
C
        COMMON /IDXDAT/ IDXREC
C
C   END OF THE DECLARATION
```

```
      PROGRAM NESUM
C++
C  THIS PROGRAM SUMS UP SEVERAL NE-213 DATA RECORDS IN
C  ORDER TO GET A BETTER ANALYSIS DATA SET.
C++
      IMPLICIT INTEGER(A-Z)
      INCLUDE   'NECOM.FTN'
      INTEGER*4 FSTSHT,LSTSHT
      INTEGER*4 TOTAL(4)
      INTEGER   ADC1S(240),ADC2S(240),ADC3S(240)
      INTEGER   ADC4S(240),ASDATE(5),ASTIME(4)
      CHARACTER*1  YESNO
C
C  ASK FOR START SHOT NUMBER
      WRITE (5,900)
900   FORMAT('$  ENTER START SHOT NUMBER >> ')
      READ (5,910) FSTSHT
910   FORMAT(I6)
C
C  ASK FOR LAST SHOT NUMBER
      WRITE (5,920)
920   FORMAT('$  ENTER THE LAST SHOT NUMBER >> ')
      READ (5,910) LSTSHT
C
C  SEARCH FOR THE FIRST RECORD
      OPEN (UNIT=1,FILE='NE213.IDX',READONLY,
     1   FORM='UNFORMATTED',BUFFERCOUNT=2,STATUS='OLD',
     2   RECORDTYPE='FIXED',RECL=3)
      READ (UNIT=1) IDXREC
C
C  IS THE SHOT NUMBER OUT OF RANGE ?
      IF (FSTSHT.GT.IXSHOT) THEN
       WRITE (5,930) FSTSHT
930    FORMAT(' START SHOT NO ',I7,'  OUT OF RANGE')
       CALL EXIT
      ENDIF
C
10    READ (UNIT=1) IDXREC                  \READ RECORD BY RECORD
      IF (FSTSHT.LE.IXSHOT) GOTO 20
      GO TO 10
C
20    RECNO=IDXREC(1)                       \KEEP THE RECORD NUMBER
      CLOSE (UNIT=1)
C
C  OPEN FILE 'NE213.DAT' TO GET THE REAL DATA
      OPEN (UNIT=1,FILE='NE213.DAT',READONLY,STATUS='OLD',
     1   FORM='UNFORMATTED',BUFFERCOUNT=2,
     2   RECORDTYPE='FIXED',RECL=512,ACCESS='DIRECT')
C
30    READ (UNIT=1,REC=RECNO) NEREC
      RECNO=RECNO+1                 \NEXT SLOT
C
C  CONVERT DATE AND TIME TO BE PRINTED
      CALL B2ADAT(ASDATE,HDATE(1),HDATE(2),HDATE(3))
      CALL B2ATIM(ASTIME,HTIME(1),HTIME(2),HTIME(3))
C
C  PRINT ONE-LINE RECORD INFORMATION
      WRITE (5,940) ASDATE,ASTIME,HSHOT,TOTCNT
940   FORMAT(/,' ',5A2,' ',4A2,' SHOT:',I6,'  TOTAL:',T40,
     1   4(I7),/,'$ INCLUDE THIS REC?  Y/N>> ')
      READ (5,950) YESNO
950   FORMAT(A1)
      IF (YESNO.EQ.'Y') THEN
       DO 40, I=1,240
       ADC1S(I)=ADC1S(I)+ADC1(I)              \ADD CHANNEL BY CHANNEL
       ADC2S(I)=ADC2S(I)+ADC2(I)
       ADC3S(I)=ADC3S(I)+ADC3(I)
       ADC4S(I)=ADC4S(I)+ADC4(I)
40     CONTINUE
```

```
C
        DO 50,I=1,4
50      TOTAL(I)=TOTAL(I)+TOTCNT(I)
C
C  WRITE OUT THE CURRENT RUNNING TOTAL
        WRITE (5,960) TOTAL
960     FORMAT('  ******** RUNNING TOTAL ********',T40,
     1   4(I7))
        ENDIF
C
C  IS IT THE LAST RECORD?
        IF(LSTSHT.GT.HSHOT) GOTO 30
        CLOSE (UNIT=1)          \CLOSE FILE 'NE213.DAT'
C
C  ASK FOR SLOT NUMBER 1-5, ENTER Ø IF DO NOT WANT IT
60      WRITE (5,970)
970     FORMAT(//,'  ENTER SLOT NUMBER (1 TO 5) TO SAVE THE DATA'.
     1          /,'$ ENTER Ø IF YOU DO NOT WANT TO SAVE IT >> ')
        READ (5,980) NSLOT
980     FORMAT (I2)
C
        IF (NSLOT.EQ.Ø) CALL EXIT
        IF (NSLOT.LT.Ø .OR. NSLOT.GT.5) THEN
         WRITE (5,990)
990      FORMAT('  ERROR??? VALID SLOT IS FROM 1 TO 5, TRY AGAIN')
         GOTO 60
        ENDIF
C
C  HOW ABOUT THE RECORD DESCRIPTION?
70      WRITE (5,1000) SUMID
1000    FORMAT('  REC. ID >> ',64A1,
     1          /,'$ DO YOU WANT TO CHANGE THIS? Y/N >> ')
        READ (5,950) YESNO
        IF (YESNO.NE.'N') THEN
         WRITE(5,1010)
1010     FORMAT(/,'  ENTER NEW RECORD ID ON THE NEXT LINE, 64 CHAR MAX'.
     1           /,'$ ENTER >>')
         READ (5,1020) SUMID
1020     FORMAT(64A1)
         GO TO 70
        ENDIF
C
C  WRITE THE DATA INTO RECORD
        DO 80,I=1,240
        ADC1(I)=ADC1S(I)
        ADC2(I)=ADC2S(I)
        ADC3(I)=ADC3S(I)
        ADC4(I)=ADC4S(I)
80      CONTINUE
C
        DO 90,I=1,4
        TOTCNT(I)=TOTAL(I)
90      CONTINUE
        HSHOT=FSTSHT            \RECORD THE FIRST SHOT
        CALL DATE(HDATE)
        CALL TIME(HTIME)        \RECORD DATE AND TIME
C
        OPEN(UNIT=1,FILE='NESUM.DAT',ACCESS='DIRECT',
     1   FORM='UNFORMATTED',BUFFERCOUNT=2,STATUS='OLD',
     2   RECORDTYPE='FIXED',RECL=512)
        WRITE(UNIT=1,REC=NSLOT) NEREC
        CLOSE (UNIT=1)
C
        WRITE (5,1030)
1030    FORMAT(/,'  ********** DATA SAVED **********')
        CALL EXIT
        END
```

ORNL/TM-9561
Dist. Category UC-20d

INTERNAL DISTRIBUTION

1-2.	L. S. Abbott	25.	M. W. Rosenthal
3.	R. G. Alsmiller, Jr.	26.	R. T. Santoro
4.	J. B. Ball	27-31.	R. R. Spencer
5.	S. J. Ball	32.	A. Zucker
6.	J. M. Barnes	33.	P. W. Dickson, Jr. (consultant)
7-12.	J. K. Dickens	34.	G. H. Golub (consultant)
13.	A. C. England	35.	D. Steiner (consultant)
14-18.	N. W. Hill	36-37.	Central Research Library
19.	D. L. Hillis	38.	Fusion Energy Division Library
20.	N. M. Larson	39.	Fusion Energy Division Reports Office
21.	F. C. Maienschein	40.	ORNL-Y-12 Technical Library
22-23.	J. W. McConnell	41-42.	Laboratory Records
24.	R. W. Peelle	43.	Laboratory Records - RC
		44.	ORNL Patent Section

EXTERNAL DISTRIBUTION

45. Office of Assistant Manager for Energy Research and Development, DOE-ORO, Oak Ridge, TN 37831

46. S. E. Berk, Division of Development and Technology, Office of Fusion Energy, ER-532, US Department of Energy, Washington, DC 20545

47. Library, Princeton Plasma Physics Laboratory, Princeton University, P. O. Box 451, Princeton, NJ 08540

48. Library, Lawrence Livermore National Laboratory, P. O. Box 808, Livermore, CA 94550

49. C. E. Clifford, Princeton Plasma Physics Laboratory, Princeton University, P. O. Box 451, Princeton, NJ 08540

50. H. Conrads, Princeton Plasma Physics Laboratory, Princeton University, P. O. Box 451, Princeton, NJ 08540

51. S. L. Davis, Princeton Plasma Physics Laboratory, Princeton University, P. O. Box 451, Princeton, NJ 08540

52. J. File, Princeton Plasma Physics Laboratory, Princeton University, P. O. Box 451, Princeton, NJ 08540

53. D. J. Grove, Princeton Plasma Physics Laboratory, Princeton University, P. O. Box 451, Princeton, NJ 08540

54. H. Hendel, Princeton Plasma Physics Laboratory, Princeton University, P. O. Box 451, Princeton, NJ 08540

55. F. S. Hou, Princeton Plasma Physics Laboratory, Princeton University, P. O. Box 451, Princeton, NJ 08540

56. D. L. Jassby, Princeton Plasma Physics Laboratory, Princeton University, P. O. Box 451, Princeton, NJ 08540

57. J. Kolibal, Princeton Plasma Physics Laboratory, Princeton University, P. O. Box 451, Princeton, NJ 08540

58. L-P. Ku, Princeton Plasma Physics Laboratory, Princeton University, P. O. Box 451, Princeton, NJ 08540

59. S. Liew, Princeton Plasma Physics Laboratory, Princeton University, P. O. Box 451, Princeton, NJ 08540

60. R. Little, Princeton Plasma Physics Laboratory, Princeton University, P. O. Box 451, Princeton, NJ 08540

61. D. M. Meade, Princeton Plasma Physics Laboratory, Princeton University, P. O. Box 451, Princeton, NJ 08540

62. E. B. Nieschmidt, Princeton Plasma Physics Laboratory, Princeton University, P. O. Box 451, Princeton, NJ 08540

63. C. W. Pierce, Princeton Plasma Physics Laboratory, Princeton University, P. O. Box 451, Princeton, NJ 08540

64. B. Pritchard, Princeton Plasma Physics Laboratory, Princeton University, P. O. Box 451, Princeton, NJ 08540

65. P. Sager, General Atomic Company, P. O. Box 81608, San Diego, CA 92138

66. N. R. Sauthoff, Princeton Plasma Physics Laboratory, Princeton University, P. O. Box 451, Princeton, NJ 08540

67. J. Sinnis, Princeton Plasma Physics Laboratory, Princeton University, P. O. Box 451, Princeton, NJ 08540

68. D. L. Slaughter, Lawrence Livermore National Laboratory, P. O. Box 808, Livermore, CA 94550

69. J. Stencel, Princeton Plasma Physics Laboratory, Princeton University, P. O. Box 451, Princeton, NJ 08540

70. W. M. Stacey, Jr., School of Nuclear Engineering, Georgia Institute of Technology, Atlanta, GA 30332

71. J. D. Strachen, Princeton Plasma Physics Laboratory, Princeton University, P. O. Box 451, Princeton, NJ 08540

72. K. M. Young, Princeton Plasma Physics Laboratory, Princeton University, P. O. Box 451, Princeton, NJ 08540

73. F. Y. Tsang, Princeton Plasma Physics Laboratory, Princeton University, P. O. Box 451, Princeton, NJ -8540

74. Bibliothek, Institut fur Plasmaphysik, D-8046, Garching bei Munchen, Federal Republic of Germany.

75. Bibliothek, Institut fur Plasmaphysik, KFA, Postfach 1913, D-5170, Julich 1, Federal Republic of Germany

76. Bibliotheque, Service du Confinement des Plasmas, CEA, B.P. No. 6, 92, Fontenay aux Roses (Seine), France

There are some interesting results that may be deduced from these tables, although one must be cautious not to over-speculate since the model is only an approximation to the actual configuration, and the assumed incident neutron spatial distribution is not likely to be that studied in the TCB. For our present measurement purposes in the TCB, the magnitudes of the perturbations due to the iron shield are no larger than other experimental uncertainties and are much smaller than present-day transport-calculation uncertainties. Clearly, though, when the latter reach a stage of sophistication to reverse the relative uncertainties vis-a-vis the experiment, then the transport calculations will need to include the details of the detector configuration given in Fig. 1.

77. Documentation, S.I.G.N., D.P.PFC CEN, P.O. 85, Centre de Tri, 38041 Cedex, Grenoble, France

78. Institute of Physics, Academia Sinica, Peking, Peoples Republic of China

79. Library, Centre de Recherches en Physique des Plasmas, 21 Avenue des Bains, 1007, Lausanne, Switzerland

80. Library, Jet Joint Undertaking, Culham Laboratory, UKAEA, Abingdon, Oxon, OX14-3DB, England

81. Library, FOM Institute voor Plasma-Fysica, Rijnhuizen, Jutphass, Netherlands

82. Library, Institute for Plasma Physics, Nagoya University, Nagoya 464, Japan

83. Library, International Centre for Theoretical Physics, Trieste, Italy

84. Library, Laboratoria Gas Ionizzati, Frascati, Italy

85. Library, Plasma Physics Laboratory, Kyoto University, Gokasho Uji, Kyoto, Japan

86. Plasma Research Laboratory, Australian National University, P. O. Box 4, Canberra ACT.2000, Australia

87. Thermonuclear Library, Japan Atomic Energy Research Institute, Tokai, Naka, Ibaraki, Japan

88-211. Given distribution as shown in TID-4500, Magnetic Fusion Energy (Distribution Category UC-20d: Fusion Systems).